IEEE Access
Multidisciplinary | Rapid Review | Open Access Journal

Received 14 February 2024, accepted 26 February 2024, date of publication 29 February 2024, date of current version 7 March 2024.

Digital Object Identifier 10.1109/ACCESS.2024.3371493

TOPICAL REVIEW

Review on the Advancements in Wind Turbine Blade Inspection: Integrating Drone and Deep Learning Technologies for Enhanced Defect Detection

MAJID MEMARI, PRAVEEN SHAKYA, MOHAMMAD SHEKARAMIZ, (Member, IEEE), ABDENNOUR C. SEIBI, AND MOHAMMAD A. S. MASOUM, (Senior Member, IEEE)
Machine Learning and Drone Laboratory, Engineering Department, Utah Valley University, Orem, UT 84058, USA

Corresponding author: Mohammad Shekaramiz (mshekaramiz@uvu.edu)

This work was supported by the Utah System of Higher Education (USHE)-Deep Technology Initiative Grant 20210016UT.

ABSTRACT The increasing demand for wind power requires more frequent inspections to identify defects in the Wind Turbine Blades (WTBs). These defects, if not detected, can compromise the structural integrity and safety of wind turbines. As WTBs are crucial and costly components, they may suffer material degradation and fatigue failure, which affects their performance and safety. Thus, the urgency for efficient and regular monitoring to maintain their structural integrity is greater than ever. This review paper explores innovative methods in fatigue testing, damage detection, and structural reliability in WTBs, focusing on the use of recent inspection methods, including those that take advantage of drones. Drones are used to identify defects such as cracks, erosion, and coating irregularities using high-resolution imagery with the onboard cameras. Various investigators have developed novel data-driven approaches, incorporating machine learning and deep learning, to accurately identify these defects. Although deep learning-based image processing has been successful in other public infrastructure contexts, its application to wind turbine inspection from aerial images presents unique challenges. This paper also highlights the critical role of failure inspection in enhancing the operational integrity of WTBs, showcasing state-of-the-art deep learning techniques that are pivotal for identifying and analyzing failures in WTBs from images captured by drones. The paper provides insights into the latest developments in using drone imagery for blade defect detection, contrasting this method with traditional non-destructive techniques. This approach could significantly transform the wind energy industry by offering a more efficient, automated, and precise way of ensuring the structural health of wind turbines. Unlike previous studies that predominantly focus on isolated aspects such as inspection or fatigue, this review paper not only integrates the three major aspects of WTBs integrity in terms of aerial inspection, image processing using machine learning, and structural integrity of the blade but also undertakes an extensive examination of the prevailing methodologies in the field, pinpointing crucial gaps and challenges. It provides a detailed review of existing research, covering various areas including automated inspection, image processing techniques, fatigue analysis, and the reliability of wind turbines. This approach enriches the discourse by offering a multifaceted perspective on WTB maintenance, thereby advancing the understanding of operational integrity within the field of wind energy.

INDEX TERMS Wind turbine blades, defect detection, drones, anomaly detection, fault identification, feature extraction, image processing, deep learning, aerial imagery, crack detection, turbine maintenance, fatigue, reliability.

The associate editor coordinating the review of this manuscript and approving it for publication was Yiming Tang.

I. INTRODUCTION

With the growing global demand for sustainable energy solutions, wind turbines have increased rapidly in number and

scale. Consequently, this surge has led to a simultaneous rise in the number of turbine blade failures, making identification of their surface defects of paramount importance for ensuring their operational efficiency and longevity. If not addressed in a timely manner, such defects can compromise the structural integrity of the turbines, leading to possible catastrophic failures. WTBs are intricately designed with thin-walled and pre-twisted structures to withstand the dynamic deformations experienced during operation. Their preset angle relative to airflow remains relatively constant, thereby optimizing their aerodynamic performance. The blades feature suction and pressure sides formed at their leading and trailing edges, further enhancing their aerodynamic efficiency. To withstand complex loads encountered during routine operation, WTBs are engineered to withstand harsh environmental conditions, including high humidity, wind gusts, fatigue, and even lightning strikes.

Wind turbine damage can arise from both natural and human factors. Improper handling during manufacturing, transportation, installation, and maintenance can cause damage. Additionally, WTBs are often located in environmentally challenging locations, making them susceptible to various forms of damage. Recognizing the early stages of damage is crucial, as the gradual accumulation of micro-damage can compromise efficiency and even result in catastrophic failures over time. Timely detection and diagnosis of blade health through Structural Health Monitoring (SHM) can mitigate these risks and extend the lifespan of wind turbines.

Several methods are employed for diagnosing WTB damage, including Non-Destructive Testing (NDT), Supervisory Control And Data Acquisition (SCADA)-based approaches, and vibration signal analysis. NDT technology, in particular, has gained prominence in recent years for its effectiveness in fault diagnosis. This paper also examines the latest advancements in WTB damage detection, encompassing methods such as visual inspection, wave propagation analysis, impedance measurement, photogrammetry, ultrasonic, thermal, and radiographic methods. It is also focused on the experimental and numerical study of the structural reliability and fatigue of WTBs.

Recent advances in aerial technology, particularly the development and use of drones, present a promising avenue for early defect detection. Harnessing the potential of drones for defect identification not only ensures accurate data acquisition but also promises reduced human intervention, addressing the challenges posed by an aging workforce and rising labor costs. Drawing parallels from previous research, methods rooted in image processing have been pivotal in defect detection across various infrastructures. However, aerial images of wind turbines present a unique challenge. These aerial shots encompass a myriad of complexities, including varying environmental data, necessitating robust image processing techniques to identify potential structural flaws.This review paper also delves into the innovative realm of utilizing drone-captured imagery for WTB defect detection.

We highlight the evolution of defect identification techniques, ranging from vibration detection technology and acoustic emission detection to more recent computer vision-based methodologies. More specifically, we shed light on how machine learning, especially deep learning algorithms, are revolutionizing the domain of WTB defect detection, paving the way for automated, real-time surveillance, and quick preventive maintenance. This article also includes the various WTB reliability models and how they are used to predict their remnant service life.

Historically, defect detection largely relied on non-destructive methods. While these traditional methods are still relevant, their limitations in terms of cost, scalability, and accuracy have propelled the research community to explore alternative avenues. The integration of drones with deep learning algorithms stands out as a viable solution, offering unprecedented levels of accuracy and scalability.

The following sections will provide a comprehensive understanding of the various wind turbine failures, their structural integrity, and will elucidate recent strides made in deep learning algorithms and their application, present real-world case studies, and evaluate the scalability and overall impact of these novel methodologies. The following sections consist of three major parts related to wind turbine damage and reliability models, autonomous inspections, and image processing. We aim to present a comprehensive review that encompasses all activities ensuring a sustainable energy supply through timely autonomous inspection, image processing, and wind turbine blades structural reliability.

II. OVERVIEW OF DAMAGES ON WTB

Wind loads acting on the blades cause them to rotate and generate electricity. However, for a prolonged period, cyclic loading induces fatigue degradation to these blades, thereby inducing cracks that lead to blade failure before their intended service life. Furthermore, WTB damage can be caused by erosion, heavy rain, lightning, ice accumulation, strong winds, manufacturing defects, and collision of birds as shown in Figure 1 taken from [1].

For the safety of WTBs, most wind turbines operate at cut-in (3-4 m/s) and cut-out (25 m/s) wind speeds to avoid damage from high winds. However, it has been seen that the WTBs are damaged due to a fierce storm and very high wind. This is usually avoided by installing wind farms in areas with low probability of a strong storm and regions with very high wind.

During the operation of wind turbines, the presence of air mixed with sand and water droplets can lead to significant erosion of WTBs as shown in Figure 2. The blades experienced significant force due to rapid impacts from tiny particles within milliseconds, particularly at the tip where the rotational speed is highest. The impact of a water droplet on the blade surface induces significant shear stress. Continuous scouring by sand particles and water droplets imposes a persistent load on the blade surface, resulting in a gradual reduction of the blade surface fatigue strength and causing substantial damage to the blade material. Erosion at

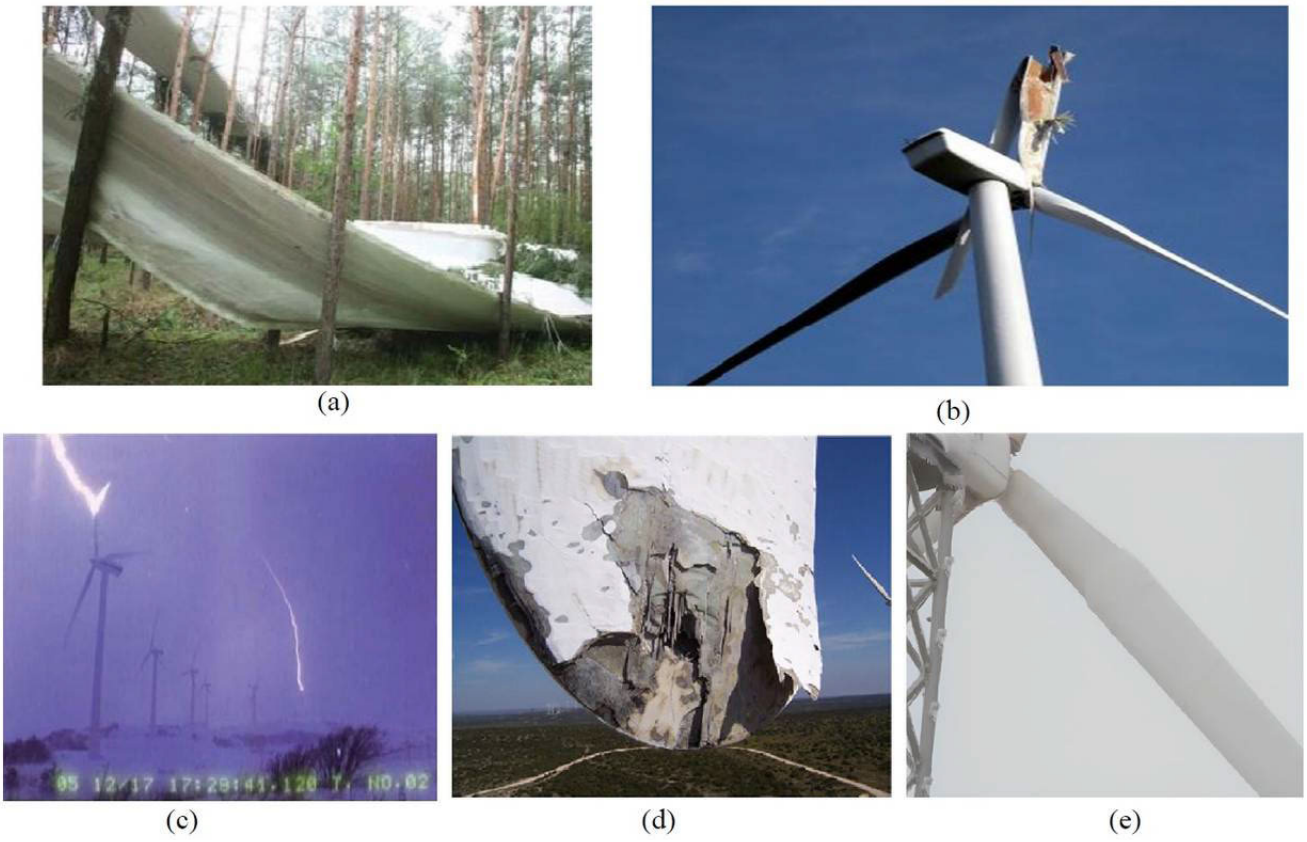

FIGURE 1. WTB damaged due to (a) Fierce storm (b) High winds (c) Lighting strike (d) Damage due to lightning strike (e) Ice accumulation [1].

the leading edge of WTBs stands out as a notable example of a subtractive process, frequently arising from the high-speed impact of the blade's leading edge with rain droplets or hailstones [2]. Zarate et al. [3] studied erosion at the tip of WTB considering aerodynamic analysis, modal analysis and predictive ML modelling. Location of erosion and erosion level were automatically detected using multi-layer neural network and adaptive networks with fuzzy inference system. Campobasso et al. [2] presented a novel probabilistic analysis framework that combines Computational Fluid Dynamics (CFD), uncertainty propagation, and high-performance computing to assess the performance degradation of WTBs due to erosion. The study quantified statistical moments of power and energy yield losses for eroded turbines at offshore and onshore sites, revealing potential Annual Energy Production (AEP) losses of 2% and 3%, respectively (with low standard deviations). Their findings emphasized the importance of considering turbulence intensity at the installation site in understanding turbine loss variability. Castorrini et al. [4] employed open source CAD functionalities to model leading edge erosion on WTB, and simulating pits and gouges using CFD.Their research on a 5 MW WTB revealed AEP loss of 1-2% due to leading edge damages. They further emphasized the potential benefits of adaptive power control strategies to mitigate erosion-induced energy losses. Lopez et al. [5] proposed a framework to estimate erosion evolution and energy degradation overtime by considering weather uncertainty. They utilized wind and rain data derived from site observations, ERA5 reanalysis (atmospheric data), and whirling arm test data. The assessment of erosion effects on airfoils was conducted using aerodynamic polar curves. Their case study of a 5 MW NREL wind turbine in the North Sea revealed potential AEP loss of 1.6-1.75% and the predicted inital erosion failure between 2-6 years.

Wind turbines that are hundreds of feet above ground become easy targets for lightning. In the presence of moisture on the WTBs struck by lightning, the accumulated dust in the air generates a destructive internal shock wave that harms the blades. Researchers are actively working on the development of a lightning protection system to protect blades from such damage. The National Renewable Energy Lab (NREL) has developed a new type of material (thermoplastic resin composites) to protect the blade from lightning [7]. The advantage of using thermoplastic materials is that they can be easily recycled compared to commonly used thermoset materials. Moreover, thermoplastic composites can cure at room temperature, thus reducing the blade manufacturing time and cost. The experimental findings indicate that approximately 80% of the electrical current is channeled into the expanded aluminum foil layer for lightning protection instead of the blade skin when subjected to a high current. Moreover, the carbon fiber remained unharmed beneath the

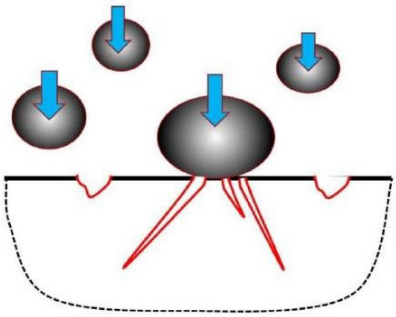

(a) WTB Erosion Schema

(b) Eroded WTB surface

FIGURE 2. Erosion on WTB [6].

affected region of the tip. Consequently, this design enhances the safety of the blades against lightning strikes.

During cold weather, ice accumulation on WTBs emerges as a significant concern for safety and operational efficiency, particularly due to the high speed at which the blades are moving at the tip. This accumulation of ice on the blades results in a reduction of lift and an increase in drag, both of which detrimentally impact power production. Bragg and others have highlighted these effects in their studies [8]. Additionally, experimental observations by Gao and colleagues have shed further light on these dynamics [9]. In a detailed field study, Gao et al. [10] specifically examined the impact of ice accretion on utility-scaled 50 m WTBs, focusing on the resultant effects on power production. In their innovative approach, they utilized a drone equipped with a digital camera to capture detailed images of the ice accretion on WTBs. Their findings are crucial, indicating that even under conditions of high winds, the power production can be reduced to 80% due to the presence of ice on the blades.

In addition to complex environmental damage, human errors are also the reason for blade failure due to faulty manufacturing. Figure 3 illustrates an example of broken blades due to poor manufacturing [1]. In this blade, wrinkles appeared in the carbon fiber within the spar. When subjected to cyclic loading from strong winds, these wrinkles spread extensively, resulting in damage to the WTB.

The majority of WTBs consist of composite materials, wherein the spar box contains spar and shear webs responsible for bearing the primary loads. Sørensen et al. [11] carried out an experimental study to investigate various types of

FIGURE 3. Example of a damaged WTB [1].

TABLE 1. List of most common damage types on WTB [11].

Type	Description
Type 1	Damage formation and growth in the adhesive layer that joins the skin and the main spar flanges (skin/adhesive debonding and/or main spar/adhesive layer debonding)
Type 2	Damage formation and growth in the adhesive layer that joins the skins of the up and downwind along the leading and / or trailing edges (adhesive joint failure between the skins)
Type 3	Damage formation and growth at the interface between the face and the core in sandwich panels in the skins and the main spar web (sandwich panel face/core debonding)
Type 4	Formation and growth of internal damage in laminates in the skin and / or the main flanges of the flanges, under a tensile or compression load (delamination driven by a tension or buckling load)
Type 5	Splitting and fracture of separate fibers in skin and main spar laminates (fiber failure in tension; laminate failure in compression)
Type 6	Skin buckling due to the formation of damage and the growth of the bond between the skin and the main spar under compressive load (skin/adhesive debonding induced by buckling, a specific type 1 case)
Type 7	Formation and growth of cracks in the gel-coat; debonding of the gelcoat from the skin (gelcoat cracking and gelcoat / skin debonding)

damage that occurred in WTB. Figure 4 sho ws most common types of damage and defects on WTB. In summary, Table 1 summazied these types of damage occuring on WTB.

III. WTB TESTING METHODS AND NUMERICAL SIMULATIONS

The structural integrity of WTBs has been studied through intensive experimental investigations and numerical simulations. WTB testing methods are generally categorized into two types: static and fatigue. Depending on the objective of the experiment, the test load can be either load-based or strength-based. Load-based testing aims to demonstrate the blade's ability to withstand intended loads without any failure, which is part of the certification process. Strength-based testing, on the other hand, focuses on evaluating the material properties and durability of the blades. It involves applying static and dynamic loads to identify potential weaknesses in the blade's construction

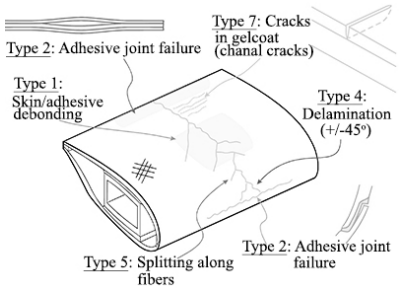

(a) Blade section subjected to a compressive load

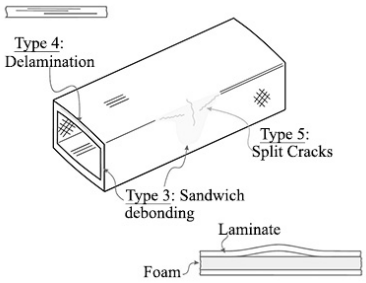

(b) Damage to main spar outer surface

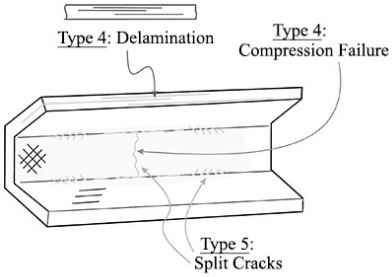

(c) Damage caused to internal surface of the main spar

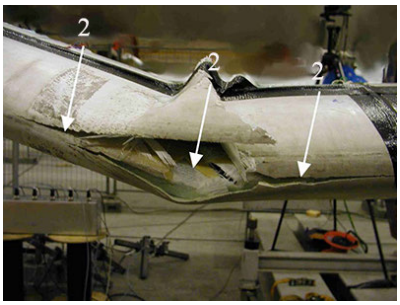

(d) Damage in blade section at the leading edge (Type 2: Adhesive joint failure)

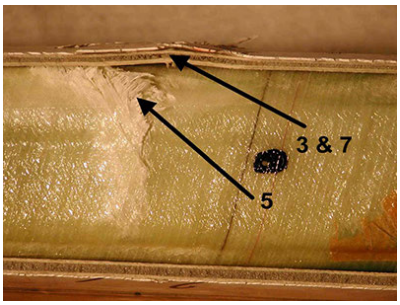

(e) Damage at outer surface of main spar with Type 3, Type 5 and Type 7 damages

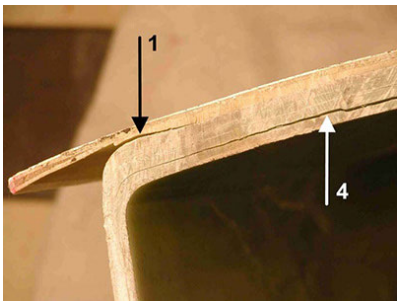

(f) Damage at main spar flanges of blade section with Type 1 and Type 4 damages

FIGURE 4. Types of common damages induced on a WTB [11].

and materials. By combining load-based and strength-based testing, engineers can gain comprehensive insights into the overall performance, structural resilience, and safety margins of WTBs to meet rigorous standards and withstand the harsh conditions of wind energy environments.

The experimental study and the numerical analysis of static testing, fatigue, and reliability in WTB are essential components of the design and validation process. Experimental studies involve subjecting physical prototypes to static tests, where the blades are subjected to static loads to assess their structural behavior and integrity under various conditions. Concurrently, fatigue testing involves simulating cyclic loading conditions to replicate the long-term stresses experienced during the operational life of the blade. These experiments provide invaluable information on potential weaknesses, deformation patterns, and failure modes. However, numerical studies utilize advanced modeling techniques to simulate and predict the static and dynamic behavior of WTBs. This numerical analysis helps optimize the design, predict stress distributions, and assess long-term reliability of the blades. Combining experimental and numerical studies leads to a comprehensive understanding of the static, fatigue, and reliability aspects, enabling engineers to refine designs and ensure the structural integrity of WTBs throughout their operational lifespan.

A. EXPERIMENTAL STUDY OF WTBS

The experimental study of WTBs is a crucial aspect that focuses on static testing and fatigue analysis. The aim of the experimental study is to improve the performance and durability of wind turbine systems, contributing to the overall efficiency of wind energy generation. Static testing involves subjecting the blades to various loads and forces to assess their structural integrity and material strength under different conditions. This phase helps researchers understand how the blades respond to static forces, ensuring that they can withstand the environmental challenges they may encounter during their operational life. Additionally, fatigue testing is essential to evaluate the long-term reliability of the blades by simulating cyclic loading, similar to the conditions experienced during wind-induced oscillations. By comprehensively investigating both static and fatigue aspects, scientists and engineers can refine blade designs, leading to more robust and sustainable wind turbines that can withstand the diverse challenges of harnessing wind power for renewable energy production.

1) STATIC TESTING

WTBs undergo extreme loads during operation. Therefore, it is crucial to perform static testing of WTBs to determine structural integrity and its ability to withstand extreme loads. When loads are applied to the blades in a static manner, the loads are held constant in one direction to determine the ultimate strength of the blades and predict its performance under various conditions. The objective of this test is to ensure that the blades comply with the International Electrotechnical Commission (IEC) Technical Specification 61400-23, which defines the requirements for full-scale strutural testing of WTBs.

During static testing, the blade is subjected to loads that simulate the forces it may experience during its operational lifespan. The testing can be intentionally destructive or

non-destructive, depending on the objectives. Static testing is typically performed in specialized facilities where the blade is secured and loads can be accurately applied, as shown in Figure 5. The testing process usually involves gradually increasing the load until a pre-determined limit is reached. This procedure assesses the blade's ability to withstand the expected loads without experiencing any failure or deformation. The results obtained from static testing are crucial for wind turbine manufacturers and operators, as they provide valuable information about the blade's structural performance, ultimate strength, and the overall reliability. This information also helps optimize the design and ensure the safety and durability of WTBs [12].

In this area, Yang et al. [13] studied a full-scale collapse test under flapwise loading for a 40m composite WTB. Integral and local WTB deformations under flap loading conditions were measured using a videometric technique. At maximum load, the blade tip deflected about 11 m, which was 160% of the extreme design load for the tested blade. Their study revealed that the initial failure mechanism occurred due to the debonding of the aerodynamic shells of the adhesive joints resulting in a complete blade failure.

Fagan et al. [14] conducted an experimental investigation on a 13 m long composite WTB. The results of the test were used to calibrate the finite element model for an optimized design study using a genetic algorithm. In their setup, two blades were mounted on a support structure and loaded using chains and chain blocks. Three load saddles located at 5 m, 10 m, and 12 m from the root of the blade were used to transfer the load. The results did not show signs of cracking, surface buckling, or acoustic emissions during the test.

Chen et al. [15] conducted a failure analysis on a 52.3 m long 2.5 MW composite WTB under static loading. Static bending tests were performed for two sets of 2.5 MW and 3 MW blades. The initial set of tests was designed to evaluate the performance of the blades under design loads applicable to 2.5 MW turbines. These tests were conducted in accordance with certification body requirements for full-scale blades. In contrast, the second set of tests, was conducted on 3.0 MW turbines, aimed to push the limits of the blade's capabilities and exploring potential failure points. For each set of experiments, the loads were applied stepwise, with a specific loading procedure of 0%, 40%, 60%, 80%, and 100%, followed by an unloading procedure of 80%, 60%, 40%, and 0%, relative to the target loads, in each individual test case. Following the successful completion of the blade certification with the 2.5 MW load set, testing was continued with the 3.0 MW load set. During this testing phase, the blade experienced a catastrophic failure in the transition region at approximately 90% of the target test loads. The main failure regions were found to be between 3.5-5.5 m exhibiting several typical failure modes, including Laminate Fracture (LF), Composite Delamination (DL), and sandwich skin-core Debonding (DB).

In another study, Gage et al. [16] conducted static testing on the NRT Blade, a 13 m WTB. The blade was subjected to extreme negative flapwise bending and static edgewise bending moments. These test moments included the combined effects of blade self-weight, tear load from the weight of the load saddles, as well as external loads applied through an overhead crane and ballast weights. For each load scenario, the bending moments were applied in three load ramps, corresponding to approximately 25%, 50%, and 100% of the target load. Remarkably, the blade successfully withstood each of the proof load cases, displaying no signs of damage or evident changes in physical shape.

Jørgensen et al. [17] conducted a failure test on a 25 m WTB subjected to flapwise load. The blade was tested to failure at three different locations. For static tests, more than 100 strain gauges were used to detect the strain in the blade. Rumsey and Paquette [18] performed static and fatigue tests on a 9m long composite WTB. Thirty thousand Ohm metal foil strain gauges were installed on the gel-coat surface of the blade and strain gauges were zeroed at the flapwise load. The commercial off-the-shelf acoustic emission NDT system effectively monitored the blade, revealing diagnostic signs of failure after 4,000,000 fatigue cycles. The study emphasized safety concerns, prompting the test's interruption prior to complete blade failure. Lee et al. [19] proposed optimal sensor placement on the WTB without Finite Element (FE) model and displacement estimation. They have employed a simplified experimental blade model through modal testing interpolation, which proved practical for operational wind turbine applications. Additionally, a wireless sensor network, utilizing open-source hardware, was implemented on a 300 W scale wind turbine to analyze blade vibrations during operation.

As stated above, static testing of WTBs is an essential step in ensuring their structural integrity and performance. This type of testing involves evaluating the blades under static (non-moving) conditions to assess their strength, stiffness, and overall structural behavior. Through static testing, the strength and structural behavior of WTB structures at different locations were determined in the aforementioned experimental studies. However, it is crucial to recognize that assessing the long-term durability and performance of these blades requires more than static testing alone. This is particularly true because static testing may not fully capture the dynamic loading conditions a blade encounters during its operational life. In cases where static testing is lacking, the significance of conducting comprehensive fatigue testing is heightened to ensure the blades' reliability. Fatigue testing is a critical procedure, which subjects the blade to repeated loading cycles, simulating the conditions throughout its operational lifespan. The next section will delve into a study focused on fatigue testing for different WTBs.

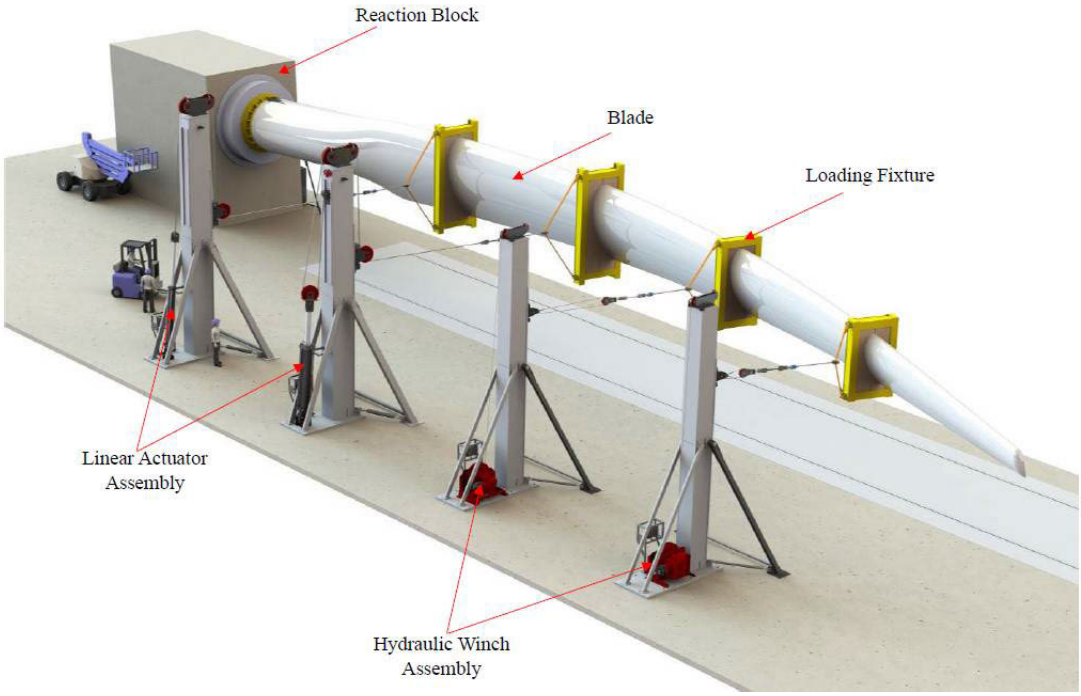

FIGURE 5. Static testing of WTB [12].

2) FATIGUE TESTING

The primary goal of fatigue testing is to ascertain the structural characteristics of a blade, including its fatigue strength and failure modes. Moreover, such testing is instrumental in evaluating the capability of new sensor technologies to detect damage and conduct SHM. Evaluation of the blade's service life can be achieved either experimentally or numerically by subjecting a typical blade to cyclic loading in the form of millions of load cycles. Figure 6 presents the fatigue certification test method of WTB.

The size of composite WTBs has continuously grown over the past decade. Therefore, the utilization of testing technology that takes advantage of the resonance phenomenon has become increasingly common. The moment distribution on WTBs is a critical aspect of its structural analysis, as it directly influences the overall performance and reliability of the blade. It is necessary to determine the moment distribution on the blade using modal analysis and test amplitude using damping analysis for resonance-type fatigue testing.

Desmond et al. [21] performed structural tests on a 8.3 mm long WTB made of different materials (glass fibers and carbon fibers) to investigate their reliability by inducing damage to both blades. The load was applied through a hydraulic actuator and damage was detected using Acoustic Emission (AE) sensors. The testing concentrated on applying loads to specific spanwise regions of the blade (i.e., 7m, 6m, and 4.37m) where the deliberate defects were located. The fiberglass blade showed out-of-plane and root laminate failure at different loading stations, however, the carbon fiber showed failure of the in-plane and out-of-plane.

(a) Along flapwise direction

(b) Along edgewise direction

FIGURE 6. Fatigue certification test of WTB [20].

Lee and Park [20] studied fatigue damage effect on the residual strength of full-scale composite WTB. They initially performed a static test followed by fatigue testing on a 48.3 m WTB in accordance to IEC TS 61400-23. The blade was sequentially loaded in positive flapwise,

positive edgewise, and negative flapwise directions. During the static loading test, the blade withstood positive flapwise loading. For edgewise loading, the blade sustained the static loading; however, there were some cracking sounds due to peeling strains in the trailing edge bonding line, resulting in delamination in the fatigue-damaged layers. During negative flapwise loading, the blade collapsed at 70% of static loading due to interfacial failure in the bonding line which was unable to sustain the shear flow. A sudden drop in the torsional rigidity was observed showing oblique cracks in the shear webs that lead to the breakage of the pressure-side spar cap.

Al-Khudairi et al. [22] conducted fatigue testing and examined damage propagation by introducing a crack to study the performance of a full-scale WTB, specifically a 47.5 m long WTB was selected for static testing, fatigue testing and modal analysis. A total of 30 strain gauges were used on the pressure and suction side of the blade, and inside the shear web. They conducted three studies (i) full blade without crack, (ii) a crack of 200 mm was introduced between the spar cap and the web, and (iii) a crack was extended to 1000 mm. The first natural blade frequency for each state was used for fatigue testing. The results showed that for a 200 mm crack between the shear web and the spar cap at a location of 9 m from the root it did not propagate at 50% of the target bending moment up to 62110 cycles. When the load increased to 70% of the target bending moment, damage was observed on the pressure side of the blade. For 1000 mm, the crack started to propagate and the blade experienced delamination, adhesive joint failure, compression, and sandwich core failure.

Chen [23] presented an experimental observation on structural degradation of a 47 m long full-scale composite WTB subjected to fatigue loading up to 2 million cycles. In composite WTB, the unidirectional laminates form a major portion of the spar caps, which are responsible for the overall stiffness and load carrying capacity of the blade. Changes in bending stiffness, damping ratio, and natural frequencies were calculated at different fatigue cycles. The fatigue test was stopped at five intervals (0, 0.5, 1, 1.5, and 2 million), a pulling force was applied at a blade section of 39.5 m and deflections were measured in sections of 19 m, 28 m and 39.5 m using drawwire displacement transducers. No fatigue degradation of the bending stiffness was observed in the blade section ranging from 0 to 19 m. However, a clear trend of degradation was observed from 19 to 39.5 m blade section. The stiffness degradation was a result of the density of matrix cracks in these off-axis laminates (biaxial and triaxial), which might enter saturation phase and unidirectional laminates were taking the primary load. Changes in the natural frequencies were negligible in fatigue loading and the damping ratios increased by 20% for two flapwise modes.

Fremmelev et al. [24] explored damage detection in a commercial 52 m long WTB under fatigue testing. To detect damage, different artificial damages were introduced in the form of cracks to the blade. Damages induced in the WTB were manually increased to see propagation and delamination during fatigue loading. Various number of sensors such as Strain Gauges (SG), AE sensors, accelerometers, and an active vibration monitoring system were employed along the blade to monitor the structural health of damaged and healthy states of the blade. SG measurements demonstrated the local detection of damage initiation and propagation through changes in the strain range, providing a simple interpretation with limited data processing. AE sensors revealed that damage to sandwich panels, such as the web and the shell, could be detected within 0.5 m. The Distributed Accelerometer System (DAS) showed potential for modal identification, suggesting improved modal separation with increased ambient excitation. The Active Vibration Monitoring System, utilizing Power Spectral Density (PSD), was found to be sensitive to small damages, enabling the formulation of a damage index to quantify severity and track progression.

Melcher et al. [25] performed an experimental study on a 60-70 m long commercial WTB to study elliptical bi-axial resonance fatigue testing. In their method, they used phase-locked resonant bi-axial excitation with a 1:1 frequency ratio, streamlining the assessment of damage-equivalent load cycles as compared to bi-axial tests involving multiple frequencies. One spring element, two decoupled mass elements, and two hydraulic actuators were used to maintain the 1:1 biaxial frequency ratio. The elliptical bi-axial rotor blade fatigue test, utilizing resonant excitation, effectively simulated realistic loading conditions similar to field scenarios. The validated design model, which integrates transient and harmonic simulations, aligned closely with the experimental results, showcasing the agreement in displacements and loads along the blade.

Castro et al. [26] presented an optimized fatigue testing of WTB using the strain-based damage method experimentally. A linear optimization method was used to determine the optimal mix of different uniaxial and multiaxial test blocks, allowing the attainment of material-based damage across the blade while minimizing the test time duration. The experimental results demonstrated a nearly 50% reduction in the duration of the total testing. The total experimental Equivalent Damage Ratios (EDRs) achieved after conducting the three test blocks within the optimized test was assessed. These findings were presented for various cross-section regions, including the Trailing-Edge (TE), TE panel, Spar Cap (SC), and Leading Edge (LE), on both the Suction Side (SS) and Pressure Side (PS), and at various span-wise locations along the blade.

Flapwise vibration is the dominant vibration in WTB that leads to out-of-plane alternating loads that break the blade when the load exceeds the blade strength limit. Su et al. [27] experimentally studied the areas of fatigue failure of WTB rotating at the fundamental frequency. Strain gauges were used to collect strain data at various locations. To identify

the locations that are vulnerable to fatigue damage, the strain power spectral density amplitude along the spanwise direction was examined. Through accurate identification, the region of the rotating blade that is susceptible to fatigue failure is precisely determined except for the position at 0.10 R (R defines blade radius), the spanwise region of the blade ranges between 0.70-0.75 R is particularly prone to failure. This is attributed to the combination of flapwise bending and vortex excitation coupling, which leads to a higher amplitude in the strain.

Reliability monitoring is possible using Radar sensors with other sensor types. However, there are some limitations that need to be addressed, such as the effect of the environment and operational conditions. In this area Simon et al. [28] presented the design and experimental implementation of a cooperative radar network for blade SHM. During manufacturing 40 Frequency-Modulated Continuous Wave (FMCW) radar sensors operating at 58-63.5 GHZ were installed on a 31 m long WTB. Ten embedded material sensors were installed in the core material of the blade, and the remaining 30 sensors were placed on the inner surface of the rotor blade. Fatigue testing on a full-scale turbine blade with artificial damage such as a hole was performed in the laboratory. It was found that icing is also detected using the same sensors. All of the Radar measurements used in their investigation were made with the rotor blade unloaded. Therefore, the data analysis must take into account both mechanical vibrations and the effects of mechanical stress. Moll et al. [29] studied the radar sensors in WTB which operate in microwave and millimeter wave frequency range, to conduct remote and in-service inspection. Radar sensors were mounted on the wind turbine tower, emitting the electromagnetic waves in the direction of the rotating blade. Their observation revealed successful damage detection in the Glass-Fiber Reinforced Plastics (GFRP) plate and the tip of the blade in the laboratory environment.

Zhang et al. [30] employed highly stable BuckyPaper (BP) sensors to monitor the structural health of a repaired composite blade specimen under fatigue. To check the health monitoring of the specimen, BP sensors were initially calibrated through the quasi-static tensile failure test and graded loading and unloading after which these sensors were used to monitor glass-fiber-reinforced composite specimens through axial-tensile fatigue tests. The sensor results were compared with the actual damage of the specimen and a non-destructive inspection chart revealed comparable results.

Staffa et al. [31] developed and validated a low-cost damage detection sensor in real-time through an experimental investigation using small samples. The system comprises both hardware components and a signal processing algorithm, designed to identify and continuously monitor changes in structural responses caused by the accumulation of damage. The efficacy of the device is substantiated through experimental validation conducted on a basic Y-shaped specimen exposed to fatigue loading. The device is capable of accurately predicting structural damage and giving real-time feedback on the health of the structure. The experimental results revealed promising use for industrial applications.

An experimental study on WTB fatigue involves a systematic investigation to comprehend how these crucial components respond to cyclic loading, simulating the operational stresses they endure during their lifespan. Through a carefully designed testing protocol, the study aims to identify potential failure modes, assess fatigue life, and gain insight into the structural behavior of the blades under various loading conditions. Experimental setups typically include subjecting the turbine blades to repeated loading cycles, monitoring strains, and observing any visible signs of damage. By quantifying the effects of cyclic loading on structural integrity, this experimental approach provides valuable data to validate computational models, optimize blade designs, and ultimately ensure reliable and enduring performance of wind energy systems. The findings of such previous studies contribute significantly to advancing the understanding of fatigue phenomena in WTBs, influencing design improvements and operational strategies in the renewable energy sector. In the next section, we discuss the integration of experimental studies with numerical simulations in the fatigue analysis of WTBs which constitutes a comprehensive approach to understanding and predicting the structural behavior of these critical components.

B. NUMERICAL SIMULATIONS

Experimental studies involve subjecting turbine blades to realistic loading conditions in controlled settings, monitoring responses, and collecting empirical data on fatigue performance. These experimental data become invaluable in the validation of numerical simulation models. Numerical simulations, employing finite element analysis (FEA) or other computational techniques, complement these experiments by providing a platform for predictive modeling under various scenarios. By combining the insights gained from physical testing with the capabilities of numerical simulations, engineers can refine and validate computational models, enhancing their accuracy and reliability. This integrative approach not only strengthens the understanding of fatigue mechanisms, but also enables the development of more robust and optimized WTB designs, which ultimately contributes to the overall efficiency and longevity of wind energy systems.

The assessment of WTB reliability offers two distinct approaches, i.e., deterministic methods and stochastic (probabilistic) methods. International design standards endorse semiprobabilistic approaches, representing an enhancement over deterministic methods. The semiprobabilistic strategy involves examining a range of design load scenarios, conducting short-term numerical simulations on a validated wind turbine model, and using extrapolation techniques to estimate higher load levels for long-term exceedance probabilities [32], [33]. During the design check for the ultimate and fatigue limit states, partial safety factors for loads or materials are applied, considering specific reliability levels.

Calibrated partial safety factors contribute to maintaining a consistent reliability level across structural components subjected to varying load conditions. However, challenges arise, particularly in novel wind turbine technologies, such as offshore Floating Wind Turbines (FWTs), where site-specific parameters, positioning systems, control strategies, and drivetrain technologies introduce uncertainties. Large partial safety factors may lead to less cost-effective designs of WTBs. On the contrary, the probabilistic approach explicitly addresses uncertainties related to loads, materials, and analysis methods, improving the overall design level. This approach, proven effective in various industrial designs, utilizes Structural Reliability Analysis (SRA) to calculate and predict the probability of limit-state violations during a reference period, incorporating stochastic variables into the formulation of limit states regarding ultimate strength, fatigue failure, structural stability, or critical deflection [34].

One noteworthy technique is the utilization of Monte Carlo (MC) simulation, a probabilistic methodology that involves executing numerous simulations with randomized input values to evaluate a spectrum of potential outcomes. Specifically in the realm of wind turbines, applying MC simulations allows modeling of uncertainties related to wind conditions and material properties. This method provides a comprehensive perspective on the reliability of the system in a spectrum of scenarios [33], [35], [36]. Additionally, Weibull analysis proves to be a common practice for scrutinizing the distribution of wind speeds [35]. Engineers leverage this method by fitting a Weibull distribution to the observed wind speed data, thereby estimating the likelihood of various wind speed occurrences. These reliability analysis methods, among others, significantly contribute to the progression of wind turbine technology, ensuring not only optimal performance under anticipated conditions, but also fortifying resilience against unpredictable environmental variables.

In this area, Abdusamad [35] employed a robust approach based on MC simulation to assess the reliability of wind energy systems. The simulation utilizes Weibull distribution to model the wind speed. The study reveals that as the number of simulations increases, there is a slight decrease in the probability of failure, accompanied by a substantial reduction in computational errors and a noticeable increase in run time.

Dao et al. [36] introduced a probabilistic approach to address uncertainty in reliability data by quantitatively estimating parameters from available resources. The study incorporates fuzzy logic to model the uncertainty in failure costs, establishing a connection between a component's failure cost, capital cost, and downtime. The researchers employ a time-sequential MC simulation to replicate the operational sequences of Offshore Wind Turbine (OWT) components. The findings highlight that uncertainties have a more pronounced impact on OWT performance, particularly in databases where component reliability is low. In addition, the study emphasizes that both reliability and cost uncertainties can collectively contribute to variations that exceed 10% in the cost of energy.

Sichani et al. [33] performed the estimation of the probabilities of wind turbine failure using an enhanced Monte Carlo (EMC) method. The proposed method offers distinct advantages over both Peak-Over-Threshold (POT) and Standard Monte Carlo (SMC) techniques, demonstrating superior performance in terms of computational efficiency and accuracy. The SMC method involves generating random samples from a given probability distribution to approximate numerical results, particularly for inteactable integrals. On the contrary, the EMC method incorporates variance reduction methods, importance sampling, stratified sampling, or control variates to improve the efficiency and accuracy of the simulation. The goal of these enhancements is to reduce computational burden and achieve more accurate results by more effectively allocating computational resources. While SMC is a basic and widely used technique, the researchers applied the EMC method to a low-order numerical model representing a 5 MW wind turbine equipped with a pitch controller and subjected to turbulent inflow conditions. The study explored scenarios involving constant rotational speed and variable rotational speed controlled by the pitch controller. The results indicate that the EMC method effectively estimates the failure probabilities of the model, aligning with values relevant to the required 50-year return period of the wind turbine.

Gamma Process Model (GPM) is a stochastic model that particularly well-suited for modeling the degradation and deterioration mechanisms inherent in various materials over time. In the context of structural reliability, Gamma process serves as a versatile framework for capturing the uncertainties associated with complex loading conditions, material properties, and structural responses. By incorporating probabilistic parameters, such as shape and scale parameters, Gamma process facilitates a more comprehensive representation of structural deterioration and failure modes. Researchers and engineers often employ GPM to perform probabilistic assessments, enabling a more accurate prediction of the probability of failure and the remaining structural life. This approach contributes significantly to advancing our understanding of structural reliability and aids in optimizing maintenance strategies to enhance overall safety and longevity of engineering systems. Zhang et al. [37] presented a stochastic deterioration modeling method and a fatigue damage assessment of offshore composite WTBs. NREL 5 MW blade was used to determine fatigue damage and applicability of the stochastic deterioration modeling method. The aerodynamic loads in the wind turbine were determined using the Blade Element Momentum (BEM) method. GPM was used for modeling progressive damage such as wear, fatigue, and corrosion. The results showed that the proposed approach serves as a valuable tool for assessing the performance and evaluating the fatigue damage in composite WTBs operating in harsh offshore wind field environments.

Lee et al. [38] studied the root cause failure of a full-scale WTB of 3 MW during fatigue testing and revealed that the blade failure at its root end. In their study, the blade was modeled as full-scale shell elements and the sub-component as solid elements to perform finite element analysis. They observed that the blade's bumping motion led to a modification in the load distribution at the root end, resulting in an increased load at other locations. This incremental load was a contributing factor to the partial separation of the T-bolt joints, which ultimately led to delamination at the end of the blade root.

Haselbach and Branner [39] investigated the trailing edge failure numerically and experimentally tested on a 34 m long WTB to the ultimate failure. Aeroelastic simulations were conducted to ultimate load failure using HAWC2 software (second generation horizontal axis WTB code). All relevant Design Load Cases (DLC) were computed to predict the design load according to IEC 61400-1. Abaqus software (an FEA solver) was used to discretize the blade geometry having 67000 8-noded double-curve thick shell elements. The adhesive bond line between the upper and lower aerodynamic shells at the trailing edge was simulated using 8-node linear brick elements featuring reduced integration and hourglass control. Various failure criteria were used to identify critical strains, stresses, and progressive damage and failure models. The results showed that the combination of solid elements and shell elements using multi-point constraints leads to a highly accurate prediction of tailing edge failure. The combined loading, which is critical for load directions, subjects the training edge to a compressive load, thereby leading to a deformation-induced blade failure.

Haselbach et al. [40] provided a comprehensive numerical analysis of energy release rates at the tip of a transversely oriented crack on the trailing edge of the 1.5 MW blade. Four ASM Posiwire 6250 draw wire transducers were mounted on the suction-side cap and two more ASM Posiwire 6250 were at the trailing edge to validate optical displacement measurements. Strain gauges were used to validate longitudinal strains glued to the laminate. HAWC2 software was used for aeroelastic simulation to predict the bending moment distribution and forces at the cross-section of the blade for various loads. For both numerically and experimentally, a geometric non-linear longitudinal trailing-edge wave occurs in blades, which were designed to prevent local buckling. These waves can damage the integrity of the adhesive trailing-edge joint.

Lahuerta et al. [41] investigated a sub-component of the blade tailing edge failures attributed to static and fatigue loading, mainly characterized by the edge-wise moment. For the static test, the $3 \times 2 \times 400$ mm blade segment was tested at the 24 m blade station. The experimental and numerical findings were evaluated and explained using criteria related to the strength and stability of the trailing edge. In static tests, a buckling wave was formed along the trailing edge until the point of failure occurred at the trailing edge adhesive joint. The global loading curve response exhibited distinct pre-buckling and post-buckling regions, revealing a non-linear structural response. The blade failed at 2.4 million cycles.

Liu et al. [42] studied the reliability of offshore WTBs with and without the support of the floating foundation. OpenFAST, an open-source engineering tool for simulating the dynamics of wind turbines, was used to determine the motion of the floating wind turbine and the blade was modeled in ANSYS software. Calculations include the probabilities of blade root overload failure, blade root fatigue failure, and excessive blade tip displacement. The blade failure probability for a floating wind turbine was revealed to be higher than for a fixed wind turbine. Different piezoelectric materials on floating WTBs were tested to determine the effect of piezoelectric material on floating blades. It was observed that the blade with piezoelectric materials showed, respectively, a decrease in the stress level at the blade root and blade tip displacement as well as the probability of failure.

Tarfaoui et al. [43] conducted a numerical study of static and fatigue modeling of a NACA 4424 airfoil WTB. The maximum thickness of the blade was taken as 24% of the chord length. The blade was modeled as a hollow structure with thin walls and shell type elements. Aerodynamic load was calculated at each segment using BEM theory. Hashin's criteria assume the occurrence of two distinct fiber and matrix failure modes occurring in two different fracture planes. It was used to evaluate the different modes of failure. The results showed that the blade failure occurred near the hub and spar of the blade.

Bos et al. [44] proposed a new technique consisting of a quadrature rule to determine the fatigue design load of the offshore NREL 5MW blade. The DLC of 1.2 as specified in IEC 61400 standard described the simulation in the regular environment that results in power production of offshore wind turbines. For fatigue testing a DLC value of 1.2 was used. The main advantage of using the implicit quadrature rule is that it has positive weights and can be constructed directly using the environment measurements. This method revealed a good accuracy with less computational time as compared to the standard binning approach.

Liu et al. [45] presented a modified fatigue damage model proposed by Wu and Yao [46] by introducing sine/cosine trigonometric terms to simulate damage progress in a WTB. The 3.4 MW Sinoma 68.6 m long WTB was selected for full fatigue testing to meet the 20-year service life requirement. For fatigue testing, the blade was fixed to a bench through the flange bolts with the tip cut at 61.5 m distance from the root. Instead of line stiffness, bending stiffness is selected as the evaluation standard with the advantage of having stiffness in real-time to avoid additional calibration test. In their simulation, the humidity effect was ignored. It was observed that as the temperature increases, the stiffness of the blade drops. The fatigue damage indexes of the composite under different cycles through the stiffness degradation experiment

was obtained and observed that the modified sine and cosine models have the ability to simulate the damage process with a higher fitting degree than other models.

Castro et al. [47] presented an optimized method for multi axial fatigue testing of WTBs and they applied it to a commercial WTB. The response of the blade was analyzed at the material level by incorporating strain-based damage targets. All regions along this blade were observed to have the damage based on strain and no fatigue or static failure occurred. The total test time was 50% less than the current standard test.

Avendano-Valencia et al. [48] proposed a data-driven model to predict the short-term fatigue Damage Equivalent Loads (DEL) on a wind turbine affected by wake. This model relies on wind field inflow sensors and load sensors deployed on up-wind wind turbines. Gaussian Process Regression (GPR) is a probabilistic model that captures and predicts relationships in data by assigning a distribution over functions [49]. They have used GPR model and calibrated it to effectively predict the loads on a wake affected wind turbines. For the DELs of the blade, the overall prediction error was less than 1%. In the fore and aft direction, the maximum normalized mean squared error for tower base DELs in wake affected zone was nearly 4%.

Shaler et al. [50] presented a sensitivity analysis approach to identify which wind-inflow and wake-related parameters have the greatest influence on fatigue and ultimate loads under normal operations of turbines in a wind farm. A total of 28 parameters were identified which can lead to largest variation of fatigue and ultimate loads. NREL 5 MW blade was considered at normal operating conditions and gusts, start-ups, shutdown, and idling conditions were neglected. The results show that ambient turbulence in primary wind direction and shear are the most important parameters for fatigue and ultimate loads for both waked and non-waked turbines. Yaw misalignment, integral length of the u direction, and the u component of the IEC coherence model also affected fatigue and ultimate loads.

Hu et al. [51] addressed rain-induced fatigue damage in WTB coatings, which requires significant repair and maintenance costs. It introduces an advanced computational framework for analyzing rain erosion-induced fatigue. An extended stochastic rain field simulation model was considered to model the different types of raindrop shapes (flat, spindle, and spherical), sizes, impact angle, and wind speed. A stress interpolation method was used to determine the impact stress of raindrops with effective computational time. The accuracy of the framework was verified against data from the literature. The study demonstrated that by incorporating rainfall statistics, this framework can estimate the fatigue life of the blade coating due to rain erosion effectively.

Moraras et al. [52] studied the variation of the equivalent stress at high stress points of the blade with respect to the applied torque. A finite element analysis was performed on the scalable WTB to determine the locations of high stress values along the blade. Electrotensiometric transducers were strategically placed at various locations on the blade to ascertain both the primary stresses at those specific points and their fluctuations during the torsion test, which were subsequently computed through numerical simulation. The results of the finite element correlated well with the experimental data.

Zhang et al. [53] proposed an RDT-SSI method to estimate the operational frequency of an OWT under ambient excitation using combined Kalman filter, the Random Decrement Technique (RDT), and stochastic subspace identification (SSI) methods. RDT technique used to pick up the free-time-decaying signal of a structure having unknown excitation and SSI estimate the modal properties of large-scale turbine having high noise level. Both combined as RDT-SSI method is used for the identification of modal parameters. RDT-SSI method is easy to implement for field application due to non-requirement of input loads. The accuracy of RDT-SSI method is validated with the experimental study of small-scale OWT. The small-scale OWT was submerged at varying depths to replicate the impact of scouring phenomena. As the embedment depth decreased, the frequency of the OWT also diminished.

Aeroelastic tailoring, that is, Bend-Twist Coupling (BTC), is generally used to reduce the fatigue loading on WTB. Bend-twist coupling suggests that due to bending the blade can also twist. This phenomenon alleviates aerodynamic loads due to a decrease in the angle of attack when the load is suddenly increased. Hayat and Ha [54] used bend-twist coupling to alleviate aerodynamic loads through unbalanced laminate composite. Three kinds of unbalances (i.e. ply angle, ply-material and ply-thickness) were used to get aeroelastic tailoring of a 5 MW WTB. Fully coupled aeroelastic analysis of the 5 MW variable speed and collective-pitch controlled wind turbine rotor blade showed a reduction in fatigue load due to aeroelastic tailoring.

Meng et al. [55] investigated fatigue loads due to the effect of BTC under different wake conditions using the stress-based method. An anisotropic 1-D beam model was used in aeroelastic simulation. Static and dynamic analyses were performed to verify the anisotropic beam model for the NREL 5MW WTB with different fiber angle orientations. The study suggests that the predicted life of NREL 5MW is in close agreement with the design life.

During the flap-wise fatigue test, a large aerodynamic drag was experienced on the WTB. To mitigate this, a drag reducer was installed along the outboard blade. However, this caused an increased torsion that creates an extra twist deformation along the blade, which was unfavorable to the normal conduction of the testing. To tackle this problem, Guangxing et al. [56] proposed a shuttle-shaped airfoil design in WTBs to reduce the drag. A highly efficient aero-structure integrated numerical method was utilized to construct an optimization design framework. An optimal

airfoil was designed at NREL 60 m blade to reduce the drag. The results obtained indicated that using the shuttle airfoil the drag coefficient reduced by 25% compared to the ellipse airfoil. This design helps to meet the target testing loads, thereby, improving the excitation motor efficiency and reducing the power consumption.

Peng et al. [57] developed a multi-scale modeling method for a jacket-type offshore wind turbine. The local joints of the jacket were modeled using solid elements and other components as beam elements. Equivalent Mises and Lemaitre methods were used to analyze the multi-axial fatigue damage utilizing the multiaxial S-N curve to account for the multiaxial stress conditions in the local joint. The multiaxial S-N curve considers the influence of varying stress directions, providing information on the durability of a material. This curve is crucial for designing components exposed to multiaxial loading in diverse applications. It was revealed that the tubular joint of the jacket leg and brace connections can be effectively represented using the multi-scale methods which yields a 15% difference in the degree of uniaxial fatigue damage. Using multi-scale finite element model, uniaxial and multiaxial fatigue comparison showed a difference of about 15%. For better accuracy, multi-scale finite element model can be used for multiaxial fatigue analysis of the jacket-type offshore wind turbines.

In summary, static and fatigue testing play pivotal roles in evaluating the structural integrity and performance of WTBs, crucial components of wind energy systems. Static testing involves subjecting the blades to controlled loads to assess their strength, stiffness, and deformation characteristics under various conditions. However, fatigue testing simulates the cyclic load that WTBs experience throughout their operational life, helping to identify potential fatigue failures and ensuring long-term reliability. Experimental studies involve subjecting turbine blades to controlled loading conditions, collecting empirical data on fatigue performance, and validating numerical simulation models. Numerical simulations, employing advanced FEA and predicting the aerodynamic loads based on different methods such as computational fluid dynamics, blade element momentum method, and complement experimental findings by predicting the structural and aerodynamic performance under different operating conditions. Innovative approaches include bend-twist coupling for fatigue load reduction and drag reduction through shuttle-shaped airfoil design. The reliability of WTBs is a critical factor that influences the overall efficiency and safety of wind energy systems. Robust reliability assessments consider factors such as material properties, manufacturing variability, and environmental conditions to ensure that the blades can withstand the complex and dynamic forces encountered during their operational lifespan. Probabilistic methods such as MC, EMC, and GPM predicts the failure of WTBs. These advances contribute to optimizing WTB designs, enhancing their reliability, and ensuring efficient, durable performance in the evolving field of wind energy technology.

Table 2 presents the comparison of various studies based on different NDT techniques, loading, sensors, software, and WTB length. The table containing the acronyms listed in Table 2 can be found in Table 3.

IV. WTB INSPECTION METHODS

The monitoring process for the health of WTBs is primarily focused on early detection of blade damage, thereby identifying potential safety risks promptly. This approach is imperative to avert severe and catastrophic failures and ensure the uninterrupted, safe, and efficient operation of wind turbines. Performing periodic maintenance on identified faults and potential safety hazards can substantially mitigate operational and maintenance costs, minimize downtime, improve power generation efficiency, and reduce economic losses.

SHM of WTBs is regularly carried out using quality control during manufacturing and in-service inspections to detect various kinds of damage. NDT methods serve as valuable techniques for detecting, assessing, and monitoring these blades without requiring the dismantling of the structure or causing harm to the materials being tested. These NDT processes often include specialized applications tailored to test and evaluate composite materials to produce reliable data.

NDT techniques on WTBs can be performed using sensors or a visual inspection. Visual inspection can spot obvious deterioration or significant fissures. However, cutting-edge sensor technology is relied on to evaluate elements such as fracture propagation, inherent damage, or delamination. SG sensors measure the expansion or contraction of the material, which is directly related to the amount of strain or stress experienced by that material. Accelerometer sensors are used to measure the dynamic response of the blade. Advances in technology have led to the development of modern emerging sensors capable of detecting damage in ways that were not possible with traditional strain gauges and accelerometers. Technologies such as optical fiber, AE, pezoelectric lead zirconate titanium (PZT), macro-fiber composites (MFC), scanning laser Doppler spectroscopy (SLDV), and radio detection and range (RADAR) sensors are employed to measure inherent blade damage based on different NDT techniques.

There are a spectrum of methods to detect structural and material damage to WTBs, including strain, acoustic emission, ultrasonic, vibration, thermal imaging, and machine vision monitoring. This section provides a comprehensive review of the principles of each monitoring technique and discusses ongoing advances in research in these areas. A detailed analysis will be conducted on the merits and drawbacks of each of these monitoring techniques, offering a more nuanced understanding of their applicative value and limitations.

The integration of remote sensing technologies, particularly drones equipped with high-resolution cameras and specialized sensors, has revolutionized the inspection process.

TABLE 2. Comparison of techniques, analysis methods, and sensors for WTB Testing.

Authors	Study	Sensor	Technique/ Software	Testing	Axial Loading	Damage Types	Detection	Blade length	Scale
Yang et al. (2013) [13]	Exp	SG	Videometric	Static	Uni	DB	Local	40m	Full
Chen et al. (2014) [15]	Exp	SG, DWDT	N/A	Static	N/A	DL, DB, LF	Point	52.3m	Full
Fagan et al. (2017) [14]	Exp, Num	SG	GA	Static	N/A	N/A	Point, Local	13m	Full
Melcher et al. (2007) [25]	Exp	SG	Phase-locked	Fatigue	Uni, Multi	DL	Global	60m	Full
Desmond et al. (2015) [21]	Exp	AE	N/A	Static, Fatigue	Uni	Crack, DL, LF	Point	8.3m	Full
Lee and Park (2017) [20]	Exp	N/A	N/A	Static, Fatigue	Uni	DB, DL	N/A	48.3m	Full
Chen (2019) [23]	Exp	SG, DWDT	N/A	Static, Fatigue	Uni	Fatigue Deg	Point	47m	Full
Gage et al. (2021) [16]	Exp	SG, ACC	N/A	Static, Fatigue	Uni	N/A	Point	13m	Full
Fremmel et al. (2022) [24]	Exp	SG, Acc, Vibration	N/A	Fatigue	N/A	Crack, DL	Local, Point	52m	Full
Zhang et al. (2022) [30]	Exp	BP	N/A	Static, Fatigue	N/A	DB, Crack, DL	Local	N/A	Sub-component
Castro et al. (2022) [26]	Exp	SG	N/A	Fatigue	Uni, Multi	Fatigue Deg	local	14.3m	Full
Su et al. (2023) [27]	Exp	SG, Acc	N/A	Static, Fatigue	N/A	N/A	Local, Global	0.7m	Full
Hughes and Stensland (1999) [58]	Exp, Num	SG	BSTRAIN Software	Fatigue	Uni, Bi	N/A	Point	12m	Small
Lee et al. (2015) [38]	Exp, Num	SG	N/A	Fatigue	Bi	DL	Global	56m	Full
Haselbach and Branner (2016) [39], Haselbach et al. [40]	Exp, Num	DWDT, FBG, SP	HAWC2	Fatigue	Uni	DB	Point, Local	34m	Full
Lahuerta et al. (2018) [41]	Exp, Num	SG	N/A	Static, Fatigue	Uni	DB, Buck	Local	24m	Sub-component
Liu et al. (2019) [42]	Num	Piezo material	OpenFast, ANSYS	Fatigue	N/A	N/A	Global	61.5m	Full
Tarfaoui et al. (2019) [43]	Num	N/A	N/A	Static, Fatigue	N/A	N/A	Global	50m	Full
Bos et al. (2020) [44]	Num	N/A	Quadrature Technique	Fatigue	N/A	N/A	Global	61.5m	Full
Liu et al. (2020) [45]	Num	N/A	Cos/ Sin Trignometric Term	Fatigue	N/A	Stiff Deg	Global	68.6m	Full
Castro et al. (2021) [47]	Num	N/A	N/A	Static, Fatigue	Uni, Multi	Fatigue Deg	Local	14.3m	Full
Avendano-Valencia et al. (2021) [48]	Num	N/A	DEL	Fatigue	N/A	N/A	Local	61.5m	Full
Shaler et al. (2021) [50]	Num	N/A	N/A	Fatigue	N/A	N/A	Global	61.5m	Full
Zhang et al. (2021) [37]	Num	N/A	GPM	Fatigue	N/A	N/A	Global	61.5m	Full
Hu et al. (2021) [51]	Num	N/A	Abaqus	Fatigue	N/A	Fatigue Deg, Erosion	Global	100m	Sub-component
Moraras et al. (2022) [52]	Exp, Num	SG	N/A	Fatigue	Uni	N/A	Local	1.75m	Full, Sub-component
Zhang et al. (2022) [53]	Num	N/A	RDT-SSI Method	Fatigue	N/A	N/A	Local	60 cm	Small
Simon et al. (2023) [28]	Exp	Radar Sensor	N/A	Fatigue	Uni	Crack	Local, Global	31m	Full

These aerial vehicles capture detailed images and data, allowing comprehensive analysis of blade conditions from a safe distance. Advanced sensors on drones, such as infrared thermography and Light Detection And Ranging (LiDAR),

TABLE 3. List of acronyms used in Table 2.

Acronym	Full Term
ACC	Accelerometer
AE	Acoustic Emission
Buck	Buckling
BP	BuckyPaper
DB	Adhesive Joint Debond
Deg	Degradation
DEL	Damage Equivalent Load
DL	Delamination
DWDT	Draw-Wire Displacement Transducer
Exp	Experimentnal
FBG	Fiber Bragg Grating
HAWC2	Horizontal Axis Wind turbine simulation Code 2nd generation
Multi	Multiaxial loading
Num	Numerical
SG	Strain Gauge
SP	Stereophotogrammetry.
Uni	Uniaxial loading

enhance their capability to detect subtle and hidden defects.

In parallel, physical sensor technologies installed directly on the turbine blades or components provide real-time data on the structural integrity and performance of the wind turbines. Strain gauges, accelerometers, and emerging technologies such as fiber Bragg Grating (FBG) sensors and piezoelectric sensors for the detection of acoustic emission are crucial in this domain.

Despite these advances, there remain challenges in integrating these technologies into a cohesive system that can provide accurate and reliable data under diverse environmental conditions. Developing intelligent algorithms capable of automatically analyzing sensor data and identifying defects with high accuracy is essential for the future of autonomous wind turbine monitoring. The continuous evolution of these technologies promises to enhance the efficiency and safety of wind turbine operations, making renewable energy more reliable and sustainable.

A. STRAIN DETECTION

Strain Monitoring of WTBs is an established and cost-effective technology used to monitor blade deformation under operational conditions. When blades are subjected to external forces, they tend to deform. Exceeding historical deformation thresholds at any local position on the blade can indicate potential damage. Strain sensors, which are adept at detecting minor changes in blade deformation, are crucial to monitoring blade fatigue, stress concentrations, and damage.

Two primary types of strain monitoring sensors are deployed for WTBs: resistance strain gauges and Fiber Bragg Grating (FBG) sensors. Resistance strain gauges consist of a thin metal foil patterned on a plastic film base. The deformation of the blade translates into this gauge, altering the electric resistance, which is then measured and converted into strain values for effective monitoring.

Strain measurements, using physical sensors either affixed to or embedded within the WTB's surface, are essential for gauging deformation, whether tension or compression. This method enables continuous local strain monitoring, though accurate sensor placement is critical for reliable detection. Typically, multiple sensors are placed near critical areas to increase sensitivity. Electrical strain gauges, based on the principle of changing electrical parameters, come in various types, including resistance, capacitance, inductance, and semiconductor technologies [59]. For smaller WTBs, systems that use modal analysis, wireless networks, and strain gauge sensors have been developed for deflection monitoring [19]. Traditional strain gauges, when properly installed, offer a cost-effective means of detecting discontinuities in WTBs, providing favorable frequency responses and a wide measurement range. However, they have limitations in pinpointing damage accurately due to their distance from the affected area and are susceptible to environmental interference, especially temperature fluctuations. These sensors also limit the surface area available for strain measurement and are not particularly robust for prolonged installations. Figure 7 illustrates a strain gauge sensor placed on a cantilever beam [60].

FBG sensors, made of Bragg grating glass fibers, are highly sensitive to changes in strain or stress concentrations in the blade. Embedded in the blade structure, alterations in the blade's state due to strain or stress result in changes in the optical characteristics of the sensor, enabling precise damage monitoring with minimal signal attenuation or change. The sensitivity and precision of this method make it invaluable for the detection and monitoring of preventive damage to WTBs, as shown in Figure 8.

Originally used in telecommunications, optical fiber sensors are resilient against electromagnetic and radio interference and have inherent immunity to lightning strikes, common in WTB environments. They are also cost-effective and lightweight. These sensors are categorized into intensity-based sensors, phase-modulated sensors (interferometers), and wavelength-based sensors. FBG and optical fiber microbend displacement sensors are employed to detect damage in WTBs. Optical fiber sensors function by exploiting changes in light transmission properties within the fiber as the blade experiences strain or deformation. These alterations are precisely measured to detect stress, damage, or structural integrity, providing critical feedback for turbine performance and safety. Research in this area includes the work of Tian et al. [62], who developed a non-baseline damage detection method based on FBG in a WTB. Sierra-Perez et al. [63] identified nonlinear damage in a 13.5-meter blade using strain measurements and a pattern recognition technique. Wen et al. [64] investigated the feasibility of detecting damage in floating wind turbines using FBG sensors and a Fiber Optical Rotary Joint (FORJ) in wave basin tests, suggesting that FBG sensors consistently delivered reliable responses.

B. ACOUSTIC EMISSION DETECTION

Acoustic emission is a passive online detection method that uses sensors to collect transient elastic waves emitted from

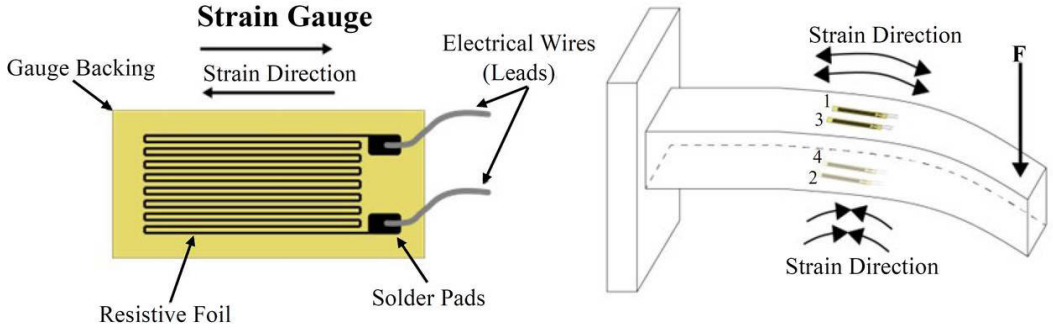

FIGURE 7. Strain gauge sensor [60].

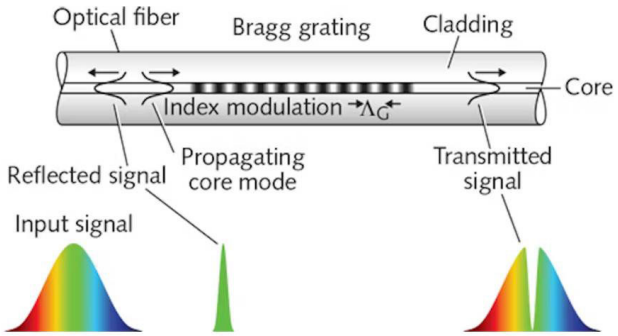

FIGURE 8. Basic principle of Fiber Bragg Grating (FBG) sensing [61].

the blade structure and materials. These waves can be caused by blade damage such as defects in a composite material, including matrix microcracking, fiber-matrix debonding, localized delamination, fiber pull-out, and breakage. Unlike other NDT techniques, acoustic emission stands out due to two key characteristics: (1) The signal's source, namely the ''sound'' produced by the released energy within an object, and (2) Its sensitivity to dynamic processes within a material, allowing detection in both static and evolving defects [65]. Acoustic emission detection is very sensitive and can detect waves much smaller than normal sound. Sensor data can be used to extract damage-related information such as rise time, duration, counting, energy, peak amplitude, and peak frequency as shown in Figure 9. This information can be used to monitor blade damage events, such as fatigue, stiffness, and cracks in turbine blades. At Sandia National Laboratories, two NDT techniques, namely acoustic emission and coherent optical, have been employed [66]. The acoustic emission technique monitors the sound energy generated by the loaded blade, while the coherent optical method is utilized as well. Experimental results indicate that both techniques effectively locate and monitor high-damage regions and flaws within the blade structure. Jungert [67] investigated two distinct acoustic techniques for the detection of damage in WTBs. The impulse-echo method is employed to detect regions of the blade that are either missing or in contact with each other, from the outer surface of the blade.

C. VISUAL INSPECTION USING RGB CAMERAS

Wind turbines play a crucial role in the global shift toward renewable energy, highlighting the need for effective maintenance strategies. Among the various methods employed, visual inspection of WTBs using RGB cameras stands out for its efficacy and technological advancement. This section examines the evolution of WTB visual inspection methodologies, highlighting the integration of cutting-edge technologies and innovative approaches. Exploration includes data-driven frameworks, advanced deep learning techniques, and the utilization of drones equipped with RGB cameras for high-resolution imaging. The focus extends to pioneering techniques in Convolutional Neural Networks (CNNs) for precise crack detection and the adoption of models such as You Only Look Once (YOLO) for improved defect identification. Furthermore, it examines the efficacy of various CNN architectures and anomaly detection methods in identifying surface damage on WTBs. The collective findings and developments discussed in this section underscore the significance of refined and automated visual inspection processes, which are crucial for the maintenance and long-term sustainability of wind energy infrastructure.

Wang and Zhang [69] focused on a novel approach to detect cracks in WTBs using drone-captured images, with a particular emphasis on the utilization of extended Haar-like features. This advanced feature set, a key element of their data-driven framework, significantly enhances crack detection capabilities. The extended Haar-like features, depicted in Figure 10, offer a more comprehensive and effective representation of the pattern compared to the original Haar-like features, as shown in parts (a) and (b) of Figure 10, respectively. These extended features achieve a higher detection rate (DR) of 97.1% and a notably lower false alarm rate (FR) of 1%, surpassing the original feature set's 80% DR and 5% FR. Integrated into an extended cascading classifier [70], these features outperform those derived from a LogitBoost-based classifier [71] in terms of DR, FR, and training efficiency. The effectiveness of this framework is corroborated through testing with drone-acquired images from a commercial wind farm, demonstrating its potential for real-time or near real-time applications.

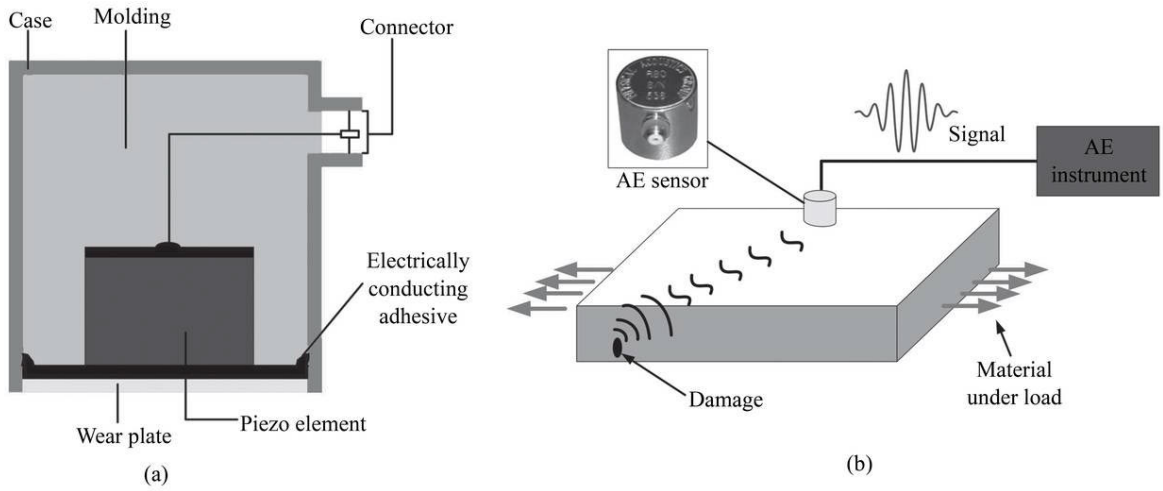

FIGURE 9. Acoustic emission technique (a) Structure of AE sensor (b) Damage identifying using AE sensor [68].

Moreno et al. [72] investigated the effectiveness of deep learning, particularly using a CNN, to improve image classification. The CNN is tailored for classifying various types of damage in WTBs from drone-captured images. This architecture includes convolutional layers, batch normalization, Rectified Linear Unit (ReLU) activation, and max pooling, culminating in a fully-connected and softmax classification layer. The model demonstrates high accuracy (92%) in classifying 10,000 images across 10 classes, surpassing other techniques. Its real-time damage identification capability, such as detecting lightning impact and wear, significantly advances wind turbine maintenance efficiency. However, the model's performance dips in low-light conditions, indicating a need for future enhancements in such scenarios.

Peng and Liu [73] presented a method to detect and analyze cracks on large-scale WTB surfaces using images captured by drones. The method involves image acquisition, pre-processing, and analysis steps to enhance crack detection accuracy and subsequently reduce operational costs. Traditional methods for monitoring WTBs are cumbersome and costly. The proposed drone-based approach addresses these challenges, leveraging real-time image transmission from a camera-equipped quadrotor drone. They utilized a quadrotor drone, shown in Figure 11, equipped with a camera for real-time image capture. Pre-processing techniques, including Wiener filtering [74], adaptive median filtering [75], and mathematical morphology [76], are applied to improve image clarity and emphasize crack details. The focus of the method is on analyzing grayscale values of crack images to study crack distribution, severity, and development trends. The advantages of using aerial images include improved worker safety, increased inspection efficiency, reduced blind areas in detection, and avoidance of interference from sensors. The proposed method outperforms traditional techniques by incorporating image restoration and noise reduction techniques [77], using mathematical algorithms to enhance image quality, and utilizing grayscale analysis [78] to provide valuable information for maintenance decisions.

Wang et al. [79] introduced a two-stage data-driven approach to detect cracks on WTBs using image analysis. The approach involves identifying crack locations and contours. Figure 12 illustrates this process, showcasing (a) the identified crack locations and (b) the detailed crack contours. The crack location is achieved through a parallel sliding window method and an extended cascading classifier. Crack contour detection employs a parallel Jaya K-means algorithm to segment crack windows and pinpoint crack contours [80]. The article emphasizes the importance of monitoring WTB health for efficient wind farm operation and discusses challenges related to inspecting blades using drones. The effectiveness of the proposed approach is validated through drone-taken images from a commercial wind farm. Challenges in inspecting WTBs using drones include handling image analysis, object detection, crack identification, broad area coverage, and safety concerns. The two-stage approach involves a parallel sliding window method and an extended cascading classifier for crack location, followed by a parallel Jaya K-means algorithm for accurate crack contour detection. The benefits of using the parallel Jaya K-means algorithm include efficient parallel processing, improved accuracy in segmenting cracks, precise boundary identification for contour extraction, and better computational performance on both high-end PCs and embedded devices such as Raspberry Pi.

Denhof et al. [81] discussed the utilization of CNNs for automating the optical surface inspection of wind turbine rotor blades. The challenges in this inspection process are highlighted, including environmental stress, effort, costs, and manual inspection limitations. The need for automation to enhance efficiency and reduce costs is emphasized. The approach involves capturing image data of rotor blades from multiple angles using a Digital Single-Lens Reflex (DSLR) camera and training CNN models using pre-trained

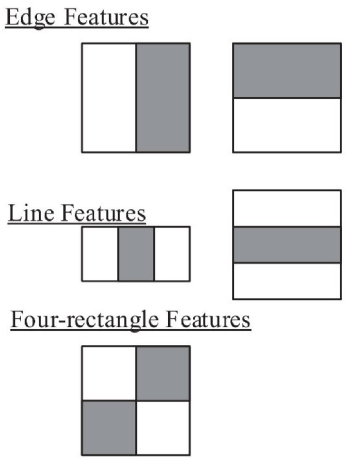

(a) Original Haar-like features.

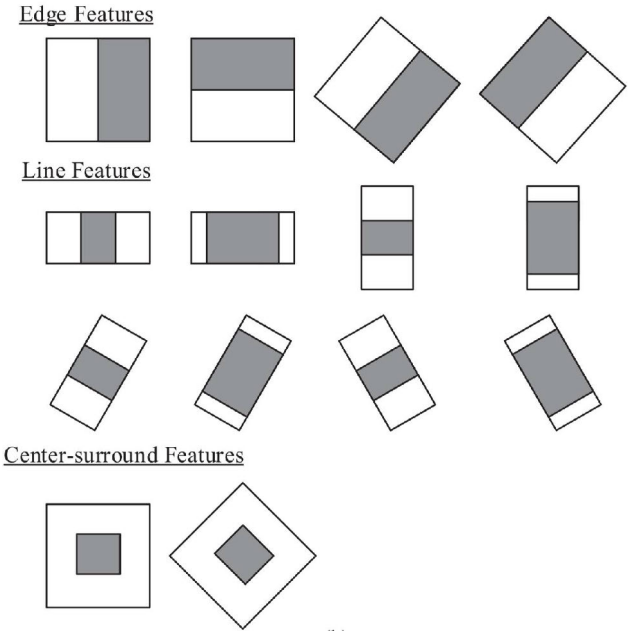

(b) Extended Haar-like features.

FIGURE 10. Two Haar-like feature sets; original Haar-like features and Extended Haar-like features [69].

FIGURE 11. Image of the drone quadrotor [73].

architectures including ResNet50 [82], DenseNet201 [83], Xception [84], and VGG19. These models learn to detect defects in the rotor blade surface and eliminate the need for manual inspection. Factors influencing model selection and hyperparameter tuning are outlined, considering hardware capabilities, training data amount, and pre-trained model performance. The article evaluates the performance of these nine common pre-trained CNN models using a 5-fold cross-validation scheme [85]. The top-performing model, ResNet50, achieved median accuracies of 97.4% and 93.8% for 8024 and 1604 samples, respectively. DenseNet169 and DenseNet201 also performed well. VGG16 demonstrated a median accuracy of 97.0%. While other models had slightly lower median accuracies, ResNet50 stood out due to its balanced trade-off between classification performance and runtime.

Qiu et al. [86] introduced the YOLO-based Small Object Detection Approach (YSODA) for automatically inspecting visual defects in WTBs. YSODA, integrating a CNN with YOLO model, specifically targets small defects such as cracks, oil pollution, and sand inclusion. The system, utilizing YOLO-V3 architecture and a multiscale feature pyramid, achieves a notable detection accuracy of 91.3% for these defects. Validated with 23,807 labeled images, YSODA demonstrated superior accuracy and robustness compared to existing methods, offering improved detection, real-time capability, adaptability, and overfitting prevention.

The bounding box decision process is depicted in Figure 13, illustrating the stages of original image presentation, division into a 13×13 grid, and defect detection results. This process highlights how the image segmentation leads to precise defect identification.

YSODA's effectiveness in detecting small-scale blade damages is visually exemplified in Figure 14, where comparisons between the original image, YOLO-v3, and YSODA results underline YSODA's superior damage detection capabilities.

Guo et al. [87] presented a vision-based approach for WTB tip detection and positioning using drone-based automatic inspection. The method employs Mask Region-based CNN (Mask R-CNN) [88] for wind turbine structure detection and shape constraints to accurately extract the pixel coordinates of the blade tip. Mask R-CNN is a deep learning model used for various computer vision tasks, particularly instance segmentation, which involves not only identifying objects in an image, but also precisely delineating their boundaries by generating pixel-wise masks. This information is then used to solve the Perspective-n-Point (PnP) problem [89] to obtain GPS coordinates for blade tips, aiding path-planning during inspections. The proposed approach is evaluated on a Wind Turbine Detection (WTD) dataset, with Mask R-CNN achieving the highest average precision of 0.989 and the lowest average blade tip extraction error of 2.27 pixels among tested network architectures, including Cascade R-CNN, Faster R-CNN, and RetinaNet. The results highlight the effectiveness of the method for blade tip detection, with potential benefits for reducing maintenance costs, improving power generation efficiency, and enhancing safety in wind turbine operations.

Figure 15 compares the performance between Horizontal Bounding Box (HBB) and Rotation Bounding Box (RBB) methods for detecting blade tips in wind turbine images. The comparison highlights the advantages of using RBB over HBB, particularly in capturing the shape and orientation of

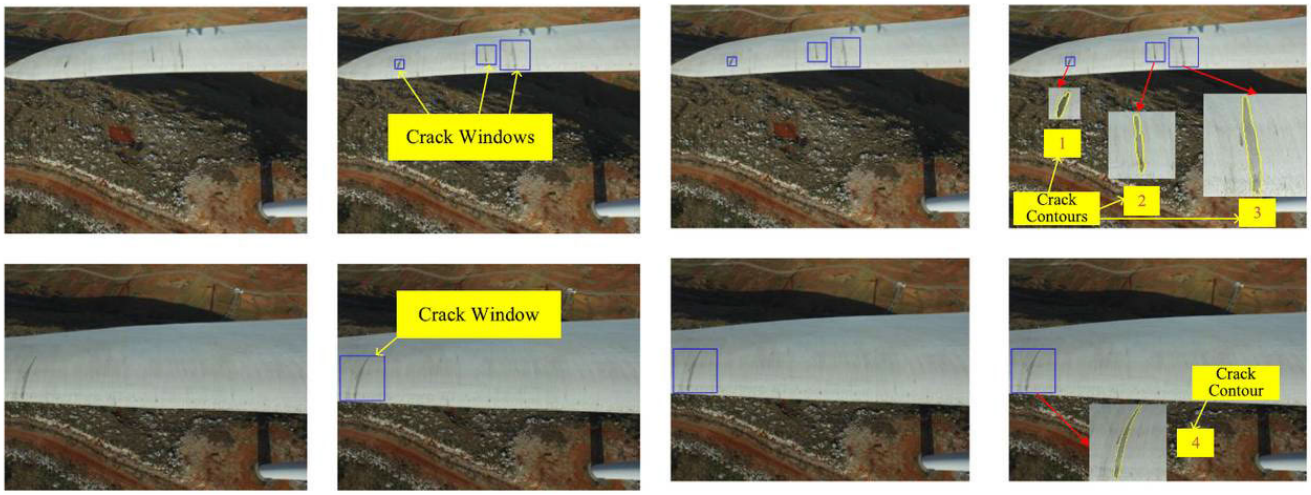

FIGURE 12. Crack contour detection results [79].

FIGURE 13. The bounding box decision process for an input image [86].

the blades more accurately. This is crucial due to the rotation characteristics of the blades, which makes HBB less effective in representing their actual shape and position. The figure visually demonstrates how RBB better fits the blade shape, enhancing detection accuracy.

Reddy et al. [90] utilized a dataset comprising WTB images captured by drones. The original images had dimensions of 3264 × 2448 pixels, but for efficient CNN model training, they were sliced into 16 smaller sections, each of 544 × 408 pixels. For binary classification, the dataset included 675 damaged images labeled as faulty data and 1,000 images categorized as non-faulty data. For multiple class classification, images were sorted based on the type of damage. Data augmentation was implemented using parameters such as shearing, zoom, and horizontal flip via Keras's ImageDataGenerator module [91]. The CNN models consisted of three convolutional layers, with parameters defined for filters, input image size, activation units, and max pooling size. The binary classification model underwent training for 200 epochs. Outcomes showed a binary classification accuracy of 94.94% over 200 epochs and a multiple class classification accuracy of 90.6% over 150 epochs. The evaluation tools included accuracy and loss curves along with a confusion matrix.

Figure 16 showcases different types of detection using a sliding window technique for WTB Structural Health Monitoring (SHM). The sub-figures are described as follows:

- Figure 16 (a) Detection of Side Erosion by Window: Highlights the detection of side erosion on a WTB using a sliding window approach. The window slides across the image, identifying regions with side erosion.
- Figure 16 (b) Detection of Tip Open by Window: Illustrates the detection of a tip open condition on a WTB using the sliding window technique. The window moves across the image, marking areas where the tip of the blade is open or damaged.
- Figure 16 (c) Mechanical Damage Detection: Demonstrates the detection of mechanical damage on a WTB using the sliding window method. The window scans the image, pinpointing sections showing signs of mechanical damage.
- Figure 16 (d) WTB Tube Crack Detection: Depicts the detection of cracks in the WTB tube using the sliding window technique. The window traverses the image, identifying regions with cracks in the WTB tube.
- Figure 16 (e) Blade Crack Detection by Sliding Window: Showcases the detection of cracks on a WTB using the

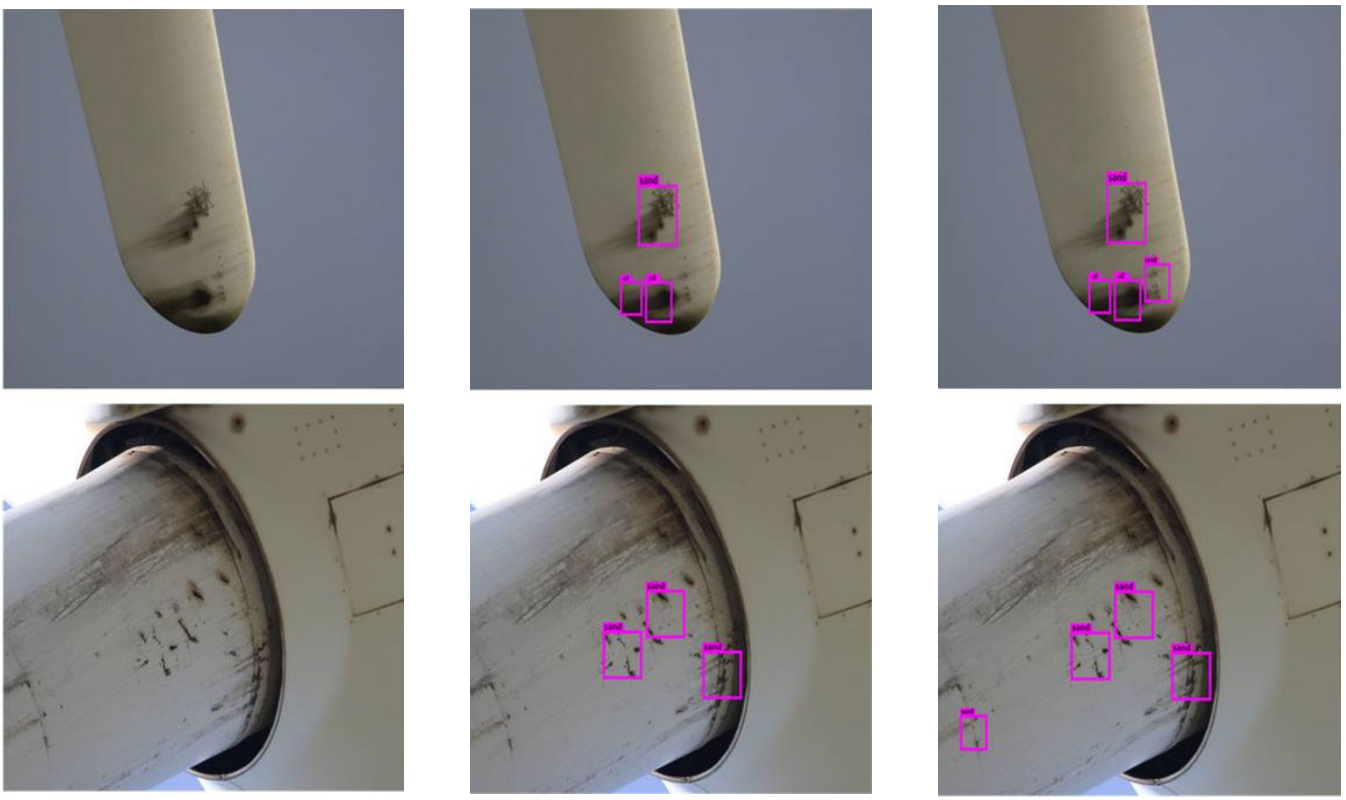

(a) Original (b) YOLOv3 (c) YSODA

FIGURE 14. Showcasing small damages on blades detected by YOLO-v3 and YSODA [86].

FIGURE 15. The performance between HBB and RBB [87].

sliding window approach. The window scans the image, identifying areas with blade cracks.

These images highlight the effectiveness of the sliding window technique in identifying specific types of damage on WTBs by systematically analyzing different areas of the image.

Wang et al. [92] introduced an unsupervised anomaly detection method for WTB images captured by drones. This technique integrates the One-Class Support Vector Machine (OCSVM) with deep features from a generic image dataset. The images are subsampled and undergo feature extraction using the VGG-16 model, after which they are dimensionally compressed with Principle Component Analysis (PCA) [93] depicted in Figure 17.

VGG stands for Visual Geometry Group designed by a research group at the University of Oxford that made significant contributions to the field of computer vision, particularly in the development of deep CNNs for image classification and object recognition.

Experiments demonstrate that deep features, specifically those from the lower layers of the network, excel in spotting anomalies in the blade images. The drone-captured images were tested using different features: Convolutional Autoencoder (CAE), Histogram of Oriented Gradients (HOG) [94], and VGG-16 layers combined with PCA. Performance metrics reveal that the VGG16 layer1 + PCA achieved the highest precision (0.630), recall (0.496), and F1 score (0.555). Despite its efficiency, the method sometimes misclassifies dirt and stains as anomalies. The research concludes that using OCSVM with deep features effectively detects anomalies in blade images, suggesting potential for combining this approach with supervised learning in future studies.

Shihavuddin et al. [95] focused on a deep learning-based automated method for detecting surface damages on WTBs using drone inspection images to reduce human intervention and enhance accuracy in damage detection. It employs various CNN architectures along with augmentation techniques including regular, pyramid, and patching [96] to enhance training sample variability. Mean Average Precision (mAP) [97] was used for performance evaluation, and results indicate that the combination of deeper architectures and augmentations produces higher mAP percentages. The proposed system achieves a precision of 81.10%, nearly

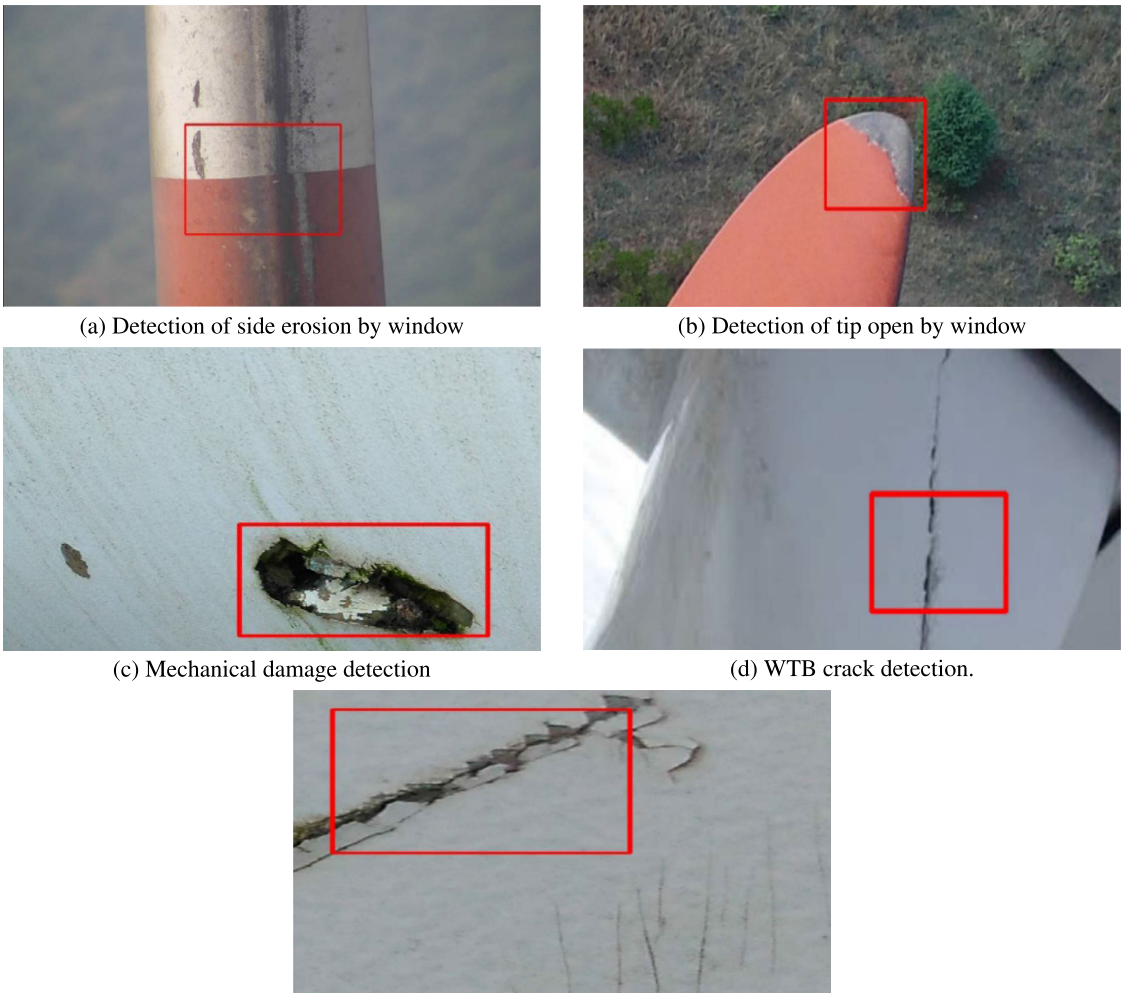

(a) Detection of side erosion by window

(b) Detection of tip open by window

(c) Mechanical damage detection

(d) WTB crack detection.

(e) Blade crack detection

FIGURE 16. Types of detection [90].

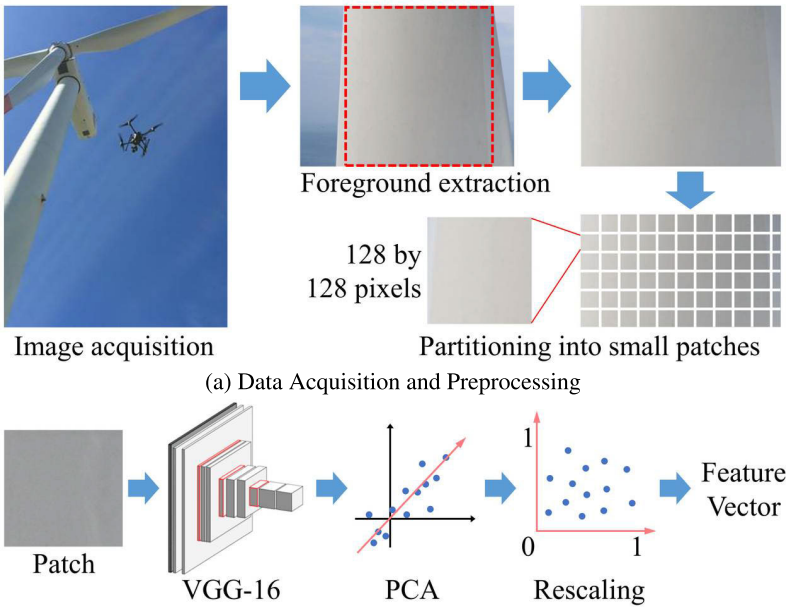

(a) Data Acquisition and Preprocessing

(b) Feature Extraction Process

FIGURE 17. Unsupervised anomaly detection with compact deep features [92].

matching human-level precision, while reducing processing time and improving accuracy compared to manual analysis. Continuous learning with human corrections is emphasized for further accuracy enhancement. The study demonstrated the effectiveness of the automated method for cost-efficient and accurate WTB damage detection. The automated damage suggestion system is depicted in Figure 18, which utilizes drone inspection images and augmentation techniques to enhance the training dataset. A deep learning model with the Faster R-CNN object detection framework is trained using these images to detect and classify damages. The system suggests the presence and location of damages on new inspection images, reducing the effort and time required for human experts. The suggestions can be verified and refined by experts, improving the trained model over time. Overall, the system aims to enhance the efficiency and accuracy of WTB inspection [95].

Yu et al. [98] introduced a novel approach for identifying defects in WTBs using Defect Semantic Features (DSF) [99], extracted with a DCNN [100]. DSF refers to the specific features that characterize defects, and DCNN, a type of artificial neural network, is adept at processing data with a grid-like topology, such as images. The DCNN employed in this study is trained on the ImageNet dataset [101], where it functions as a transfer feature extractor. This methodology aims to address current challenges in the field, notably the scarcity of labeled defect images and significant variations in blade defects. These issues are inadequately addressed by traditional methods such as Histograms of Oriented Gradients (HOG) [94], Scale-Invariant Feature Transform (SIFT) [102], Tamura Texture [103], and Local Binary Patterns (LBP) [104]. Experiments conducted on a dataset comprising 73 defective and 98 normal WTB images demonstrated the superior performance of this approach, especially for configurations named DSF-LC and DSF-PC, which achieved an impressive accuracy rate of 99.17%. In contrast, the DSF-RC configuration showed a lower accuracy rate of 25%, underscoring the effectiveness of specific configurations in the proposed method for defect identification.

Yang et al. [105] explored the application of deep learning algorithms, specifically ResNet50 [82] and AlexNet [106], in identifying surface damage on WTBs using drone-based machine vision. The architectures of these models are illustrated in Figure 19, with AlexNet depicted in Figure 19 (a) and ResNet50 in Figure 19 (b). The study utilized a dataset comprising images from 20 types of WTBs, classifying them into five categories: normal class, crack damage, sand-hole damage, mix-damage, and Background Class. In terms of performance, ResNet50 outperformed AlexNet, achieving a classification accuracy of 95.58% as opposed to 94.19% by AlexNet. The research underscored the advantages of employing drone-based machine vision for this purpose, noting improvements in accessibility, efficiency, image resolution, and safety compared to conventional manual inspection methods.

Mao et al. [107] introduced CAD Cascade R-CNN [108], a specialized model for detecting surface defects on WTBs. The model builds on Cascade R-CNN and incorporates techniques such as transfer learning [109], deformable convolution [110], and deformable Region of Interest (RoI) align for enhanced performance. ResNet-101 serves as the feature extraction backbone, and an improved bisecting k-means algorithm is used for reducing false positives. Performance is evaluated using mean Average Precision (mAP), with the model achieving a peak mAP of 92.1%. The dataset comprises over 3000 images and videos captured from different wind fields in China using an M200 drone equipped with a Z30 PTZ camera (Figure 20). The model outperforms existing approaches such as Faster R-CNN [111] and Mask R-CNN, setting the stage for future work in extending its capabilities to other defect types (Figure 21).

Guo et al [112] presented a hierarchical framework for WTB damage identification that combines Haar-AdaBoost [113] for region proposal and a DCNN for classification. Tested on a dataset of 725 blade images from Chinese wind farms, the model achieved an accuracy of 97%, outperforming VGG16 at 91% and the best-performing SVM [114] model at 88%. It also excelled in recall rates, ranging from 87% to 93% for different types of defects. The framework not only showed superior performance but also proved to be more computationally efficient compared to existing methods such as SVM and VGG16.

Deng et al. [115] introduced an innovative defect detection method for WTBs using digital image processing. This method combines an improved Particle Swarm Optimization (PSO) algorithm [116] called Lévy-based [117] Particle Swarm Optimization (LPSO) with Log-Gabor filter [118] for feature extraction. Lévy flight is a pattern of movement where particles take occasional big jumps instead of small steps, helping them explore new areas efficiently. In optimization, a Lévy flight strategy is used to improve algorithms such as Particle Swarm Optimization (PSO). It helps particles avoid getting stuck in local solutions by making occasional long jumps, leading to better solutions for complex problems. The Log-Gabor filter enhances edge detection using multiple templates, and the LPSO algorithm optimizes its parameters to prevent local optima. By employing HOG [94] + Support Vector Machine (SVM) [114] for classification, the approach successfully identifies scratch, crack, sand-hole, and spot defects with a recognition rate exceeding 92%. The proposed technique addresses the limitations of traditional methods and contributes to safer and more efficient wind power generation.

Figure 22 presents a comparison between two adaptive feature extraction algorithms. In subfigure (a), the output image is based on the PSO algorithm, while in subfigure (b), the output image is based on the Improved Adaptive LPSO algorithm.

Zhang et al. [119] evaluated the effectiveness of deep learning models YOLOv3, YOLOv4 and Mask R-CNN

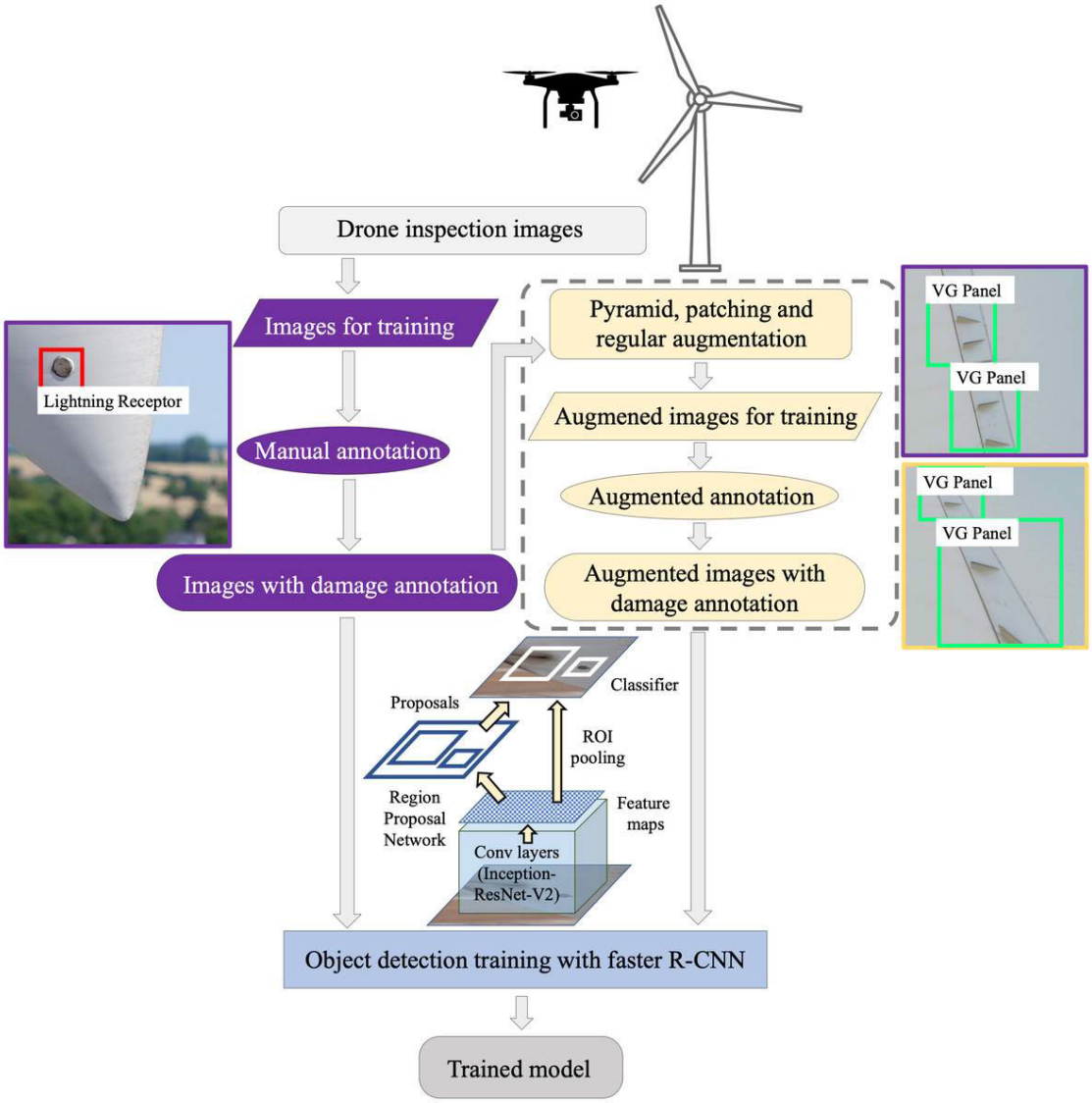

FIGURE 18. Flowchart of the proposed automated damage suggestion system VG and Vortex Generator [95].

for detecting and classifying defects in WTBs with new performance metrics such as Prediction Box Accuracy, Recognition Rate, and False Label Rate. The dataset from an industrial partner, Railston & Co. Ltd. [120], contains WTB inspection images and is augmented into three versions (D0, D1, D2, D3) using techniques such as rotation and grayscale. Mask R-CNN achieved the highest mean Weighted Average (mWA) [121] of 86.74%, outperforming YOLOv3 at 70.08% and YOLOv4 at 78.28%. The paper also proposes a new pipeline, Image Enhanced Mask R-CNN (IE-Mask R-CNN), achieving comparable performance to Mask R-CNN. Traditional metrics such as precision, recall, F1 score and mAP@IoU were also used for evaluation.

Figure 23 illustrates two types of bounding boxes: the manually labeled defect is encompassed within the yellow box, while the black box depicts a bounding box as predicted by the detection model. The Bounding Box Accuracy (BBA) metric is employed to quantify the discrepancy between these two bounding boxes by calculating the area of overlap between them. In instances where there is no overlap, the BBA value is rendered as zero.

Yang et al. [122] introduced a sophisticated deep learning model for detecting WTB damage using advanced methodologies like Otsu threshold segmentation [123] and drone imagery. They evaluated several models, including traditional SVM [114] and AlexNet [106], with SVM achieving 82.93% accuracy, and AlexNet 91.06%. The enhanced AlexNet-tl, incorporating transfer learning [124], improved accuracy to 94.67%, while AlexNet-rf, integrating a random forest classifier, reached 94.80% accuracy. The most effective model, AlexNet-tl-rf, combining AlexNet with transfer learning and a random forest classifier, achieved remarkable metrics: 98.49% accuracy, 94.60% sensitivity, and 0.9849 specificity, establishing it as the superior tool for WTB defect detection.

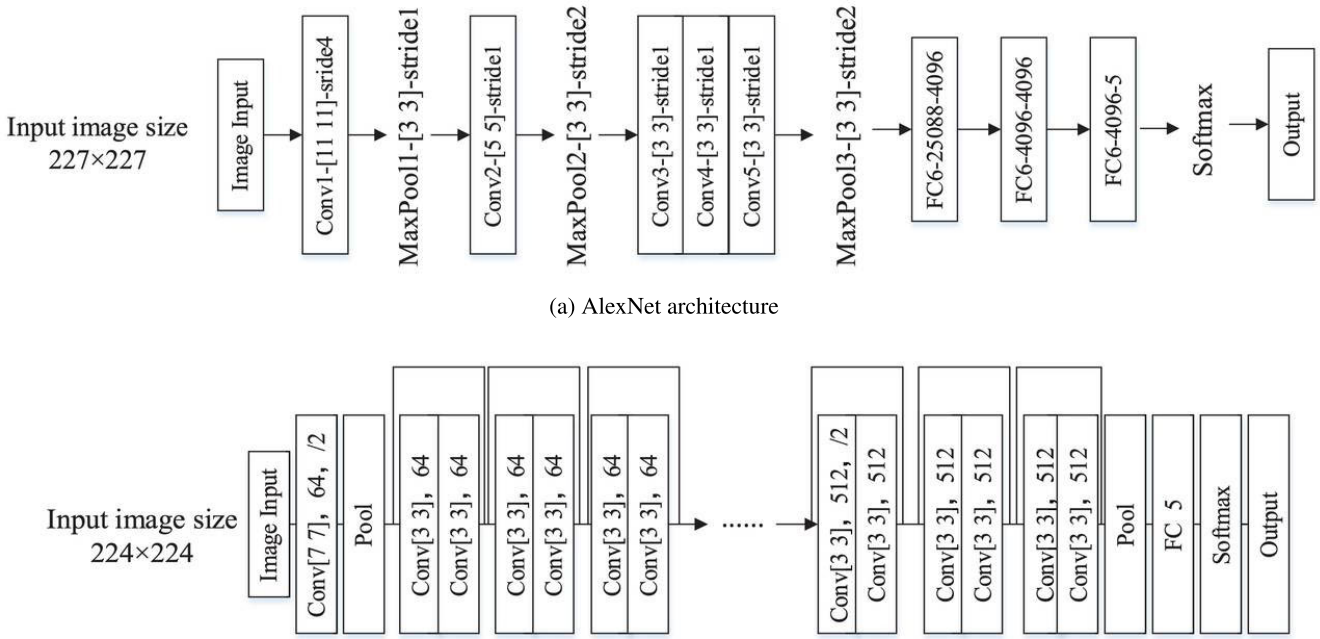

(a) AlexNet architecture

(b) ResNet50 architecture

FIGURE 19. Deep learning architectures used in drone machine vision for WTB inspection [105].

FIGURE 20. M200 drone with an onboard Z30 PTZ camera [107].

Figure 24 illustrates the structure of the proposed model for blade defect recognition, highlighting its multi-layered architecture and the integration of transfer learning and random forest classification for enhanced accuracy.

Sarkar and Gunturi [125] proposed a hybrid object detection system to monitor and assess the health of WTBs. Utilizing YOLOv3 deep learning model, the system captures and analyzes images from surveillance drones, aiming to diagnose the condition of these blades. To augment detection accuracy, the system employs a Super-Resolution CNN (SRCNN) to upgrade low-resolution images to higher resolutions. In experimental comparisons, YOLOv3 demonstrated remarkable performance. When compared with Faster R-CNN [111] and YOLOv2 models, YOLOv3 showcased increasing superiority in average accuracy as iteration numbers grew. For instance, after 5000 iterations, Faster R-CNN had an accuracy of 95%, YOLOv2 reached 93.59%, while YOLOv3 achieved the same 93.59%, but with a distinct advantage in prior iterations. In terms of efficiency, YOLOv3 was trained in 90 minutes and processed images in an average of 0.20 s, outpacing the other models. Faster R-CNN, in contrast, took 220 minutes for training and 0.652 s for image processing, while YOLOv2's metrics stood at 120 minutes and 0.522 s, respectively. Finally, with regard to precision, YOLOv3 recorded the highest mean average precision at 0.96, compared to 0.87 for Faster R-CNN and 0.90 for YOLOv2. This accentuates YOLOv3's heightened accuracy and reliability in detecting damages on WTBs.

Figure 25 elucidates the Non-Maximum Suppression (NMS) process. Figure 25 (a) displays the image post-NMS application, showcasing refined detection results, while Figure 25 (b) presents the pre-NMS image, illustrating the initial detection phase. The clarity of input images is pivotal for accurate defect detection, as depicted in Figure 26, which contrasts a blurry image against a clear one, underscoring the significance of image quality. Lastly, Figure 27 details the architecture of the YOLOv3 model, which is instrumental in the system for robust and efficient defect identification.

Ran et al. [126] introduced Attention and Feature Balanced YOLO (AFB-YOLO) algorithm, an enhancement of the popular YOLO object detection approach, tailored for the real-time detection of minor defects in WTBs. Derived from the YOLOv5s model, AFB-YOLO integrates an advanced feature pyramid network with elements such as weighted feature fusion and cross-scale connections. It also introduces a coordinate attention module for superior object representation and an Efficient Intersection over Union (EIoU) loss function for improved localization. Experimental

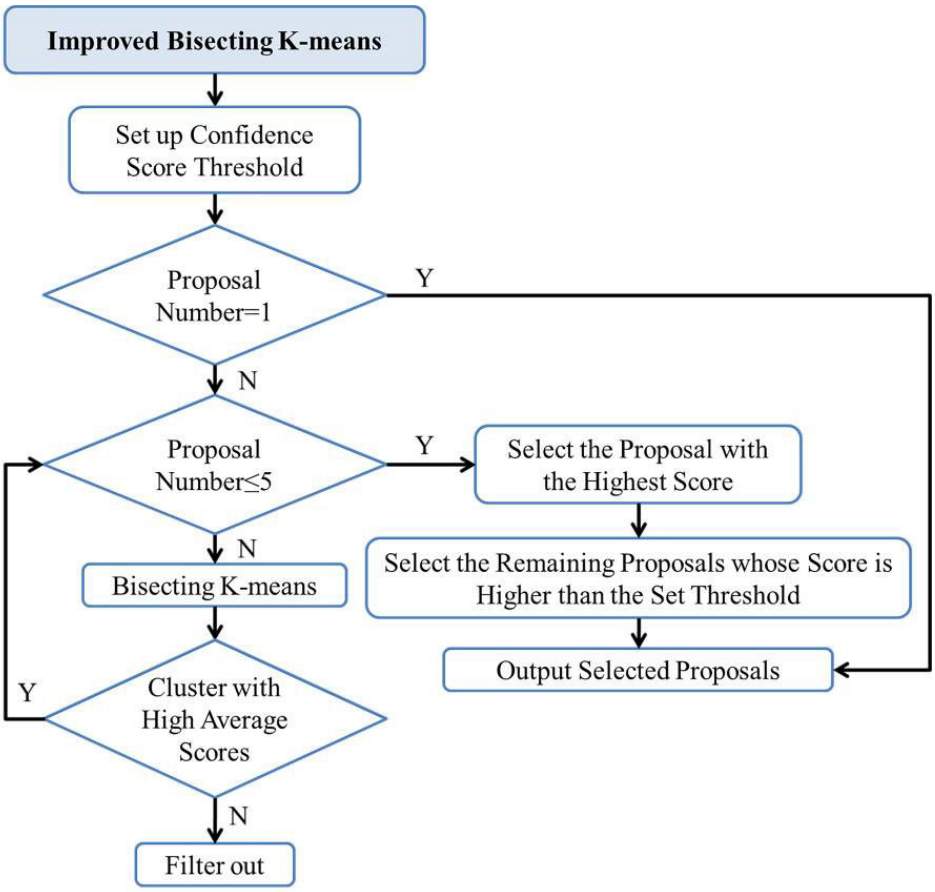

FIGURE 21. The flow chart of improved bisecting k-means [107].

outcomes indicate AFB-YOLO's superiority over traditional models in terms of detection accuracy and robustness. When compared to YOLOv3, its detection accuracy metrics such as Recall, F1-Score, and mAP50 rose by 24.1%, 13.8%, and 10.7% respectively. Furthermore, AFB-YOLO exhibited faster detection speeds than the two-stage Faster R-CNN [111] algorithm while retaining similar accuracy.

Figure 28 (a) shows the Faster R-CNN algorithm, which is known for its accuracy but slower detection speeds. Figure 28 (b) illustrates the SSD model, another important baseline in object detection. Finally, 28 (c) depicts YOLOv5, a direct predecessor and inspiration for the AFB-YOLO algorithm. These figures exemplify the evolution and comparison of various object detection models, contextualizing the improvements brought by AFB-YOLO.

Zou et al. [127] emphasized the importance of detecting damages in WTBs to prevent accidents and economic losses. A novel model, CBNLM-BLS, is introduced that combines chunking and Non-Local Means (NLMs) [128] to enhance the Broad Learning System (BLS) [129], making it more computationally efficient. In comparison tests with deep learning models such as ResNet [82], VGG19, and AlexNet [106], the CBNLM-BLS achieved the highest classification accuracy of 99.71% in detecting defects on WTBs and had a computation time of 28.662 s. This research utilized a dataset of 741 images of WTBs, with 556 used for training and 185 for testing. Variations of the CBNLM-BLS model, adjusting parameters N1, N2, and N3, were also evaluated, achieving accuracy rates as high as 99.81% with computation times ranging from 14.078 to 41.752 s. In their innovative work, Zou et al. [127] developed the CBNLM-BLS model to detect damages in WTBs. The model's efficacy is visually demonstrated through pre- and post-processing images. Figure 29 shows the dramatic improvement in image clarity: Figure 29 (a) presents the initial image before applying CBNLM, while Figure 29 (b) shows the enhanced visibility after CBNLM processing.

Zhu et al. [130] explored defect detection in WTBs using advanced deep learning techniques, specifically proposing a multi-feature fusion residual network combined with transfer learning. To train the models, a dataset of WTB images showcasing various defects was collected using drones. This data set was enhanced and adjusted for input into a deep convolutional network. The novel algorithm merges ResNet [82] and Inception structures, integrates feature fusion layers, and employs transfer learning with weights from the Pascal VOC dataset. A comparison among several models, including variants of AlexNet, VGG, GoogLeNet [131], and ResNet variants, revealed the proposed network's superior accuracy and speed. GPU performance tests on models underscored the

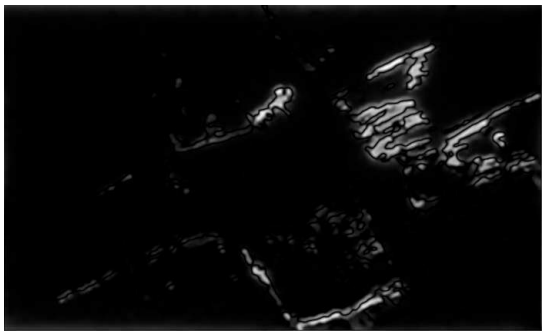

(a) Output image based on PSO

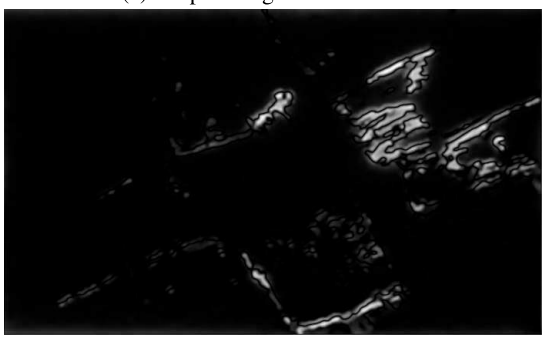

(b) Output image based on LPSO

FIGURE 22. Comparison of two adaptive feature extraction algorithms [115].

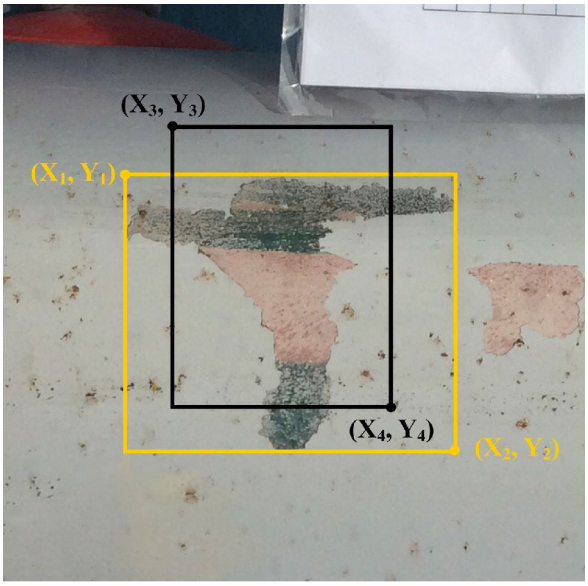

FIGURE 23. Bounding box accuracy [119].

efficiency of transfer learning; for instance, the iteration time for AlexNet on RTX2080 reduced from 51.8 s to 33.3 s with transfer learning. Furthermore, F-1 scores, a performance metric, for various defect types such as erosion and oil stain generally improved with the inclusion of transfer learning, emphasizing its value in this application.

Yu et al. [132] discussed the DMnet framework, a novel approach to detecting wind turbine surface defects. The authors did not explicitly define what the letters D and M in DMnet stand for. However, it can be inferred from the context

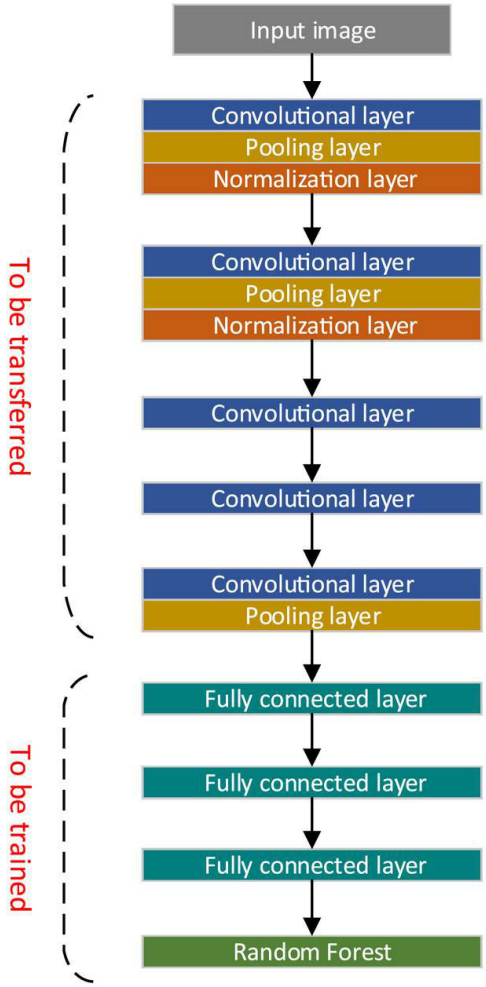

FIGURE 24. Structure of the proposed deep learning model with transfer learning and an ensemble learning classifier [122].

that D might refer to Dynamic, as the framework involves a dynamic activation mapping strategy, and M might refer to Meta-learning, as the framework is inspired by meta-learning ideology. This framework seeks to address the shortcomings of current defect detection methods, with enhanced precision for smaller, concealed defects. DMnet incorporates meta-learning [133] principles, utilizing a cross-task training strategy that reduces the need for extensive training data, a depth metric-based classification system that uses cosine distance for effective sample matching, and a dynamic activation mapping strategy to heighten task-specific information while filtering out redundancies. Comparative testing reveals DMnet's superiority over traditional machine learning and deep learning algorithms. In terms of performance metrics, DMnet achieved an accuracy of 80.41%, precision of 78.80%, recall of 75.70%, and an F1-Score of 76.83%. Ablation experiments confirmed the efficacy of the framework's components, as each contributed to its improved performance. The DMnet framework has demonstrated versatility, as it performs consistently across different deep learning models.

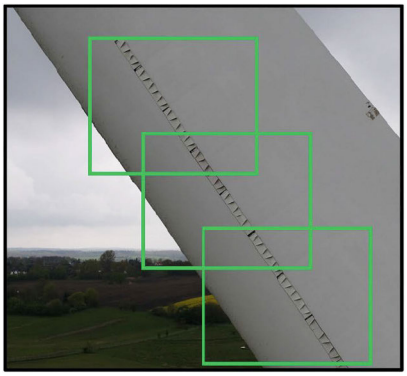

(a) After non-maximum suppression

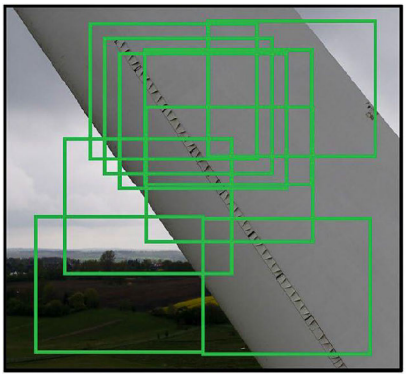

(b) Before non-maximum suppression

FIGURE 25. Non-maximum suppression process [125].

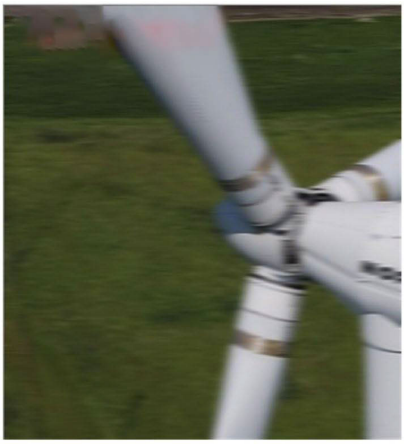

(a) Blurry image

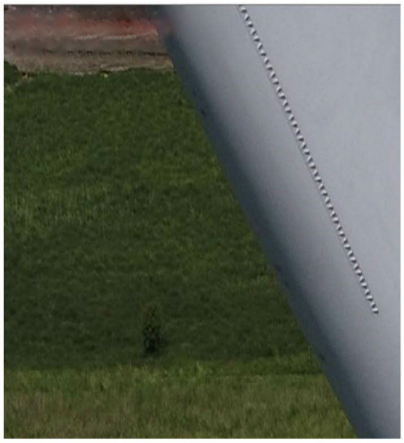

(b) Non-Blurry image

FIGURE 26. Examples of blurry images [125].

Figure 30 illustrates examples of defect visualization in the DMnet framework. The framework is capable of accurately identifying and visualizing different types of defects, such as cracks, coating breakage, and corrosion, in aerial images of wind turbine surfaces. The visualization demonstrates the effectiveness of the DMnet in pinpointing even small target defects in challenging situations. This highlights the framework's ability to enhance defect detection and aid in the inspection and maintenance of wind turbines.

Foster et al. [134] introduced a novel dataset for wind turbine surface damage detection and evaluates the performance of CNNs models, particularly ResNet-101 Faster R-CNN and YOLOv5, in this task. Offshore wind turbine inspection, a traditionally expensive and high-risk operation, can benefit from computer vision techniques, offering reductions in human exposure and costs. While YOLOv5 outperforms ResNet-101 Faster R-CNN in predicting bounding box coordinates, the latter estimates damage more holistically. Performance metrics reveal that YOLOv5S has the highest mAP@0.5 of 0.5121, but ResNet-101 Faster R-CNN excels in densely packed bounding boxes scenarios. The study underscores the potential of these models for AI-driven or autonomous inspections of active turbines and suggests future exploration into segmentation techniques and image enhancement.

Lv et al. [135] introduced a novel method for efficient and precise WTB damage detection using the Single Shot MultiBox Detector (SSD) framework with an enhanced ResNet backbone. This method leverages dense connection blocks, a bidirectional cross-scale feature pyramid, and various techniques such as data pre-processing, exponential moving average, and label smoothing to optimize damage detection. When compared with seven advanced models, the proposed method Efficient, and Accurate Damage Detector (EADD), outperforms in terms of detection accuracy and computation time, boasting an mAP of 81.2%, an Frames Per Second (FPS) of 56, 8.3 million parameters, and 12.8 billion Floating-Point Operations Per Second (FLOPS). This approach exhibits promising potential, particularly when considering the rapid growth of wind power and the imperative need for advanced damage detection mechanisms in WTBs.

Figure 31 illustrates the framework of the proposed method for WTB damage detection. The method is based on the SSD structure. However, it introduces an improved version of ResNet, which includes dense connections and lightweight bottlenecks, as the backbone of the network. The feature maps extracted by the backbone network are then aggregated through the neck component. The neck takes multiple feature maps, denoted as $Dn(n = 1, 2, 3, 4, 5)$, as input.

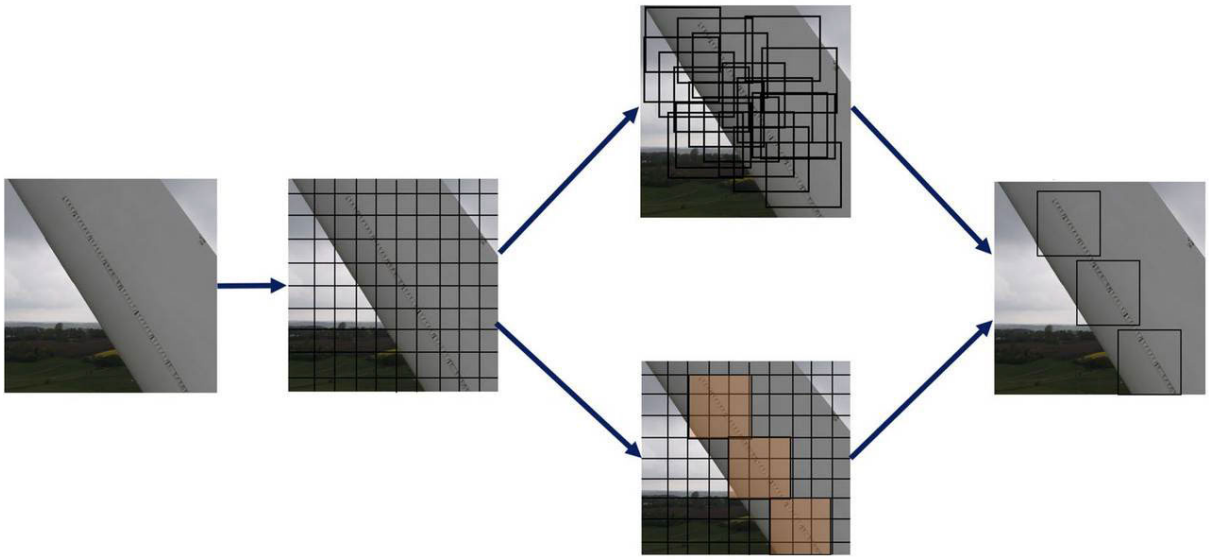

FIGURE 27. YOLOv3 Architecture [125].

Additionally, two feature maps extracted by *Conv*4(*D*1) and *Conv*5(*D*2) layers are also utilized as inputs for the neck. The aggregated feature maps are then passed to the detection head, represented by the green rectangle box. The detection head consists of two convolutional layers: a 3×3 Conv layer and a 1×1 Conv layer. These layers generate outputs of shape $N \times (C + 4)$, where N is the number of anchor boxes in each layer, C is the number of categories, and the four values represent the predicted offsets of *xywh* (coordinates x and y width and height). Overall, the framework combines the strengths of SSD with the improved ResNet backbone, dense connections, and lightweight bottlenecks to enable accurate detection of WTB damage.

Figure 32 shows the damage detection results achieved by the proposed method for WTB images. The detected damages are annotated using colored bounding boxes. In Figure 32, red boxes indicate instances of gelcoat peeling off. Gelcoat peeling off refers to the separation of the outer protective layer of the blade's surface. It is commonly caused by erosion or aging. Green boxes represent instances of surface cracking. Surface cracking refers to the formation of cracks on the surface of the blade. This can occur due to various factors such as wind-induced vibrations or material fatigue. Black boxes correspond to instances of surface corrosion. Surface corrosion refers to the gradual deterioration of the surface of the blade due to environmental factors such as moisture, salt, or chemicals. By accurately identifying and highlighting these different types of damages, the proposed method demonstrates its effectiveness in detecting and localizing various forms of damage on WTBs.

Zhang et al. [136] discussed a novel image recognition method for detecting defects in WTBs utilizing attention-based MobileNetv1 YOLOv4 combined with transfer learning. This approach is designed to enhance detection accuracy, response speed, and reduce computational complexity.

Figure 33 illustrated the concept of depthwise separable convolution, which is a fundamental operation used in the MobileNetv1 neural network architecture. In traditional convolutional operations, each input channel is convolved with a set of filters, resulting in multiple output channels. However, depthwise separable convolution decomposes this process into two separate operations: depthwise convolution and pointwise convolution. The depthwise convolution is applied independently to each input channel using a separate kernel for each channel. This operation produces a set of intermediate feature maps, where each feature map represents the convolved output of a single input channel. This step reduces the computational cost by performing spatial convolution on each channel individually. The pointwise convolution is then employed to combine the intermediate feature maps obtained from the depthwise convolution. It applies a 1×1 kernel on each location across all channels to compute a linear combination of the intermediate feature maps. This step enables the network to learn more complex representations by combining the information captured from different channels. By separating the convolution operation into depthwise and pointwise convolutions, depthwise separable convolution significantly reduces the number of parameters and computational cost compared to traditional convolutions. This makes it particularly useful for lightweight and efficient networks, such as MobileNetv1.

Figure 34 illustrates the structure of CBAM. The CBAM aims to enhance the feature map by considering both channel-wise and spatial-wise attention. In the channel

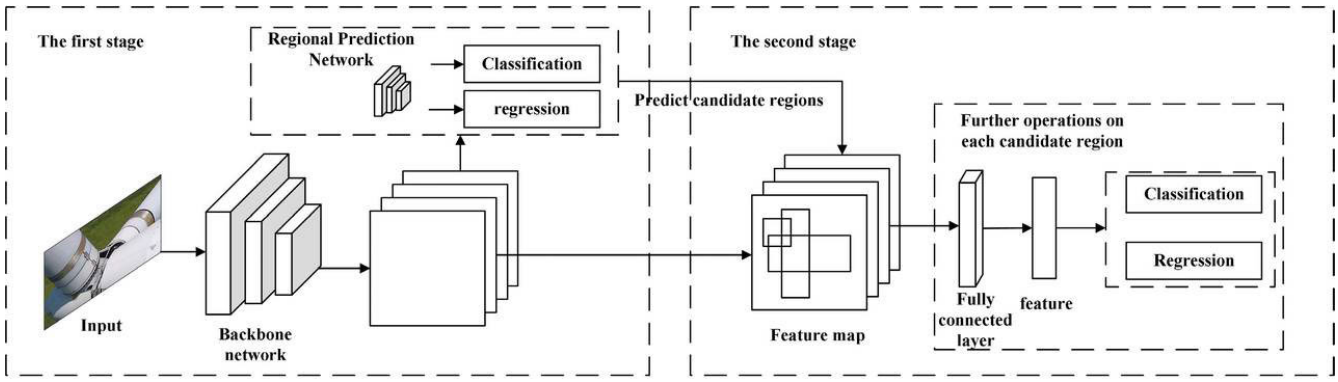

(a) Faster R-CNN

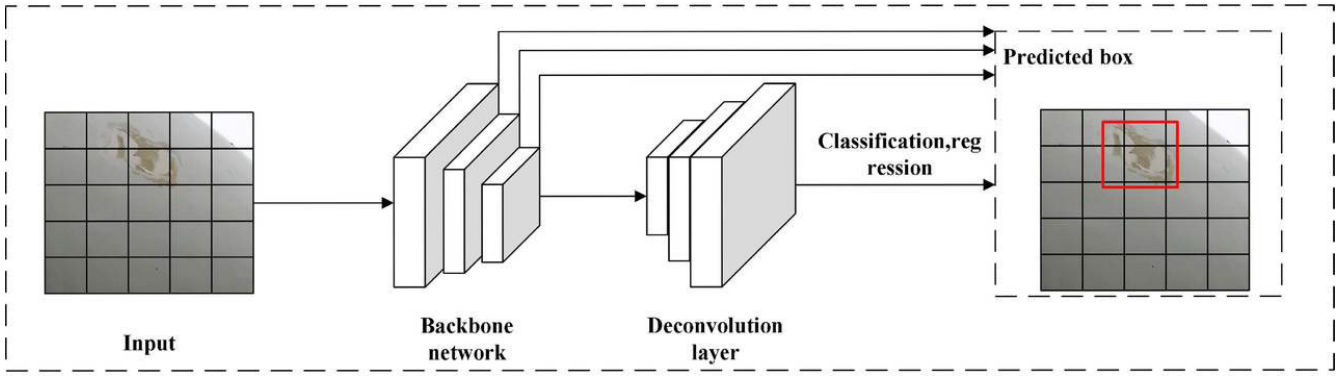

(b) SSD

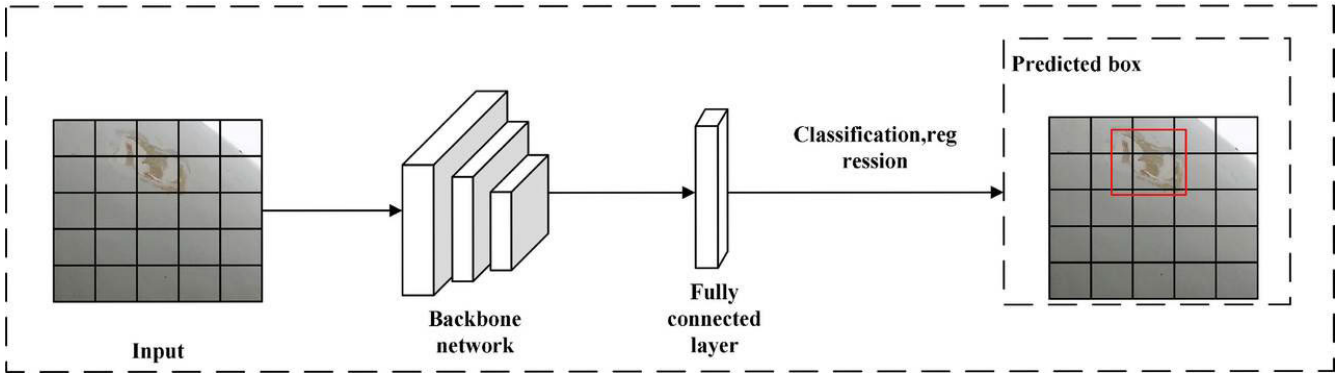

(c) YOLOv5

FIGURE 28. Representative object detection algorithms [126].

attention module, the input feature map undergoes two separate operations: average-pooling and max-pooling. These operations gather information about the spatial dimension and retain background and texture information. The output feature vectors from these operations are fed into a shared Multi-Layer Perceptron (MLP). The MLP processes these vectors to generate the channel attention feature map. The channel attention is computed by applying the sigmoid function σ to the output feature vectors obtained from the average-pooling and max-pooling operations. These vectors are multiplied by weight matrices $W0$ and $W1$ and summed element-wise to obtain the final channel attention feature map. This process allows the channel attention module to adaptively learn relevant features and suppress irrelevant ones. Overall, the channel attention module in Figure 34 emphasizes the importance of different channels in the input feature map and enhances the feature representation for better detection accuracy.

Xiaoxun et al. [138] introduced the Multivariate Information YOLO (MI-YOLO) model designed for detecting cracks in WTBs using deep learning techniques. The focus is on improving the detection of subtle cracks to enhance wind turbine efficiency. The MI-YOLO model synergizes feature extraction capabilities from networks such as Mobilenetv3

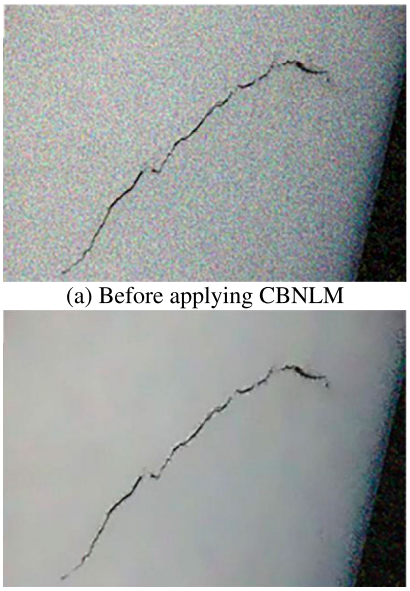

(a) Before applying CBNLM

(b) After applying CBNLM

FIGURE 29. Comparison of images before and after CBNLM processing [127].

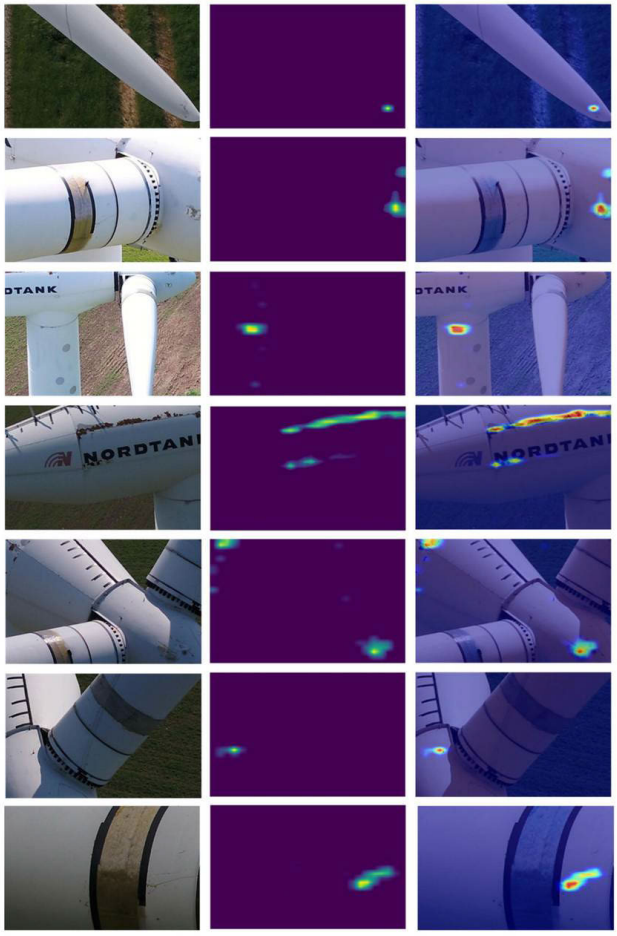

FIGURE 30. Defect visualization [132].

Algorithm 1 Blurred Image Synthesis [137]

Require: Sharp image (Is), ROI mask $Isroi$, Central point (i_c, j_c) of WTB, Additive noise N, Morphological structuring element Se with size s, Angular velocity ω, Linear fusion factor α

Ensure: Blurred image (IB)

$Idilate \leftarrow Isroi \oplus Se$
$Iedge \leftarrow Idilate - Isroi \ominus Se$
$Km \leftarrow 0$
for each pixel (i, j) in $Idilate$ **do**
  $s(i,j) \leftarrow 2\tan(\omega/2) \times \|(i,j) - (i_c, j_c)\|^2$
  $\theta(i,j) \leftarrow \arctan\left[\frac{j-j_c}{i-i_c}\right]$
  $U(i,j) \leftarrow s(i,j)\cos(\pi/2 - \theta(i,j))$
  $V(i,j) \leftarrow s(i,j)\sin(\pi/2 - \theta(i,j))$
  if $\|U(i,j), V(i,j)\|^2 < s \times \|(U(i,j), V(i,j))\|^2/2$ **then**
    $Km(i,j) \leftarrow \frac{\delta(i\sin(\theta)+j\cos(\theta))}{\|(U(i,j),V(i,j))\|^2}$
  end if
end for
for each pixel (i, j) in Is **do**
  if $Isroi(i,j)$ **then**
    $Ib(i,j) \leftarrow Km \times Is(i,j) + N$
  else if $Iedge(i,j)$ **then**
    $Ib(i,j) \leftarrow \alpha(Km \times Is(i,j) + N) + (1-\alpha) \times Is(i,j)$
  else
    $Ib(i,j) \leftarrow Is(i,j)$
  end if
end for
return IB

[139] and Ghostnet [140]. Features such as the C3TR module and Alpha-IOU are incorporated to better detect weak color cracks and balance precision-recall rates. Data enhancement techniques, including slice transposition and crack pixel reconstruction, expand the dataset to further the accuracy of the model. Performance testing on drone images reveals MI-YOLO's superiority over YOLOv5s in mAP, precision, and recall. Compared to other target detection algorithms, MI-YOLO + Alpha-IOU exhibited the highest mAP of 93.2%, a precision of 93.1%, and a recall of 92.2% against other target detection algorithms.

Zhang et al. [141] introduced a new high-precision model, SOD-YOLO, for detecting defects on WTB. Traditional methods struggle to detect small and long strip defects on WTB surfaces. SOD-YOLO overcomes these limitations by integrating foreground segmentation [142], Hough transform [143], a micro-scale detection layer, K-means [144] re-clustering of anchor frames, CBAM attention mechanism [145], and channel pruning. The method significantly enhances detection accuracy and speed. Experimental results indicate the SOD-YOLO's average accuracy on the WTB dataset is 95.1%, outpacing YOLOv5 by 7.82%. The model also boasts a 28.3% improvement in detection speed over the mainstream models.

The YOLOv5 model is a deep learning-based algorithm used for object detection tasks. The model consists of several components, including an input layer, a backbone network,

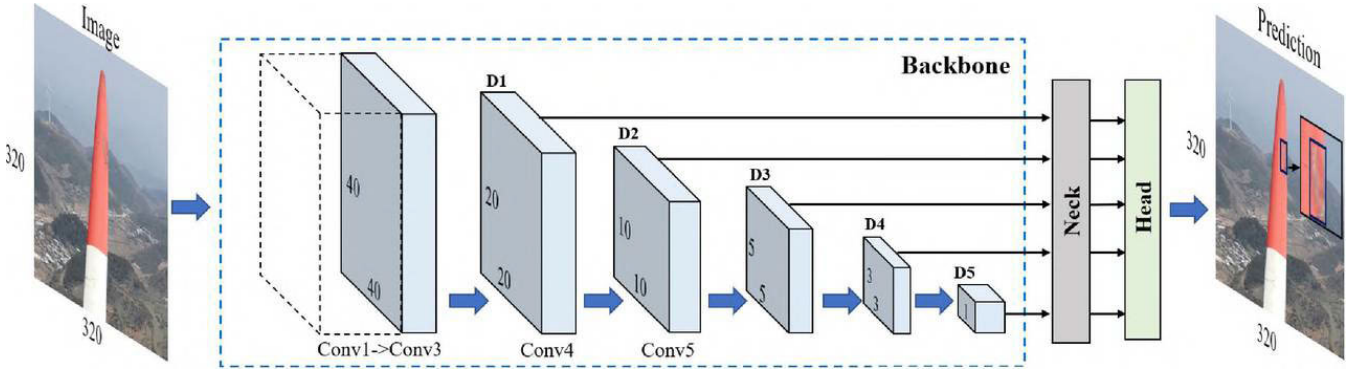

FIGURE 31. The framework of the proposed method based on SSD, the network introduces an improved ResNet with dense connections and lightweight bottlenecks as the backbone. The feature maps extracted by the backbone are aggregated through the neck and input to the detection head (green rectangle box) to obtain the detection results, where Dn (n = 1, 2, 3, 4, 5) are the input of the neck [135].

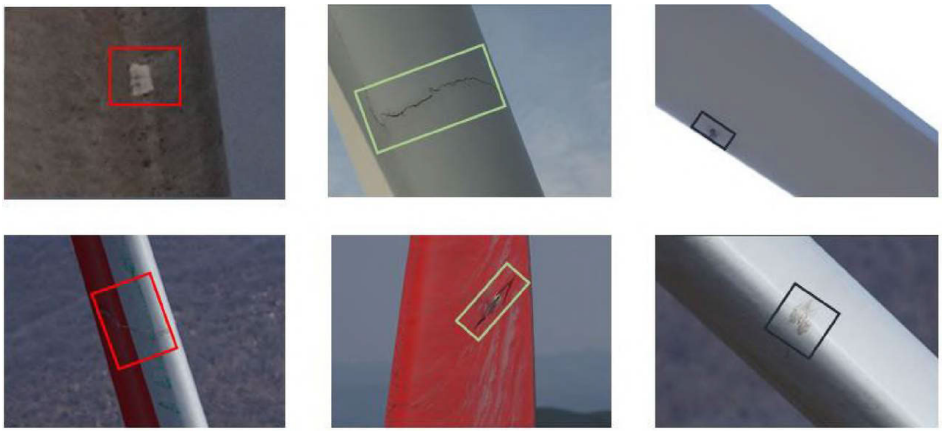

FIGURE 32. The damage detection results of the proposed method, where red boxes represent gelcoat peeling off, green boxes represent surface cracking, black boxes represent surface corrosion [135].

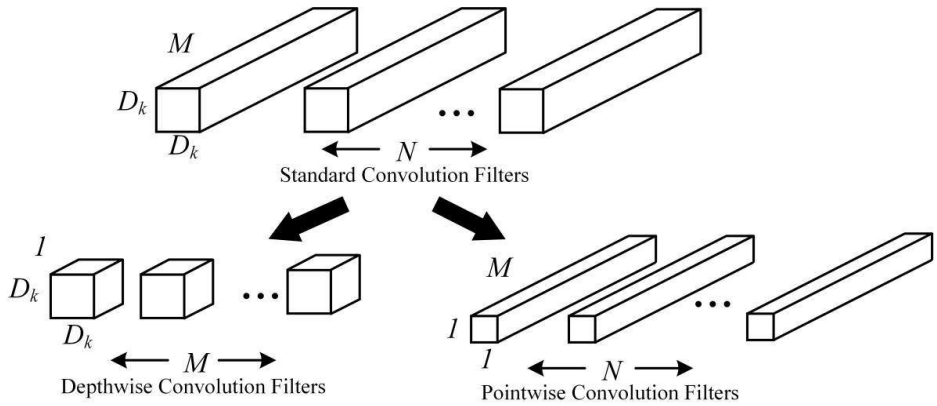

FIGURE 33. Depthwise separable convolution [136].

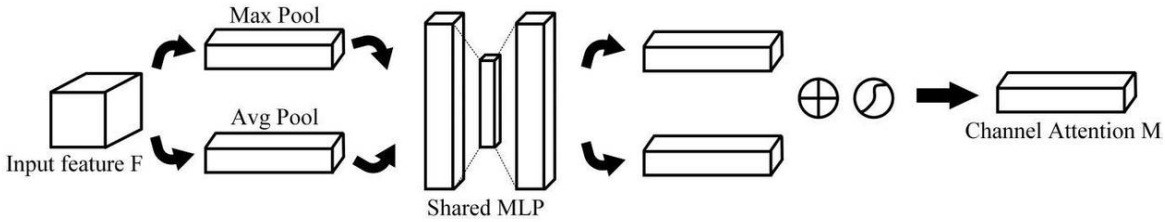

FIGURE 34. Channel attention module [136].

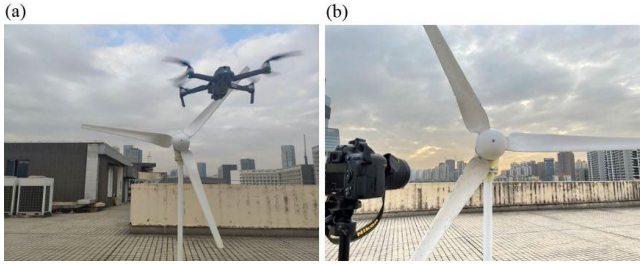

FIGURE 35. Image pair acquisition setup [137].

a neck module, and a head output [141]. The input layer takes in the image data that needs to be analyzed for object detection. The backbone network is responsible for extracting high-level features from the input images. These features capture the visual patterns and characteristics of the objects present in the image. The neck module further refines the features extracted by the backbone network. It performs additional operations such as feature fusion or upsampling to enhance the representation of the image features. Finally, the head output processes the refined features obtained from the neck module and generates the final predictions. The predictions include the bounding box coordinates and the class labels of the detected objects. Overall, the main structure of the YOLOv5 model demonstrates the sequential flow of information through the input layer, backbone network, neck module, and head output to achieve accurate and efficient object detection [141].

Figure 37 depicts the algorithm structure of SOD-YOLO, which is an improved version of the YOLOv5 model specifically designed for WTB defect detection. The algorithm incorporates several enhancements to improve the detection of small targets and long strip defects in the WTB dataset. The algorithm structure starts with the preprocessing of WTB images using foreground segmentation and the Hough transform techniques. This step helps extract the blade region and adjust the image orientation for accurate defect labeling. Next, the input images are passed through the improved YOLOv5 model, consisting of several key components: Micro-scale Detection Layer: A micro-scale detection layer is introduced to the original YOLOv5 architecture. This layer aims to improve the detection of small targets and enhance the recognition of long strip-shaped defects on the surface of WTBs. Re-clustering of Anchor Boxes: The K-means clustering algorithm is employed to re-cluster the anchor boxes used in the detection process. By recalculating the cluster centers, the model can better adapt to the characteristics of the WTB dataset and improve the accuracy of defect detection [141]. CBAM Attention Mechanism: The algorithm integrates the Convolutional Block Attention Module (CBAM) mechanism into each feature fusion layer. CBAM helps to emphasize important features related to blade defects and suppress irrelevant background information, enabling more accurate detection in complex backgrounds. The algorithm also includes additional steps for channel pruning, which reduce the computational complexity of the model and improve the detection speed. In general, the structure of the SOD-YOLO algorithm showcases the various improvements made to the YOLOv5 model to improve its performance in detecting WTB defects, particularly small targets and long strip-shaped defects [141].

Yang et al. [146] delved into the challenges and innovations in WTB inspection, highlighting the importance of accurate drone-based image stitching for defect identification. Current image stitching methods fall short due to texture-deficient blade surfaces and unstable drone positioning. Addressing this, the proposed method consists of two stages: coarse-grained stitching, which leverages blade shape features and camera-blade distance, and fine-grained stitching that fine-tunes the panorama using regression. The newly introduced ''Blade30'' dataset, containing drone images of 30 full WTBs from various environments, offers a significant resource for the industry. It is populated with 1,302 images, diverse in drone models, camera resolutions, and defect types, making it a substantial step forward in benchmarking various inspection methods.

Figure 40 shows the annotation of defects and contaminations in the Blade30 dataset. The upper part of the figure displays annotations for defects, which are areas on the WTB that indicate damage, such as cracks or chips. These defects are marked with yellow rectangles to highlight their presence. The bottom part of the figure displays annotations for contaminations, which are foreign objects or substances found on the blade surface that can affect its performance. These contaminations are also marked with yellow rectangles. These annotations provide valuable information for analyzing and evaluating the effectiveness of the proposed stitching algorithm and the deduplication method in identifying and addressing defects and contaminations on WTBs.

In this section, various techniques and applications of RGB camera technology in WTB inspection are discussed. Techniques like extended Haar-like features and adaptive median filtering are used for image pre-processing, while CNN architectures and object detection frameworks are employed for deep learning object detection models. Advanced techniques such as the LPSO strategy are applied for enhanced image denoising and motion blur removal. These methods serve critical roles in feature extraction, noise reduction, defect identification, and ensuring the clarity of images captured for inspection purposes. Refer to Table 4 for further details and specific applications of these techniques in the field.

D. VISUAL INSPECTION USING THERMAL IMAGING

Thermal imaging monitoring technology is a non-contact monitoring technology that detects thermodynamic changes on the blade surface. When the blade is damaged, the structure of the blade becomes discontinuous. The heat is locally retained at the discontinuous position with low thermal conductivity, resulting in a higher temperature at the discontinuous position. A highly sensitive infrared

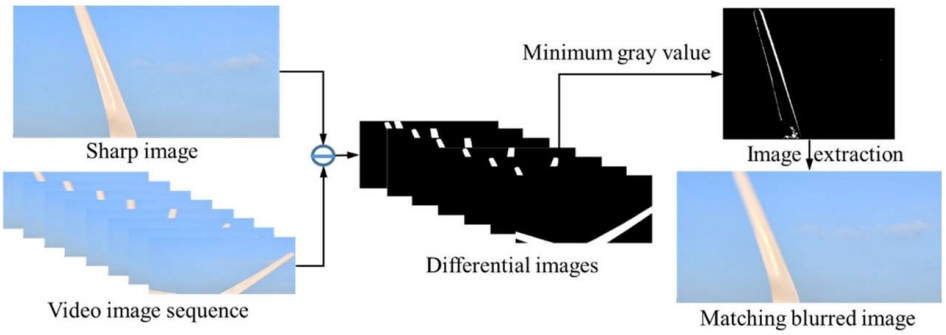

FIGURE 36. Image matching process [137].

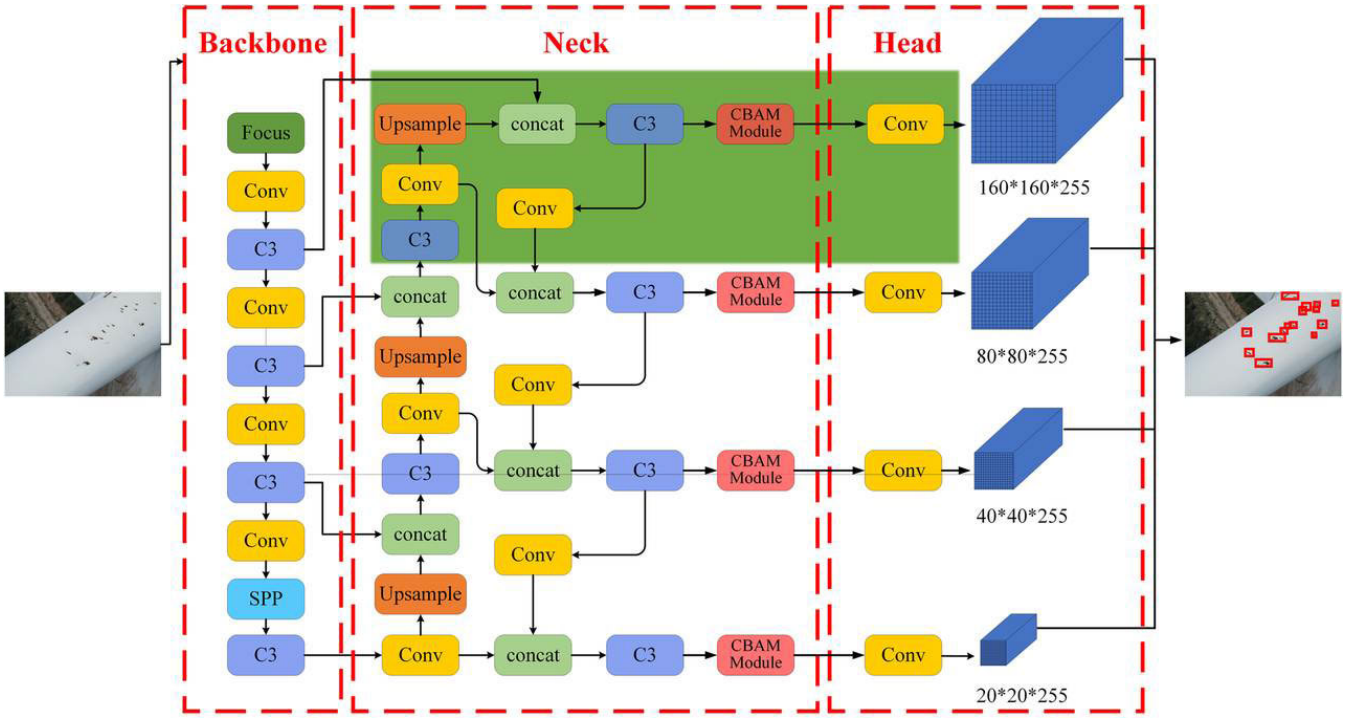

FIGURE 37. Algorithm structure of SOD-YOLO [138].

TABLE 4. Summary of techniques used in WTB visual inspection using RGB cameras.

Category	Techniques	Applications
Image Pre-processing Techniques	Extended Haar-like Features, Wiener Filtering, Adaptive Median Filtering, Log-Gabor Filter	Feature Extraction, Noise Reduction, Edge Detection
Deep Learning Object Detection Models	CNN Architectures (e.g., ResNet, DenseNet, Xception, VGG), Object Detection Frameworks (e.g., YOLO, Mask R-CNN, Cascade R-CNN), Anomaly Detection (e.g., One-Class SVM), Innovative Methods (e.g., U-Net, attention-based models)	Defect Identification, Anomaly Recognition, Targeted Defect Detection
Advanced Techniques	LPSO Strategy, CBNLM-BLS Method, I-DeblurGANv2 Network	Image Denoising, Motion Blur Removal in Aerial Images, Synthetic Images

camera can capture and visualize this temperature difference, to realize the rapid detection of blade-damage defects. In addition, the high strain area inside the blade will generate heat energy by friction, which allows the engineer to determine the high strain area of the blade. Wang and Gu [147] used the passive infrared thermal imaging detection method to detrmine the damage of the WTB under outdoor conditions, and the numerical simulation of the damage was performed. Sanati et al. [148] explored passive and active thermography techniques, employing pulsed and step heating and cooling methods. The study involved monitoring a section of a severely damaged blade and a small "plate"

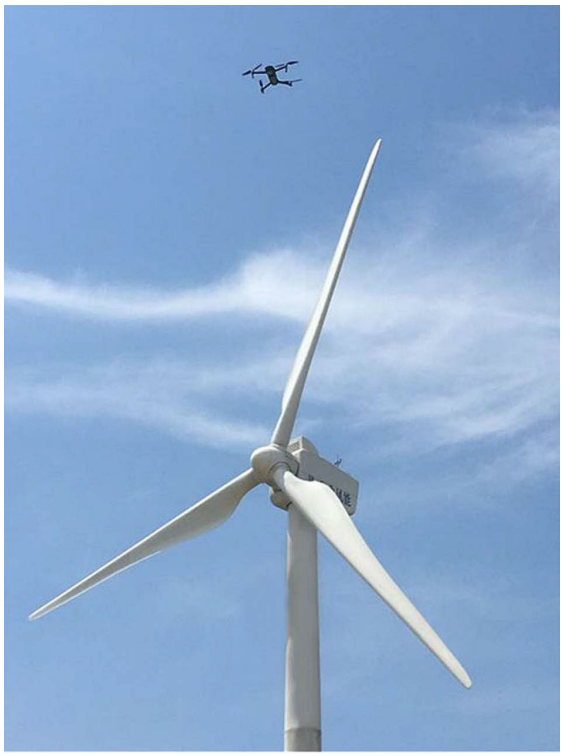

FIGURE 38. DJI AIR 2S professional drone shooting WTB defects [138].

cut from the undamaged laminate section, where holes of varying diameter and depth were drilled from the rear to create ''known'' defects. The results of image processing on both active and passive thermography revealed a significant enhancement in the quality of images and the visibility of internal defects through the applied technique.

Chen et al. [149] introduced a method using thermography and computer vision for inspecting WTBs. It focuses on detecting subsurface damages, crucial for blade maintenance and longevity. This method aims to significantly reduce inspection costs and lower the Levelized Cost Of Energy (LCOE) by 1-2% for land-based wind farms. AQUADA's non-intrusive approach enhances inspection efficiency compared to traditional methods, offering a promising solution for the wind energy industry.

Zhou et al. [150] centered on enhancing defect detection in WTBs by integrating visible and infrared image fusion. Traditional inspection techniques often lead to a high percentage of false detections due to inefficiencies. To address this, a *Regression Crop* data-processing technique was introduced, which automatically crops critical areas in WTB images, thereby increasing detection accuracy by 34.5%. This method, combined with an RGB-IR feature fusion module, further optimizes detection, attaining a precision rate of 99% for genuine defects. When compared using the YOLOv7 model, the combination of ''Regression Crop'' and RGB-IR feature fusion vastly outperformed existing methods, as evidenced by precision improvements of up to 20.8% and AP gains of 34.5%. In the exploration of efficient wind turbine detection using drones photos in Industry 4.0, Zhou et al. [150] proposed a novel Soft-Masks Guided (SMG) [151] Faster R-CNN model. This model harnesses synthetic datasets and soft masks to enhance detection accuracy. The synthetic datasets simulate real drone-captured imagery, and the soft masks guide the model's focus, suppressing domain-specific features and boosting feature extraction accuracy. Notably, soft masks have proven beneficial for variations in wind turbine sizes. On the Xilin dataset, the SMG Faster R-CNN achieved an AP@IoU0.5 of 0.409, outperforming many models including SSD, RetinaNet, and DA Faster R-CNN. Furthermore, the model performance peaked with a soft pixel value of 125, reaching an AP of 0.409, indicating that larger soft mask values enhance detection.

Figure 41 provides an overview of the methods utilized in the study [150]. It illustrates the workflow of the proposed approach for detecting defects in WTBs. The image-processing method consists of two main components: the Regression Crop data-processing method and the RGB-IR feature fusion module. The *Regression Crop* method involves reducing the size of the input image through downsampling. After the downsampling process, the image goes through a four-stage residual module to obtain the final feature maps. This method makes the process three times more efficient compared to traditional global crop methods. The RGB-IR feature fusion module focuses on combining the features extracted from RGB and InfraRed (IR) images. The module adapts the weighting coefficients of IR image features dynamically to achieve better detection accuracy. By integrating the features from both modalities, the likelihood of false detections caused by dust or other contaminants on the blades is minimized. Overall, the combination of the Regression Crop method and the RGB-IR feature fusion module enhances the accuracy and efficiency of detecting actual defects in WTBs.

Figure 42 illustrates a comparison between examples of actual and false defects within the WTB dataset used in the study [150]. The figure presents two images side by side. The left image shows an example of an actual defect on a WTB. This defect may include various types of damage such as cracks, chips, or delamination. The specific defect is annotated by professional turbine maintenance personnel to ensure accuracy. The right image, on the other hand, represents a false defect. These false positives can occur due to various factors such as dust, urine, or feces present on the blade surface, which may visually resemble actual defects. By including both examples of actual defects and false positives, Figure 42 highlights the challenges faced in accurately detecting and distinguishing between real defects and false detections. Understanding the characteristics and differences between actual defects and false positives is crucial for developing effective detection methods. The proposed approach in the study aims to address these challenges by utilizing a data-processing method and feature

FIGURE 39. Blade inspection utilizing remote and non-remote sensors [146].

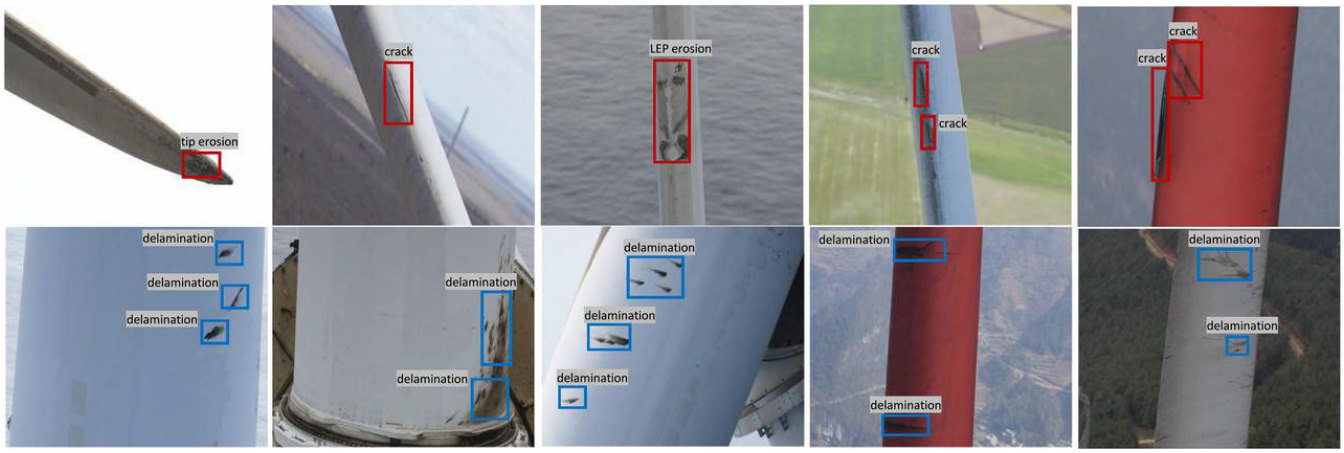

FIGURE 40. Annotation of defects [146].

fusion module to improve the accuracy and precision of detecting actual defects in WTBs.

In this section, the utilization of thermal imaging techniques for the inspection of WTBs is investigated. Thermal imaging is instrumental in detecting structural damage through thermodynamic changes on the blade surface. This section underscores the capability of sensitive infrared cameras to capture temperature differentials at the site of discontinuities, allowing for rapid identification of blade-damage defects. Furthermore, the integration of computer vision with thermography offers a non-intrusive, yet cost-effective means for subsurface damage detection. The fusion of visible and infrared imaging, as well as the application of advanced techniques like SMG Faster R-CNN with synthetic datasets, significantly improves defect detection accuracy under varying turbine conditions. The diverse applications and descriptions of these techniques are comprehensively presented in Table 5, providing a detailed overview of their effectiveness in WTB visual inspections using thermal imaging.

E. ULTRASONIC TESTING

Ultrasonic testing technology is a relatively mature technology to detect defects in composites and other materials. It is widely used to detect internal debonding, delamination, and other defects of WTB materials. An elastic wave of more than 20 kHz is introduced into the blade structure through a transmitter. The wave propagates along the structure of the blade and passes through or interacts with the defects, such as delamination, debonding, and crack, to make the wave change in the propagation process. The second sensor measures the mode changes, such as propagation, amplitude, phase, time, reflection, and attenuation of the elastic wave, to accurately judge the location and size of the damage, and Figure 43 shows the ultrasonic technique. Ultrasonic testing necessitates an assortment of transducers and coupling agents and is carried out through transmission, reflection, and backscattering modes [152]. These behaviors are influenced by the interfaces between arbitrary boundaries. The Ultrasonic non-destructive testing (NDT) method is adept at detecting the bonding area and depth of a structure by analyzing the time gap between transmission and echo signals [153]. Chakrapani et al. [154] conducted experiments utilizing the pulse-echo technique to scrutinize adhesive bonds within composite plates, which exhibited varying thickness ranging from 1.4 mm to 45.5 mm.

F. VIBRATION MONITORING

Vibration monitoring is a widely used monitoring technology for WTBs. It works by monitoring the dynamic response of the blade structure under external force excitation. Since the dynamic response of the blade depends on the characteristics of the blade material, structure, and loading conditions, any damage to the blade will lead to a change in its dynamic response. Ghoshal et al. [156] successfully detected damage in WTBs before experiencing catastrophic failure

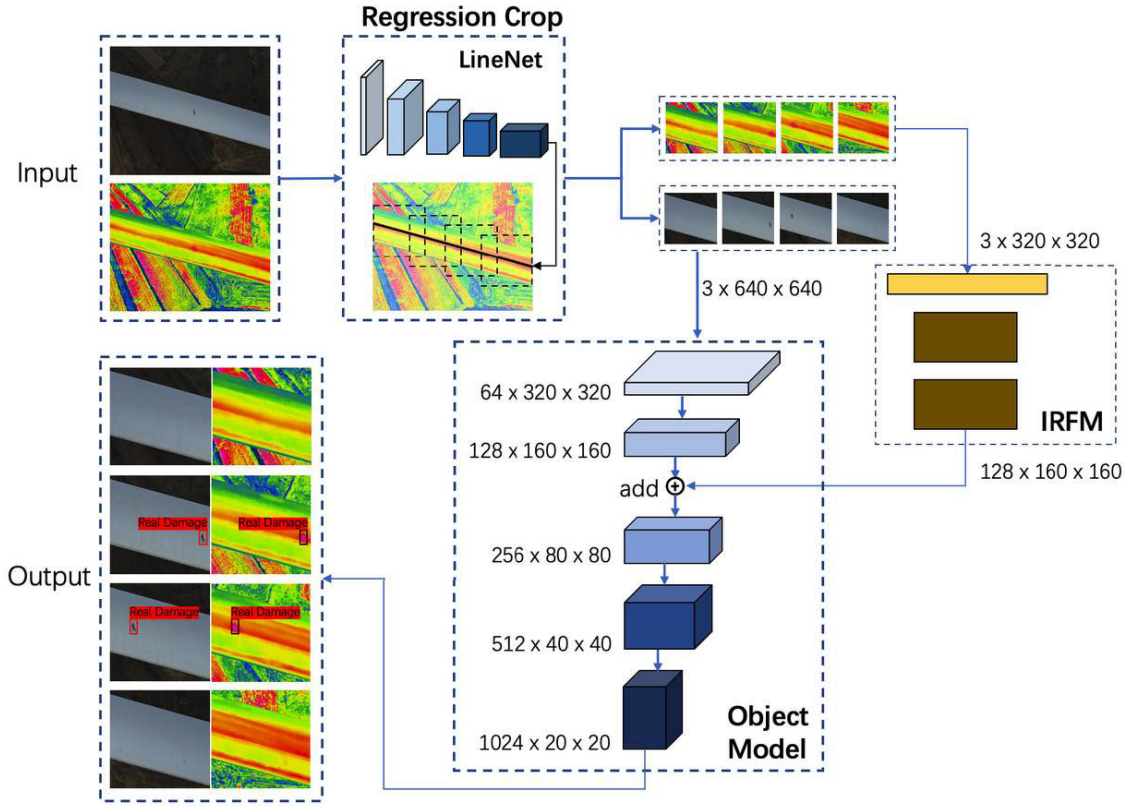

FIGURE 41. Overview of the methods in WTB defects detection based on visible and infrared image fusion [150].

TABLE 5. Summary of techniques used in WTB visual inspection using thermal imaging.

Technique	Description
Thermal Imaging	Uses both passive infrared and advanced thermography for blade damage detection in various conditions.
Computer Vision Integration	Combines thermography with computer vision for cost-effective and non-intrusive sub-surface damage detection.
Image Fusion & Processing	Merges visible and infrared imaging, employing techniques like 'Regression Crop' for enhanced defect identification.
SMG Faster R-CNN	Applies synthetic datasets and soft masks to improve detection accuracy in varied turbine conditions.

by analyzing the vibration response of the blade. Abouhnik and Albarbar [157] presented a comprehensive overview of vibration sources in wind power. They introduced a novel method utilizing Empirical Decomposition Feature Intensity Level (EDFIL) for the analysis of vibration signals and the identification of crack damage. Chen and Chen [158] conducted a study on the sensitivity of vibration modes in the blades of various sizes for damage recognition. Their findings indicated that as blade size increased significantly, vibration modes became relatively more sensitive to damage recognition.

The inspection of WTBs using NDT techniques plays a crucial role in assessing the structural integrity without causing harm or altering their functionality. Various NDT methods are employed to identify potential defects, damage, or structural irregularities in these critical components. Acoustic emission, for instance, monitors the sound energy generated by loaded blades, providing information on their structural health. Thermography techniques, involving both passive and active methods, use temperature variations to detect hidden flaws or damage. Vibration analysis, as explored in different studies, leverages the response of the blade to identify potential issues before catastrophic failure. Additionally, coherent optical techniques and EDFIL have been proposed for enhanced analysis of blade vibrations and identification of specific types of damage. These NDT approaches collectively contribute to the proactive maintenance and optimization of WTBs, ensuring their reliability and longevity in the renewable energy sector.

As the renewable energy sector continues to grow, the need for innovative and efficient maintenance solutions for energy infrastructure becomes increasingly critical. In particular, the inspection and maintenance of WTBs pose unique challenges due to their large size, complex shapes, and often remote locations. Recent technological advancements have brought forward the use of unmanned aerial vehicles,

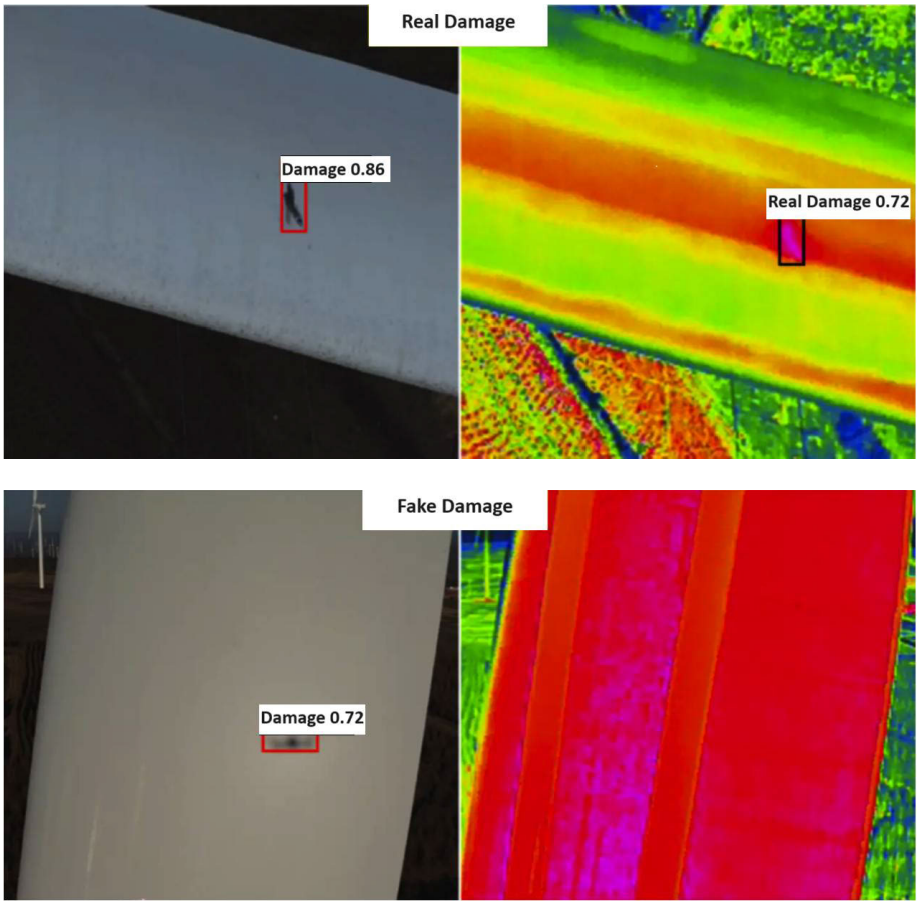

FIGURE 42. Examples of actual and false defects [150].

commonly known as drones, as a game-changing solution in this domain. Drones offer a safer, more efficient, and cost-effective alternative to traditional inspection methods, which typically involve manual inspection by technicians. This transition not only enhances the safety of the personnel involved but also significantly improves the precision and quality of the inspections. In the following section, we discuss the advances in drone path planning specifically designed for WTB inspection, highlighting the innovative approaches and technologies that are shaping the future of wind turbine maintenance.

V. DRONE PATH-PLANNING FOR WTB INSPECTION

The integration of drone technology in the field of WTB inspection marks a significant advancement in renewable energy maintenance. Drones, with their capability to navigate challenging environments, are proving to be invaluable in enhancing the efficiency and safety of WTB inspections. Recognized for their agility, energy efficiency, and prolonged operational duration, drones are increasingly becoming the preferred choice for remote and autonomous wind turbine inspections.

Different types of drones, each optimized for specific tasks, are used in WTB inspections. Low Altitude Platforms (LAPs) are favored for their agility, making them suitable for close-range inspections, while High Altitude Platforms (HAPs) are used for broader, more stable observational tasks. The choice between fixed-wing drones, known for their speed and range, and rotary-wing drones, ideal for their Vertical Take-Off and Landing (VTOL) capabilities, depends on the specific requirements of the inspection task.

Path planning is a crucial aspect of drone operation in WTB inspections. It involves developing algorithms tailored for efficient and comprehensive coverage of the turbine blades. This encompasses both uniform and mixed drone groups, with emerging trends focusing on solar-powered and hybrid drones that combine the best features of different drone types.

Drones in WTB inspections serve not only for visual assessments but also for a variety of other maintenance tasks. They are instrumental in identifying potential damages, wear and tear, and other issues that could affect the performance and longevity of wind turbines. The application of drones in this field exemplifies the convergence of advanced technology with renewable energy, leading to safer, more effective maintenance practices, and ultimately contributing to the sustainable operation of wind energy infrastructure.

Pinney et al. [159] explored the utilization of autonomous drones for the inspection of wind turbines. It aimed to reduce costs, man-hours, and safety risks associated with traditional

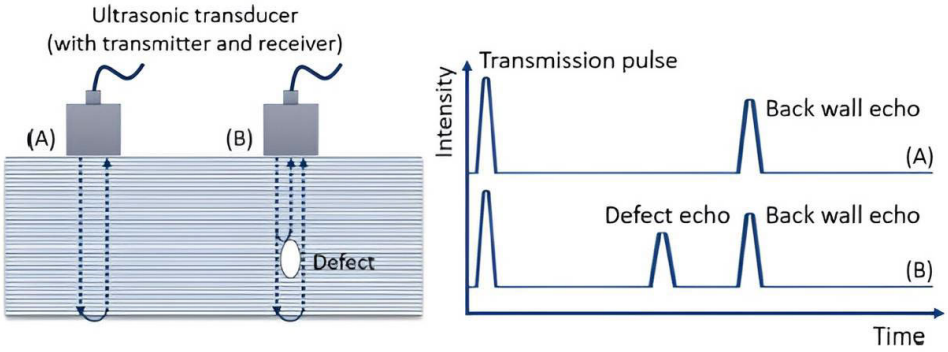

FIGURE 43. Mechanism of ultrasonic technique [155].

inspection methods. The study used a Tello EDU drone (EDU stands for education) and substituted pedestal fans for wind turbines as a small-scale proof of concept. The methodology included autonomous area exploration, target detection, Quick Response (QR) code scanning, image capture, and safe return. Key components involved using OpenCV for object detection and distance calculation, a parallel search pattern for path-planning, and precise return path tracking. The results indicated successful navigation, data collection, and return, highlighting the potential for automating wind turbine inspections to improve efficiency and safety in renewable energy operations.

In their recent work, Pinney et al. [160] focused on developing a drone-based solution for wind turbine inspection. It compared two area exploration algorithms: ''snake'' and ''spiral'', using a Tello EDU drone and pedestal fans as turbine surrogates. The study integrated object detection with OpenCV's Cascade Classifier and QR code verification. The results indicated that the snake pattern excels in battery efficiency and flight duration without object detection, while the spiral pattern outperforms with object detection. This work contributed to automated wind turbine inspections, with the aim of enhancing cost efficiency in renewable energy.

The A* (pronounced A-star) algorithm is a graph traversal and path search algorithm that is widely used in many fields of computer science due to its completeness, optimality, and optimal efficiency. It was first published in 1968 by Peter Hart, Nils Nilsson, and Bertram Raphael of Stanford Research Institute [161]. As shown in Algorithm 2, the A* algorithm is known for its efficiency in finding the shortest path between a start node and a goal node in a weighted graph. The algorithm achieves this efficiency by combining features of Dijkstra's Algorithm and Greedy Best-First-Search, effectively balancing between exploring the most promising routes and ensuring that these routes are actually feasible. A* uses a heuristic function to estimate the cost from a node to the goal, which guides the search towards the goal in an informed manner.

The A* algorithm operates by managing two sets of nodes, the 'Open Set' (OS) and the 'Closed Set'. Initially, OS contains only the start node (S). The algorithm iterates over nodes in OS, selecting the node (C) with the lowest 'f score' (FS). The 'f score' (FS) for a node is the sum of the 'g score' (GS, the cost from S to C) and a heuristic estimate (h) of the cost to the goal (G). If C equals G, the path is reconstructed and returned. Otherwise, C is processed, its neighbors (N) are examined, and their scores (GS and FS) are updated. N is added to OS if not already present. This process repeats until G is reached or OS is empty, indicating no path exists. The heuristic function (h) is crucial for efficiency, as an optimal heuristic reduces the nodes explored. Algorithm 2 outlines the pseudocode for the A* algorithm.

Alqahtani et al. [162] discussed a method for enhancing path planning robustness using Probabilistic Metric

Algorithm 2 A* Algorithm [161]

```
procedure AStar(S, G)
    OS ← {S}
    CF ← an empty map
    GS[S] ← 0
    FS[S] ← h(S)
    while OS ≠ ∅ do
        C ← the node in OS with the lowest FS[C]
        if C = G then
            return reconstructPath(CF, C)
        end if
        OS.remove(C)
        for each neighbor N of C do
            TGS ← GS[C] + d(C, N)
            if TGS < GS[N] then
                CF[N] ← C
                GS[N] ← TGS
                FS[N] ← GS[N] + h(N)
                if N ∉ OS then
                    OS.add(N)
                end if
            end if
        end for
    end while
    return failure
end procedure
```

TABLE 6. Summary of techniques used in drone path-planning for WTB inspection.

Aspect	Details
Drone Types for Inspection	LAPs for close-range, HAPs for broad-range inspections
Drone Model Choice	Fixed-wing for speed and range, Rotary-wing for VTOL and maneuverability
Path-Planning Algorithms	Efficient algorithms for blade coverage, use of uniform and mixed drone groups
Drone Application	For visual inspections and other maintenance tasks, identifying damages and wear
Technological Advancements	Solar-powered/hybrid drones, A* algorithm, autonomous exploration, SVM for turbine detection

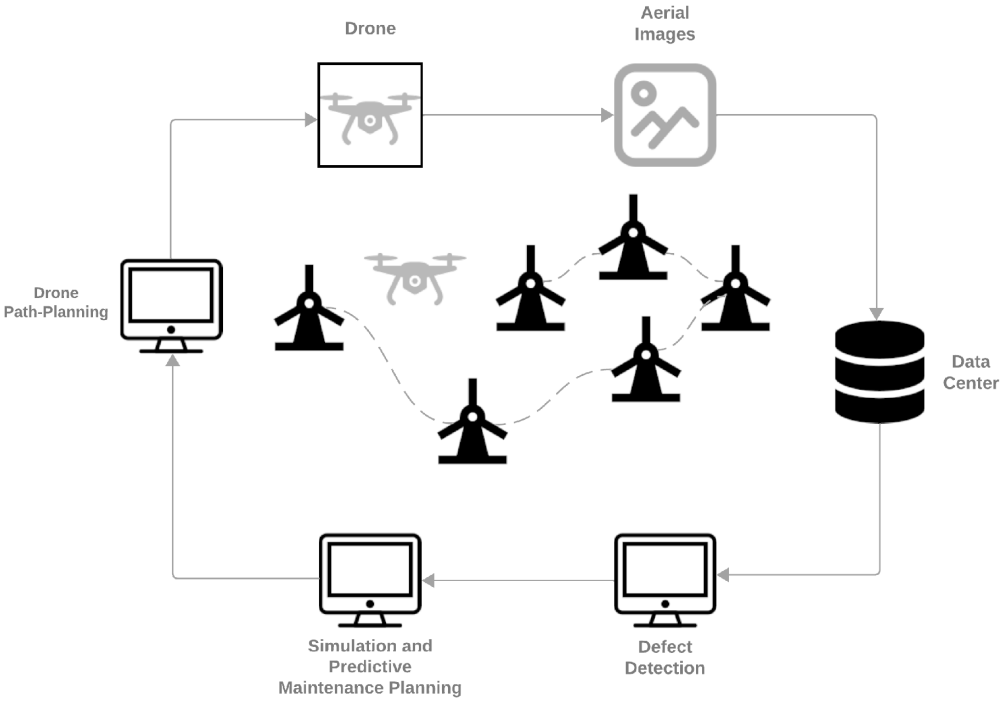

FIGURE 44. Schematic representation of the integrated and cyclic approach for comprehensive, interdisciplinary WTB maintenance research.

Temporal Logic (P-MTL). This approach aims to improve the understanding and interaction with environmental dynamics during path-planning processes, particularly for autonomous agents. Krishnan et al. [163] integrated the Bidirectional Rapidly Exploring Random Trees (RRT) algorithm with an enhanced Artificial Potential Field algorithm. The field of drone path-planning continues to grow, with contributions from Yanmaz [164], Chao et al. [165], and others, demonstrating the dynamic nature of drone path-planning in WTB inspections.

In this section, we highlighted drone integration as a key advancement in renewable energy maintenance, emphasizing drones' role in enhancing wind turbine inspection efficiency and safety. It contrasts fixed-wing drones, valued for speed and range, with rotary-wing drones, preferred for their VTOL capabilities, to meet diverse inspection needs. The discussion extends to path-planning algorithms for effective turbine coverage and technological advances like solar-powered drones, autonomous exploration, and machine learning for improved detection, underscoring drones' growing significance in sustainable inspection practices. Refer to Table 6 for detailed aspects and innovations in drone path-planning for WTB inspection.

VI. GAPS AND LIMITATIONS

Despite the significant advancements in WTB technology, there are still several gaps and limitations in the current research. Addressing these areas is vital to propel the field forward and enhance the efficiency and sustainability of wind energy.

- **Material Lifespan and Degradation:** There's a notable deficiency in long-term empirical data on the degradation of blade materials under diverse environmental conditions. This gap limits our understanding of the real-world endurance of materials and designs. Future research should not only focus on the long-term durability of new materials and designs but also develop more robust testing methodologies that simulate extreme weather conditions and operational scenarios. This will help in designing blades that can withstand harsh environments over extended periods.

TABLE 7. List of acronyms.

Acronym	Full Term	Acronym	Full Term
AE	Acoustic Emission	MC	Monte Carlo
AEP	Annual Energy Production	MFC	Macro-Fiber Composites
AFB-YOLO	Attention and Feature Balanced YOLO	MI-YOLO	Multivariate Information YOLO
AI	Artificial Intelligence	ML	Machine Learning
BEM	Blade Element Momentum	MLP	Multi-Layer Perceptron
BP	BuckyPaper	MW	Mega-Watt
BTC	Bend-Twist coupling	mWA	mean Weighted Average
CAE	Convolutional Auto Encoder	NDT	Non-Destructive Testing
CBAM	Convolutional Block Attention Module	NLM	Non-Local Mean
CNN	Convolutional Neural Network	NREL	National Renewable Energy Lab
DAS	Distributed Accelerometer System	OWT	Offshore Wind Turbine
DB	Debonding	PCA	Principal Component Analysis
DCNN	Deep Convolutional Neural Network	PnP	Perspective-n-Point
DEL	Damage Equivalent Load	POT	Peak-Over-Threshold
DL	Delamination (Composite Type)	PS	Pressure Side
DLC	Design Load Case	PSD	Power spectral density
DR	Detection Rate	PSO	Particle Swarm Optimization
DSF	Defect Semantic Features	PZT	Piezoelectric Lead Zirconate Titanate
DSLR	Digital Single-Lens Reflex	QR	Quick Response
EADD	Efficient and Accurate Damage Detector	RADAR	Radio Detection And Ranging
ECANet	Efficient Channel Attention Network	RBB	Rotation Bounding Box
EDFIL	Empirical Decomposition Feature Intensity Level	R-CNN	Region-based Convolutional Neural Network
EDR	Equivalent Damage Ratio	RDT	Random Decrement Technique
EIoU	Efficient Intersection over Union	ReLU	Rectified Linear Unit
EMC	Enhanced Monte Carlo	ResNet	Residual Network
FBG	Fiber Bragg Grating	RoI	Region of Interest
FE	Finite Element	RRT	Rapidly Exploring Random Trees
FEA	Finite Element Analysis	RUL	Remaining Useful Life
FLOPS	Floating-Point Operations Per Second	SC	Spar Cap
FMCW	Frequency-Modulated Continuous Wave	SCADA	Supervisory Control And Data Acquisition
FORJ	Fiber Optical Rotary Joint	SENet	Squeeze-and-Excitation Network
FPS	Frames Per Second	SHM	Structural Health Monitoring
FR	False Rate	SIFT	Scale-Invariant Feature Transform
FWT	Floating Wind Turbine	SLDV	Scanning Laser Doppler Vibrometer
GFRP	Glass-Fiber Reinforced Plastics	SMC	Standard Monte Carlo
GPM	Gamma Process Model	SMG	Soft-Masks Guided
GPR	Gaussian Process Regression	SNR	Signal-to-Noise Ratio
HAP	High Altitude Platform	SRA	Structural Reliability Analysis
HAWC2	Horizontal Axis WTB Code 2nd Generation	SRCNN	Super-Resolution Convolutional Neural Network
HBB	Horizontal Bounding Box	SS	Suction Side
HOG	Histogram of Oriented Gradients	SSD	Single Shot Multibox Detector
IEC	International Electrotechnical Commission	SSI	Stochastic Subspace Identification
IR	InfraRed	SVM	Support Vector Machine
LAP	Low Altitude Platform	TE	Trailing Edge
LBP	Local Binary Patterns	UAV	Unmanned Aerial Vehicle
LCOE	Levelized Cost Of Energy	VGG	Visual Geometry Group
LE	Leading Edge	VTOL	Vertical Take-Off and Landing
LF	Laminate Fracture	WTB	Wind Turbine Blade
LPSO	Levi-based Particle Swarm Optimization	WTD	Wind Turbine Detection
mAP	mean Average Precision	YOLO	You Only Look Once
MAV	Micro-Aerial Vehicle	YSODA	YOLO-based Small Object Detection Approach

- **Scalability and Real-World Application:** Current research often relies on laboratory and controlled experiments, which, while valuable, do not always accurately represent large-scale, real-world applications. The challenge lies in translating these findings into practical, scalable solutions that can be effectively implemented in operational wind farms. Future research should prioritize the development and testing of technologies in real-world settings to ensure their feasibility and efficiency on a larger scale.
- **Environmental and Ecological Impact:** The impact of WTBs on the environment and local ecosystems, particularly concerning bird and bat mortality, noise pollution, and visual aesthetics, has been insufficiently studied. Comprehensive environmental impact assessments are required to develop more ecologically harmonious designs and siting strategies, ensuring that wind turbines coexist with their natural surroundings without causing significant ecological disruptions.
- **End-of-Life Strategies:** Research on sustainable end-of-life strategies for WTBs, including recycling and disposal, is limited. The development of environmentally friendly disposal methods and the exploration

of recycling possibilities are critical. Additionally, innovation is needed in the manufacture of blades using recyclable or biodegradable materials to reduce the environmental footprint of wind turbines.

- **Cost Analysis and Economic Feasibility:** The economic evaluation of advanced WTB technologies, including a detailed cost-benefit analysis, is often overlooked. Future studies must encompass a thorough financial assessment to ascertain the economic viability of new designs and materials, ensuring that they are not only technologically advanced but also financially feasible for widespread adoption.
- **Integration with Emerging Technologies:** Although there have been strides in blade technology, its integration with emerging technologies such as Artificial Intelligence (AI), big data analytics, and the Internet of Things (IoT) for predictive maintenance and performance optimization is still nascent. Future research should investigate these integrations more thoroughly, exploring how advanced computational and analytical tools can enhance the efficiency and reliability of wind turbines.
- **Policy and Regulatory Framework:** The exploration of policy and regulatory aspects related to new WTB technologies is limited. Future research should examine how policy frameworks and regulations can evolve to support and accelerate the adoption of innovative technologies in the wind energy sector, addressing challenges such as approval processes, safety standards, and incentives for sustainable practices.
- **Multidisciplinary Approaches:** The advancement of wind turbine technology requires a synergistic, multidisciplinary approach. Collaboration across fields such as Computer Science, Mechanical Engineering, and Electrical and Computer Engineering is essential for fostering innovative solutions. This includes the development of advanced sensor technologies, sophisticated data analysis techniques, and integrated systems for enhanced inspection and maintenance of WTBs.
- **Enhanced Imaging Techniques:** The current inspection methods may lack the advanced capabilities needed for early detection of subtle or internal flaws in blade materials. Future research should focus on the application and refinement of thermal, multispectral, and hyperspectral imaging techniques. These technologies have the potential to revolutionize blade inspection by providing deeper insights into the internal health of blades and enabling predictive maintenance to prevent failures before they occur.

Addressing these gaps and limitations is essential for advancing the field of wind turbine technology, ensuring its long-term viability, and maximizing the benefits of wind energy in terms of efficiency, sustainability, and environmental friendliness.

VII. FUTURE DIRECTIONS

In the realm of Wind Turbine Blade (WTB) maintenance, our future research endeavors are set to pioneer a self-sustaining, interdisciplinary framework. This approach, inherently cyclical, is designed to ensure that advancements in one phase enrich and inform subsequent phases. Our strategy comprises several pivotal components:

- **Drone Path-Planning:** Our approach will revolutionize drone navigation by integrating next-generation path-planning algorithms. These algorithms will be designed for adaptive navigation, allowing drones to dynamically adjust flight paths in real-time, ensuring optimal routes are taken to each turbine within complex wind farm landscapes. This precision in navigation facilitates the identification and cataloging of turbines and their blades with unparalleled accuracy, laying the groundwork for targeted maintenance operations.
- **Aerial Imaging:** We aim to employ drones equipped with state-of-the-art high-resolution and multispectral cameras. This setup is not limited to capturing detailed visible spectrum images but extends to peering beneath the surface, revealing internal structural defects otherwise invisible to the naked eye. To counteract the inherent motion blur from both drone mobility and turbine blade movement, we will implement cutting-edge deblurring technologies. These advancements ensure crystal-clear imagery is obtained, providing a reliable data foundation for subsequent analysis.
- **Image Processing:** Our project intends to push the boundaries of image processing and machine learning for defect detection. The process begins with the extraction of high-fidelity images from the advanced aerial imaging phase, followed by the application of sophisticated algorithms designed to parse these images meticulously. The goal is to detect, categorize, and analyze every minute defect, distinguishing them by type, size, severity, and potential impact on turbine operation. This granular level of detail is crucial for crafting maintenance strategies that are both precise and effective.
- **Simulation and Assessment:** Utilizing cutting-edge simulation models, we will simulate the wind turbines under various defect scenarios. These models will allow us to simulate the behavior and potential impacts of defects under a range of conditions, facilitating a deep understanding of their implications on turbine health and performance. This insight feeds into a predictive maintenance framework, where data-driven predictions inform maintenance schedules, ultimately aiming to preempt potential failures, extend turbine lifespan, and optimize operational efficiency.

As depicted in Figure 44, our research methodology embodies a continuous loop of improvement, where each component feeds into the next, fostering an environment of perpetual innovation. This approach is designed to dynamically evolve, incorporating new insights and

technological advancements to refine WTB maintenance practices continually.

In summary, our dedication to advancing WTB maintenance technologies extends beyond mere technical enhancements; it is a reflection of our commitment to environmental stewardship, economic development, and societal benefit. Through this ambitious research agenda, we aspire to contribute meaningfully to the development of a sustainable, efficient, and robust global energy infrastructure.

VIII. CONCLUSION

A. SUMMARY OF KEY FINDINGS

This section encapsulates the critical insights and contributions derived from the reviewed studies in the realm of WTB technology. It particularly highlights the progress in blade design and its consequential effects on the dependability and operational efficiency of wind turbines.

- **Empirical Research and Data Acquisition:** The role of empirical research in the form of experimental testing of WTBs under controlled environments has been instrumental. Such methods have yielded valuable empirical data, especially in understanding fatigue performance, playing a key role in corroborating numerical model simulations.
- **Computational Modeling and Finite Element Method:** The application of computational models, with an emphasis on finite element analysis, has effectively supplemented empirical studies. These computational techniques have facilitated predictive modeling across varied scenarios, thus deepening the comprehension of blade dynamics in differing conditions.
- **Targeted Research Endeavors:** Specific research initiatives have focused on aspects such as fatigue failure simulations, root cause analysis, investigations of trailing edge failures and modeling fatigue induced by rain erosion. These targeted studies have been pivotal in identifying weaknesses in WTB designs and in formulating strategies for risk mitigation.
- **Innovation in Design and Techniques:** The introduction of novel approaches in design, such as bend-twist coupling mechanisms and airfoils shaped like shuttles, has been a breakthrough in reducing fatigue load and aerodynamic drag. These innovations have considerably enhanced blade design efficiency.
- **Sophisticated Numerical Analyses:** Further advancements in numerical analysis have tackled complex issues like multi-axial fatigue, predictions of remaining useful life, and short-term fatigue damage assessment using probabilistic methods. These advanced analyses are crucial for pre-emptive maintenance and for optimizing blade performance.
- **Enhancing Wind Energy Technology:** Collectively, these advances have significantly improved the reliability, operational efficiency, and durability of WTBs, ensuring their alignment with the dynamic and evolving needs of wind energy technology.
- **Interdisciplinary Collaboration:** The evolution of wind turbine blade technology is increasingly reliant on the fusion of multidisciplinary expertise. Addressing the multifaceted challenges presented by WTBs necessitates collaboration across various domains, including material science, aerodynamics, structural engineering, sensor technology, data science, and fields like robotics and AI. This integrated approach fosters innovation in material development, predictive maintenance strategies, advanced sensor technologies, and intelligent data analysis, all of which are imperative to address the complex challenges of wind turbine technology and propelling the industry towards more efficient, resilient, and cost-effective wind energy solutions.

B. IMPLICATIONS OF THE FINDINGS

The findings from the reviewed studies on WTB technology have far-reaching implications for the field of wind energy, especially in terms of enhancing sustainability. These implications are detailed below:

- **Increased Energy Efficiency:** The improvements in blade design and material, such as advanced aerodynamics and lightweight, durable materials, lead to more efficient energy capture. This efficiency is crucial for maximizing the output of wind energy systems, making them more competitive with traditional energy sources.
- **Reduced Environmental Impact:** The development of more durable blades and the focus on predictive maintenance reduce the need for frequent replacements and repairs. This, in turn, leads to a decrease in the environmental footprint of manufacturing and maintaining wind turbines, aligning with global efforts to minimize the ecological impact of energy production.
- **Enhanced Reliability and Safety:** With advancements in fatigue analysis and life prediction, wind turbines become more reliable and safer. This reliability is crucial for their acceptance and operation in diverse environments, including offshore and extreme weather locations.
- **Cost-Effectiveness:** The extended lifespan and improved efficiency of wind turbines, owing to these technological advancements, contribute to lowering the cost of wind energy. This cost reduction is essential for the broader adoption of wind energy on a global scale.
- **Support for Renewable Energy Transition:** The advancements in WTB technology significantly support the global transition towards renewable energy sources. By making wind energy more efficient and sustainable, these advancements help in reducing dependence on fossil fuels, thus contributing to mitigating climate change impacts.
- **Innovation and Economic Opportunities:** These technological advancements open up new avenues for innovation and economic growth within the renewable energy sector. They stimulate research and development,

create new job opportunities, and encourage investment in renewable energy infrastructure.

In summary, the advancements in WTB technology not only enhance the performance and sustainability of individual turbines but also have significant positive implications for the broader field of wind energy. They play a crucial role in driving the global shift towards more sustainable, reliable, and cost-effective energy sources.

REFERENCES

[1] D. Li, S.-C.-M. Ho, G. Song, L. Ren, and H. Li, "A review of damage detection methods for wind turbine blades," *Smart Mater. Struct.*, vol. 24, no. 3, Mar. 2015, Art. no. 033001.

[2] M. S. Campobasso, A. Castorrini, A. Ortolani, and E. Minisci, "Probabilistic analysis of wind turbine performance degradation due to blade erosion accounting for uncertainty of damage geometry," *Renew. Sustain. Energy Rev.*, vol. 178, May 2023, Art. no. 113254.

[3] J. Enríquez Zárate, M. D. L. Á. Gómez López, J. A. C. Troyo, and L. Trujillo, "Analysis and detection of erosion in wind turbine blades," *Math. Comput. Appl.*, vol. 27, no. 1, p. 5, 2022.

[4] A. Castorrini, L. Cappugi, A. Bonfiglioli, and M. S. Campobasso, "Assessing wind turbine energy losses due to blade leading edge erosion cavities with parametric CAD and 3D CFD," *J. Phys., Conf. Ser.*, vol. 1618, no. 5, Sep. 2020, Art. no. 052015.

[5] J. C. López, A. Kolios, L. Wang, and M. Chiachio, "A wind turbine blade leading edge rain erosion computational framework," *Renew. Energy*, vol. 203, pp. 131–141, Feb. 2023.

[6] L. Mishnaevsky, "Root causes and mechanisms of failure of wind turbine blades: Overview," *Materials*, vol. 15, no. 9, p. 2959, Apr. 2022.

[7] R. E. Murray, A. Plumer, R. Beach, and P. Broome, "Validation of a lightning protection system for a fusion-welded thermoplastic composite wind turbine blade tip," *Wind Eng.*, vol. 46, no. 1, pp. 260–272, Feb. 2022.

[8] M. B. Bragg, A. P. Broeren, and L. A. Blumenthal, "Iced-airfoil aerodynamics," *Prog. Aerosp. Sci.*, vol. 41, no. 5, pp. 323–362, Jul. 2005.

[9] L. Gao, Y. Liu, W. Zhou, and H. Hu, "An experimental study on the aerodynamic performance degradation of a wind turbine blade model induced by ice accretion process," *Renew. Energy*, vol. 133, pp. 663–675, Apr. 2019.

[10] L. Gao, T. Tao, Y. Liu, and H. Hu, "A field study of ice accretion and its effects on the power production of utility-scale wind turbines," *Renew. Energy*, vol. 167, pp. 917–928, Apr. 2021.

[11] B. F. Sørensen, E. Jorgensen, C. P. Debel, F. M. Jensen, H. M. Jensen, T. K. Jacobsen, and K. M. Hailing, "Improved design of large wind turbine blade of fibre composites based on studies of scale effects," Danmarks Tekniske Universitet, Riso Nationallaboratoriet Baeredygtig Energi, Lyngby, Denmark, Tech. Rep. Risϕ-R-1390(EN), 2004.

[12] B. Yang and D. Sun, "Testing, inspecting and monitoring technologies for wind turbine blades: A survey," *Renew. Sustain. Energy Rev.*, vol. 22, pp. 515–526, Jun. 2013.

[13] J. Yang, C. Peng, J. Xiao, J. Zeng, S. Xing, J. Jin, and H. Deng, "Structural investigation of composite wind turbine blade considering structural collapse in full-scale static tests," *Compos. Struct.*, vol. 97, pp. 15–29, Mar. 2013.

[14] E. M. Fagan, M. Flanagan, S. B. Leen, T. Flanagan, A. Doyle, and J. Goggins, "Physical experimental static testing and structural design optimisation for a composite wind turbine blade," *Compos. Struct.*, vol. 164, pp. 90–103, Mar. 2017.

[15] X. Chen, W. Zhao, X. Zhao, and J. Xu, "Failure test and finite element simulation of a large wind turbine composite blade under static loading," *Energies*, vol. 7, no. 4, pp. 2274–2297, Apr. 2014.

[16] B. Gage, R. Beach, and S. Hughes, "Laboratory wind turbine blade static testing of the Sandia national rotor testbed 13-meter wind turbine blade," Nat. Renew. Energy Lab. (NREL), Golden, CO, USA, Tech. Rep. NREL/TP-5000-79416, 2021. Accessed: Dec. 20, 2023. [Online]. Available: https://research-hub.nrel.gov/en/publications/laboratory-wind-turbine-blade-static-testing-of-the-sandia-nation

[17] E. R. Jørgensen, K. K. Borum, M. McGugan, C. L. Thomsen, F. M. Jensen, C. P. Debel, and B. F. Sørensen, "Full scale testing of wind turbine blade to failure-flapwise loading," Ris National Lab., Denmark. Forskningscenter Risoe, Risoe-R, Tech. Rep. Risϕ-R-1392(EN), 2004. Accessed: Dec. 20, 2023. [Online]. Available: https://backend.orbit.dtu.dk/ws/portalfiles/portal/7711267/ris_r_1392.pdf

[18] M. A. Rumsey and J. A. Paquette, "Structural health monitoring of wind turbine blades," *Smart Sensor Phenomena, Technol., Netw., Syst.*, vol. 6933, pp. 104–118, Apr. 2008.

[19] K. Lee, A. Aihara, G. Puntsagdash, T. Kawaguchi, H. Sakamoto, and M. Okuma, "Feasibility study on a strain based deflection monitoring system for wind turbine blades," *Mech. Syst. Signal Process.*, vol. 82, pp. 117–129, Jan. 2017.

[20] H. G. Lee and J. Park, "Static test until structural collapse after fatigue testing of a full-scale wind turbine blade," *Compos. Struct.*, vol. 136, pp. 251–257, Feb. 2016.

[21] M. Desmond, S. Hughes, and J. Paquette, "Structural testing of the blade reliability collaborative effect of defect wind turbine blades," National Renew. Energy Lab. (NREL), Golden, CO, USA, Tech. Rep. NREL/TP-5000-63512, 2015. Accessed: Dec. 20, 2023. [Online]. Available: https://research-hub.nrel.gov/en/publications/structural-testing-of-the-blade-reliability-collaborative-effect-

[22] O. Al-Khudairi, H. Hadavinia, C. Little, G. Gillmore, P. Greaves, and K. Dyer, "Full-scale fatigue testing of a wind turbine blade in flapwise direction and examining the effect of crack propagation on the blade performance," *Materials*, vol. 10, no. 10, p. 1152, Oct. 2017.

[23] X. Chen, "Experimental observation of fatigue degradation in a composite wind turbine blade," *Compos. Struct.*, vol. 212, pp. 547–551, Mar. 2019.

[24] M. A. Fremmelev, P. Ladpli, E. Orlowitz, L. O. Bernhammer, M. McGugan, and K. Branner, "Structural health monitoring of 52-meter wind turbine blade: Detection of damage propagation during fatigue testing," *Data-Centric Eng.*, vol. 3, p. e22, Jan. 2022.

[25] D. Melcher, H. Rosemann, B. Haller, S. Neßlinger, E. Petersen, and M. Rosemeier, "Proof of concept: Elliptical biaxial rotor blade fatigue test with resonant excitation," *IOP Conf. Ser., Mater. Sci. Eng.*, vol. 942, no. 1, 2020, Art. no. 012007.

[26] O. Castro, S. C. Yeniceli, P. Berring, S. Semenov, and K. Branner, "Experimental demonstration of strain-based damage method for optimized fatigue testing of wind turbine blades," *Compos. Struct.*, vol. 293, Jan. 2022, Art. no. 115683.

[27] R. Su, Z. Gao, Y. Chen, Y. Bai, and J. Wang, "Experimental on the fatigue failure areas of wind turbine blades' rotating fundamental frequency," *AIP Adv.*, vol. 13, no. 6, Jun. 2023, Art. no. 065123.

[28] J. Simon, T. Kurin, J. Moll, O. Bagemiel, R. Wedel, S. Krause, F. Lurz, A. Nuber, V. Issakov, and V. Krozer, "Embedded radar networks for damage detection in wind turbine blades: Validation in a full-scale fatigue test," *Struct. Health Monitor.*, vol. 22, no. 6, pp. 4252–4263, Nov. 2023.

[29] J. Moll, P. Arnold, M. Mälzer, V. Krozer, D. Pozdniakov, R. Salman, S. Rediske, M. Scholz, H. Friedmann, and A. Nuber, "Radar-based structural health monitoring of wind turbine blades: The case of damage detection," *Struct. Health Monitor.*, vol. 17, no. 4, pp. 815–822, Jul. 2018.

[30] L. Zhang, X. Wang, S. Lu, X. Jiang, C. Ma, L. Lin, and X. Wang, "Fatigue damage monitoring of repaired composite wind turbine blades using high-stability buckypaper sensors," *Compos. Sci. Technol.*, vol. 227, Aug. 2022, Art. no. 109592.

[31] A. Staffa, M. Palmieri, G. Morettini, G. Zucca, F. Crocetti, and F. Cianetti, "Development and validation of a low-cost device for real-time detection of fatigue damage of structures subjected to vibrations," *Sensors*, vol. 23, no. 11, p. 5143, May 2023.

[32] K. Freudenreich and K. Argyriadis, "Wind turbine load level based on extrapolation and simplified methods," *Wind Energy*, vol. 11, no. 6, pp. 589–600, Nov. 2008.

[33] M. T. Sichani, S. R. Nielsen, and A. Naess, "Failure probability estimation of wind turbines by enhanced Monte Carlo method," *J. Eng. Mech.*, vol. 138, no. 4, pp. 379–389, Apr. 2012.

[34] I. Enevoldsen and J. D. Sørensen, "Reliability-based optimization in structural engineering," *Struct. Saf.*, vol. 15, no. 3, pp. 169–196, Sep. 1994.

[35] K. Abdusamad, "Wind energy reliability analysis based on Monte Carlo simulation method," in *Proc. 1st Conf. Eng. Sci. Technol.*, Nov. 2018, pp. 734–745.

[36] C. D. Dao, B. Kazemtabrizi, and C. J. Crabtree, "Offshore wind turbine reliability and operational simulation under uncertainties," *Wind Energy*, vol. 23, no. 10, pp. 1919–1938, Oct. 2020.

[37] C. Zhang, H.-P. Chen, K. F. Tee, and D. Liang, "Reliability-based lifetime fatigue damage assessment of offshore composite wind turbine blades," *J. Aerosp. Eng.*, vol. 34, no. 3, May 2021, Art. no. 04021019.

[38] H. G. Lee, M. G. Kang, and J. Park, "Fatigue failure of a composite wind turbine blade at its root end," *Compos. Struct.*, vol. 133, pp. 878–885, Dec. 2015.

[39] P. U. Haselbach and K. Branner, "Initiation of trailing edge failure in full-scale wind turbine blade test," *Eng. Fract. Mech.*, vol. 162, pp. 136–154, Aug. 2016.

[40] P. U. Haselbach, M. A. Eder, and F. Belloni, "A comprehensive investigation of trailing edge damage in a wind turbine rotor blade," *Wind Energy*, vol. 19, no. 10, pp. 1871–1888, Oct. 2016.

[41] F. Lahuerta, N. Koorn, and D. Smissaert, "Wind turbine blade trailing edge failure assessment with sub-component test on static and fatigue load conditions," *Compos. Struct.*, vol. 204, pp. 755–766, Nov. 2018.

[42] L. Liu, H. Bian, Z. Du, C. Xiao, Y. Guo, and W. Jin, "Reliability analysis of blade of the offshore wind turbine supported by the floating foundation," *Compos. Struct.*, vol. 211, pp. 287–300, Mar. 2019.

[43] M. Tarfaoui, M. Nachtane, O. R. Shah, and H. Boudounit, "Numerical study of the structural static and fatigue strength of wind turbine blades," *Mater. Today, Proc.*, vol. 13, pp. 1215–1223, Jan. 2019.

[44] L. van den Bos, W. Bierbooms, A. Alexandre, B. Sanderse, and G. van Bussel, "Fatigue design load calculations of the offshore NREL 5 MW benchmark turbine using quadrature rule techniques," *Wind Energy*, vol. 23, no. 5, pp. 1181–1195, May 2020.

[45] H. Liu, Z. Zhang, H. Jia, Y. Liu, and J. Leng, "A modified composite fatigue damage model considering stiffness evolution for wind turbine blades," *Compos. Struct.*, vol. 233, Feb. 2020, Art. no. 111736.

[46] F. Wu and W. Yao, "A fatigue damage model of composite materials," *Int. J. Fatigue*, vol. 32, no. 1, pp. 134–138, Jan. 2010.

[47] O. Castro, F. Belloni, M. Stolpe, S. C. Yeniceli, P. Berring, and K. Branner, "Optimized method for multi-axial fatigue testing of wind turbine blades," *Compos. Struct.*, vol. 257, Feb. 2021, Art. no. 113358.

[48] L. D. Avendaño-Valencia, I. Abdallah, and E. Chatzi, "Virtual fatigue diagnostics of wake-affected wind turbine via Gaussian process regression," *Renew. Energy*, vol. 170, pp. 539–561, Jun. 2021.

[49] M. Shekaramiz, T. K. Moon, and J. H. Gunther, "Exploration vs. data refinement via multiple mobile sensors," *Entropy*, vol. 21, no. 6, p. 568, Jun. 2019.

[50] K. Shaler, A. Robertson, and J. Jonkman, "Sensitivity analysis of turbine fatigue and ultimate loads to wind and wake characteristics in a small wind farm," *Wind Energy Sci. Discuss.*, vol. 2021, pp. 1–21, Dec. 2021.

[51] W. Hu, W. Chen, X. Wang, Z. Jiang, Y. Wang, A. S. Verma, and J. J. E. Teuwen, "A computational framework for coating fatigue analysis of wind turbine blades due to rain erosion," *Renew. Energy*, vol. 170, pp. 236–250, Jun. 2021.

[52] C. I. Morăraş, V. Goanţă, B. Istrate, C. Munteanu, and G. S. Dobrescu, "Structural testing by torsion of scalable wind turbine blades," *Polymers*, vol. 14, no. 19, p. 3937, Sep. 2022.

[53] P. Zhang, Z. He, C. Cui, L. Ren, and R. Yao, "Operational modal analysis of offshore wind turbine tower under ambient excitation," *J. Mar. Sci. Eng.*, vol. 10, no. 12, p. 1963, Dec. 2022.

[54] K. Hayat and S. K. Ha, "Load mitigation of wind turbine blade by aeroelastic tailoring via unbalanced laminates composites," *Compos. Struct.*, vol. 128, pp. 122–133, Sep. 2015.

[55] H. Meng, F.-S. Lien, G. Glinka, and P. Geiger, "Study on fatigue life of bend-twist coupling wind turbine blade based on anisotropic beam model and stress-based fatigue analysis method," *Compos. Struct.*, vol. 208, pp. 678–701, Jan. 2019.

[56] G. Guangxing, Z. Weijun, S. Zhenye, S. Wenzhong, C. Jiufa, and F. Shifeng, "Drag reducer design of wind turbine blade under flap-wise fatigue testing," *Compos. Struct.*, vol. 318, Aug. 2023, Art. no. 117094.

[57] M. Peng, M. Liu, S. Gu, and S. Nie, "Multiaxial fatigue analysis of jacket-type offshore wind turbine based on multi-scale finite element model," *Materials*, vol. 16, no. 12, p. 4383, Jun. 2023.

[58] S. Hughes, W. Musial, and T. Stensland, "Implementation of a two-axis servo-hydraulic system for full-scale fatigue testing of wind turbine blades," National Renew. Energy Lab. (NREL), Golden, CO, USA, Tech. Rep. NREL/CP-500-26896, 1999.

[59] P. J. Schubel, R. J. Crossley, E. K. G. Boateng, and J. R. Hutchinson, "Review of structural health and cure monitoring techniques for large wind turbine blades," *Renew. Energy*, vol. 51, pp. 113–123, Mar. 2013.

[60] (2023). *Michigan Scientific Corporation*. Accessed: Sep. 26, 2023. [Online]. Available: https://www.michsci.com/what-is-a-strain-gauge/

[61] (2023). *Fiber-Optic Sensing: Leveraging Three Decades of Fiber Bragg Grating Sensing Technology*. Accessed: Sep. 26, 2023. [Online]. Available: https://www.laserfocusworld.com/fiber-optics/article/16555204/fiberoptic-sensing-three-decades-of-fiber-bragg-grating-sensing-technology

[62] S. Tian, Z. Yang, X. Chen, and Y. Xie, "Damage detection based on static strain responses using FBG in a wind turbine blade," *Sensors*, vol. 15, no. 8, pp. 19992–20005, Aug. 2015.

[63] J. Sierra-Pérez, M. A. Torres-Arredondo, and A. Güemes, "Damage and nonlinearities detection in wind turbine blades based on strain field pattern recognition. FBGs, OBR and strain gauges comparison," *Composite Struct.*, vol. 135, pp. 156–166, Jan. 2016.

[64] B. Wen, X. Tian, Z. Jiang, Z. Li, X. Dong, and Z. Peng, "Monitoring blade loads for a floating wind turbine in wave basin model tests using fiber Bragg grating sensors: A feasibility study," *Mar. Struct.*, vol. 71, May 2020, Art. no. 102729.

[65] S. Gholizadeh, "A review of non-destructive testing methods of composite materials," *Proc. Struct. Integrity*, vol. 1, pp. 50–57, Jan. 2016.

[66] H. Sutherland, A. Beattie, B. Hansche, W. Musial, J. Allread, J. Johnson, and M. Summers, "The application of non-destructive techniques to the testing of a wind turbine blade," Sandia Nat. Lab. (SNL-NM), Albuquerque, NM, USA, 1994. Accessed: Dec. 20, 2023. [Online]. Available: https://www.osti.gov/servlets/purl/10184661

[67] A. Jüngert, "Damage detection in wind turbine blades using two different acoustic techniques," *NDT Database J. (NDT)*, vol. 2075, pp. 1–10, Sep. 2008.

[68] Y.-K. An, M. Kim, and H. Sohn, "Piezoelectric transducers for assessing and monitoring civil infrastructures," in *Sensor Technologies for Civil Infrastructures*. Woodhead Publishing, 2014, pp. 86–120.

[69] L. Wang and Z. Zhang, "Automatic detection of wind turbine blade surface cracks based on UAV-taken images," *IEEE Trans. Ind. Electron.*, vol. 64, no. 9, pp. 7293–7303, Sep. 2017.

[70] E. Alpaydin and C. Kaynak, "Cascading classifiers," *Kybernetika*, vol. 34, no. 4, pp. 369–374, 1998.

[71] J. Friedman, R. Tibshirani, and T. Hastie, "Additive logistic regression: A statistical view of boosting (with discussion and a rejoinder by the authors)," *Ann. Statist.*, vol. 28, no. 2, pp. 337–407, Apr. 2000.

[72] S. Moreno, M. Peña, A. Toledo, R. Treviño, and H. Ponce, "A new vision-based method using deep learning for damage inspection in wind turbine blades," in *Proc. 15th Int. Conf. Electr. Eng., Comput. Sci. Autom. Control (CCE)*, Sep. 2018, pp. 1–5.

[73] L. Peng and J. Liu, "Detection and analysis of large-scale WT blade surface cracks based on UAV-taken images," *IET Image Process.*, vol. 12, no. 11, pp. 2059–2064, Nov. 2018.

[74] J. Chen, J. Benesty, Y. Huang, and S. Doclo, "New insights into the noise reduction Wiener filter," *IEEE Trans. Audio, Speech Language Process.*, vol. 14, no. 4, pp. 1218–1234, Jul. 2006.

[75] H. Hwang and R. A. Haddad, "Adaptive median filters: New algorithms and results," *IEEE Trans. Image Process.*, vol. 4, no. 4, pp. 499–502, Apr. 1995.

[76] E. Dougherty, *Mathematical Morphology in Image Processing*, vol. 1. Boca Raton, FL, USA: CRC Press, 2018.

[77] M. R. Banham and A. K. Katsaggelos, "Digital image restoration," *IEEE Signal Process. Mag.*, vol. 14, no. 2, pp. 24–41, Mar. 1997.

[78] E. J. Leavline and D. A. A. G. Singh, "Salt and pepper noise detection and removal in gray scale images: An experimental analysis," *Int. J. Signal Process., Image Process. Pattern Recognit.*, vol. 6, no. 5, pp. 343–352, Oct. 2013.

[79] L. Wang, Z. Zhang, and X. Luo, "A two-stage data-driven approach for image-based wind turbine blade crack inspections," *IEEE/ASME Trans. Mechatronics*, vol. 24, no. 3, pp. 1271–1281, Jun. 2019.

[80] H. D. Cheng, X. H. Jiang, Y. Sun, and J. Wang, "Color image segmentation: Advances and prospects," *Pattern Recognit.*, vol. 34, no. 12, pp. 2259–2281, Dec. 2001.

[81] D. Denhof, B. Staar, M. Lütjen, and M. Freitag, "Automatic optical surface inspection of wind turbine rotor blades using convolutional neural networks," *Proc. CIRP*, vol. 81, pp. 1166–1170, Jan. 2019.

[82] K. He, X. Zhang, S. Ren, and J. Sun, "Deep residual learning for image recognition," in *Proc. IEEE Conf. Comput. Vis. Pattern Recognit. (CVPR)*, Jun. 2016, pp. 770–778.

[83] G. Huang, Z. Liu, L. Van Der Maaten, and K. Q. Weinberger, "Densely connected convolutional networks," in *Proc. IEEE Conf. Comput. Vis. Pattern Recognit. (CVPR)*, Jul. 2017, pp. 2261–2269.

[84] F. Chollet, "Xception: Deep learning with depthwise separable convolutions," in *Proc. IEEE Conf. Comput. Vis. Pattern Recognit. (CVPR)*, Jul. 2017, pp. 1800–1807.
[85] Y. Bengio and Y. Grandvalet, "No unbiased estimator of the variance of k-fold cross-validation," in *Proc. Adv. Neural Inf. Process. Syst.*, vol. 16, 2003, pp. 1–8.
[86] Z. Qiu, S. Wang, Z. Zeng, and D. Yu, "Automatic visual defects inspection of wind turbine blades via YOLO-based small object detection approach," *J. Electron. Imag.*, vol. 28, no. 4, Aug. 2019, Art. no. 043023.
[87] H. Guo, Q. Cui, J. Wang, X. Fang, W. Yang, and Z. Li, "Detecting and positioning of wind turbine blade tips for UAV-based automatic inspection," in *Proc. IEEE Int. Geosci. Remote Sens. Symp. (IGARSS)*, Jul. 2019, pp. 1374–1377.
[88] K. He, G. Gkioxari, P. Dollár, and R. Girshick, "Mask R-CNN," in *Proc. IEEE Int. Conf. Comput. Vis. (ICCV)*, Oct. 2017, pp. 2980–2988.
[89] S. Li, C. Xu, and M. Xie, "A robust O(n) solution to the perspective-n-point problem," *IEEE Trans. Pattern Anal. Mach. Intell.*, vol. 34, no. 7, pp. 1444–1450, Jul. 2012.
[90] A. Reddy, V. Indragandhi, L. Ravi, and V. Subramaniyaswamy, "Detection of cracks and damage in wind turbine blades using artificial intelligence-based image analytics," *Measurement*, vol. 147, Dec. 2019, Art. no. 106823.
[91] F. Chollet, "Keras: The Python deep learning library," in *Astrophysics Source Code Library*, 2018. [Online]. Available: https://github.com/keras-team/keras
[92] Y. Wang, R. Yoshihashi, R. Kawakami, S. You, T. Harano, M. Ito, K. Komagome, M. Iida, and T. Naemura, "Unsupervised anomaly detection with compact deep features for wind turbine blade images taken by a drone," *IPSJ Trans. Comput. Vis. Appl.*, vol. 11, no. 1, pp. 1–7, Dec. 2019.
[93] M. Ringnér, "What is principal component analysis?" *Nature Biotechnol.*, vol. 26, no. 3, pp. 303–304, Mar. 2008.
[94] N. Dalal and B. Triggs, "Histograms of oriented gradients for human detection," in *Proc. IEEE Comput. Soc. Conf. Comput. Vis. Pattern Recognit. (CVPR)*, Jun. 2005, pp. 886–893.
[95] A. Shihavuddin, X. Chen, V. Fedorov, A. N. Christensen, N. A. B. Riis, K. Branner, A. B. Dahl, and R. R. Paulsen, "Wind turbine surface damage detection by deep learning aided drone inspection analysis," *Energies*, vol. 12, no. 4, p. 676, Feb. 2019.
[96] P. Chlap, H. Min, N. Vandenberg, J. Dowling, L. Holloway, and A. Haworth, "A review of medical image data augmentation techniques for deep learning applications," *J. Med. Imag. Radiat. Oncol.*, vol. 65, no. 5, pp. 545–563, Aug. 2021.
[97] P. Henderson and V. Ferrari, "End-to-end training of object class detectors for mean average precision," in *Proc. Asian Conf. Comput. Vis.* Cham, Switzerland: Springer, 2016, pp. 198–213.
[98] Y. Yu, H. Cao, X. Yan, T. Wang, and S. S. Ge, "Defect identification of wind turbine blades based on defect semantic features with transfer feature extractor," *Neurocomputing*, vol. 376, pp. 1–9, Feb. 2020.
[99] S. Wang, T. Liu, and L. Tan, "Automatically learning semantic features for defect prediction," in *Proc. IEEE/ACM 38th Int. Conf. Softw. Eng. (ICSE)*, May 2016, pp. 297–308.
[100] Y. LeCun, Y. Bengio, and G. Hinton, "Deep learning," *Nature*, vol. 521, no. 7553, pp. 436–444, 2015.
[101] J. Deng, W. Dong, R. Socher, L.-J. Li, K. Li, and L. Fei-Fei, "ImageNet: A large-scale hierarchical image database," in *Proc. IEEE Conf. Comput. Vis. Pattern Recognit.*, Jun. 2009, pp. 248–255.
[102] D. G. Lowe, "Distinctive image features from scale-invariant keypoints," *Int. J. Comput. Vis.*, vol. 60, no. 2, pp. 91–110, Nov. 2004.
[103] Y.-L. Qi, "A relevance feedback retrieval method based on Tamura texture," in *Proc. 2nd Int. Symp. Knowl. Acquisition Model.*, vol. 3, Nov. 2009, pp. 174–177.
[104] M. Pietikäinen, "Local binary patterns," *Scholarpedia*, vol. 5, no. 3, p. 9775, 2010.
[105] P. Yang, C. Dong, X. Zhao, and X. Chen, "The surface damage identifications of wind turbine blades based on ResNet50 algorithm," in *Proc. 39th Chin. Control Conf. (CCC)*, Jul. 2020, pp. 6340–6344.
[106] A. Krizhevsky, I. Sutskever, and G. E. Hinton, "ImageNet classification with deep convolutional neural networks," in *Proc. Adv. Neural Inf. Process. Syst.*, vol. 25, 2012, pp. 1–12.
[107] Y. Mao, S. Wang, D. Yu, and J. Zhao, "Automatic image detection of multi-type surface defects on wind turbine blades based on cascade deep learning network," *Intell. Data Anal.*, vol. 25, no. 2, pp. 463–482, Mar. 2021.
[108] Z. Cai and N. Vasconcelos, "Cascade R-CNN: Delving into high quality object detection," in *Proc. IEEE/CVF Conf. Comput. Vis. Pattern Recognit.*, Jun. 2018, pp. 6154–6162.
[109] L. Torrey and J. Shavlik, "Transfer learning," in *Handbook of Research on Machine Learning Applications and Trends: Algorithms, Methods, and Techniques*. Hershey, PA, USA: IGI Global, 2010, pp. 242–264.
[110] J. Dai, H. Qi, Y. Xiong, Y. Li, G. Zhang, H. Hu, and Y. Wei, "Deformable convolutional networks," in *Proc. IEEE Int. Conf. Comput. Vis. (ICCV)*, Oct. 2017, pp. 764–773.
[111] R. Girshick, "Fast R-CNN," in *Proc. IEEE Int. Conf. Comput. Vis. (ICCV)*, Dec. 2015, pp. 1440–1448.
[112] J. Guo, C. Liu, J. Cao, and D. Jiang, "Damage identification of wind turbine blades with deep convolutional neural networks," *Renew. Energy*, vol. 174, pp. 122–133, Aug. 2021.
[113] Q. Yu and Y. Zhou, "Traffic safety analysis on mixed traffic flows at signalized intersection based on Haar-AdaBoost algorithm and machine learning," *Saf. Sci.*, vol. 120, pp. 248–253, Dec. 2019.
[114] W. S. Noble, "What is a support vector machine?" *Nature Biotechnol.*, vol. 24, no. 12, pp. 1565–1567, Dec. 2006.
[115] L. Deng, Y. Guo, and B. Chai, "Defect detection on a wind turbine blade based on digital image processing," *Processes*, vol. 9, no. 8, p. 1452, Aug. 2021.
[116] J. Kennedy and R. Eberhart, "Particle swarm optimization," in *Proc. IEEE ICNN*, vol. 4, Nov./Dec. 1995, pp. 1942–1948.
[117] G. Viswanathan, V. Afanasyev, S. V. Buldyrev, S. Havlin, M. Da Luz, E. Raposo, and H. E. Stanley, "Lévy flights in random searches," *Phys. A, Stat. Mech. Appl.*, vol. 282, nos. 1–2, pp. 1–12, 2000.
[118] P. Yao, J. Li, X. Ye, Z. Zhuang, and B. Li, "Iris recognition algorithm using modified log-Gabor filters," in *Proc. 18th Int. Conf. Pattern Recognit. (ICPR)*, vol. 4, 2006, pp. 461–464.
[119] J. Zhang, G. Cosma, and J. Watkins, "Image enhanced mask R-CNN: A deep learning pipeline with new evaluation measures for wind turbine blade defect detection and classification," *J. Imag.*, vol. 7, no. 3, p. 46, Mar. 2021.
[120] R. C. Ltd. (2023). *A Software Solutions Provider*. [Online]. Available: https://railstons.com/
[121] S. R. M. Sekhar, S. G. Matt, S. S. Manvi, and S. K. Gopalalyengar, "Identification of essential proteins in yeast using mean weighted average and recursive feature elimination," *Recent Patents Comput. Sci.*, vol. 12, no. 1, pp. 5–10, Jan. 2019.
[122] X. Yang, Y. Zhang, W. Lv, and D. Wang, "Image recognition of wind turbine blade damage based on a deep learning model with transfer learning and an ensemble learning classifier," *Renew. Energy*, vol. 163, pp. 386–397, Jan. 2021.
[123] X. Xu, S. Xu, L. Jin, and E. Song, "Characteristic analysis of Otsu threshold and its applications," *Pattern Recognit. Lett.*, vol. 32, no. 7, pp. 956–961, May 2011.
[124] S. J. Pan and Q. Yang, "A survey on transfer learning," *IEEE Trans. Knowl. Data Eng.*, vol. 22, no. 10, pp. 1345–1359, Jan. 2009.
[125] D. Sarkar and S. K. Gunturi, "Wind turbine blade structural state evaluation by hybrid object detector relying on deep learning models," *J. Ambient Intell. Humanized Comput.*, vol. 12, no. 8, pp. 8535–8548, Aug. 2021.
[126] X. Ran, S. Zhang, H. Wang, and Z. Zhang, "An improved algorithm for wind turbine blade defect detection," *IEEE Access*, vol. 10, pp. 122171–122181, 2022.
[127] L. Zou, Y. Wang, J. Bi, and Y. Sun, "Damage detection in wind turbine blades based on an improved broad learning system model," *Appl. Sci.*, vol. 12, no. 10, p. 5164, May 2022.
[128] Y. Wu, B. Tracey, P. Natarajan, and J. P. Noonan, "Probabilistic non-local means," *IEEE Signal Process. Lett.*, vol. 20, no. 8, pp. 763–766, Aug. 2013.
[129] C. L. P. Chen and Z. Liu, "Broad learning system: An effective and efficient incremental learning system without the need for deep architecture," *IEEE Trans. Neural Netw. Learn. Syst.*, vol. 29, no. 1, pp. 10–24, Jan. 2018.
[130] J. Zhu, C. Wen, and J. Liu, "Defect identification of wind turbine blade based on multi-feature fusion residual network and transfer learning," *Energy Sci. Eng.*, vol. 10, no. 1, pp. 219–229, Jan. 2022.
[131] C. Szegedy, W. Liu, Y. Jia, P. Sermanet, S. Reed, D. Anguelov, D. Erhan, V. Vanhoucke, and A. Rabinovich, "Going deeper with convolutions," in *Proc. IEEE Conf. Comput. Vis. Pattern Recognit. (CVPR)*, Jun. 2015, pp. 1–9.

[132] J. Yu, K. Liu, L. Qin, Q. Li, F. Zhao, Q. Wang, H. Liu, B. Li, J. Wang, and K. Li, "DMnet: A new few-shot framework for wind turbine surface defect detection," *Machines*, vol. 10, no. 6, p. 487, Jun. 2022.
[133] R. Vilalta and Y. Drissi, "A perspective view and survey of meta-learning," *Artif. Intell. Rev.*, vol. 18, no. 2, pp. 77–95, 2002.
[134] A. Foster, O. Best, M. Gianni, A. Khan, K. Collins, and S. Sharma, "Drone footage wind turbine surface damage detection," in *Proc. IEEE 14th Image, Video, Multidimensional Signal Process. Workshop (IVMSP)*, Jun. 2022, pp. 1–5.
[135] L. Lv, Z. Yao, E. Wang, X. Ren, R. Pang, H. Wang, Y. Zhang, and H. Wu, "Efficient and accurate damage detector for wind turbine blade images," *IEEE Access*, vol. 10, pp. 123378–123386, 2022.
[136] C. Zhang, T. Yang, and J. Yang, "Image recognition of wind turbine blade defects using attention-based MobileNetv1-YOLOv4 and transfer learning," *Sensors*, vol. 22, no. 16, p. 6009, Aug. 2022.
[137] Y. Peng, Z. Tang, G. Zhao, G. Cao, and C. Wu, "Motion blur removal for uav-based wind turbine blade images using synthetic datasets," *Remote Sens.*, vol. 14, no. 1, p. 87, Dec. 2021.
[138] Z. Xiaoxun, H. Xinyu, G. Xiaoxia, Y. Xing, X. Zixu, W. Yu, and L. Huaxin, "Research on crack detection method of wind turbine blade based on a deep learning method," *Appl. Energy*, vol. 328, Dec. 2022, Art. no. 120241.
[139] A. Howard, M. Sandler, B. Chen, W. Wang, L.-C. Chen, M. Tan, G. Chu, V. Vasudevan, Y. Zhu, R. Pang, H. Adam, and Q. Le, "Searching for MobileNetV3," in *Proc. IEEE/CVF Int. Conf. Comput. Vis. (ICCV)*, Oct. 2019, pp. 1314–1324.
[140] K. Han, Y. Wang, Q. Tian, J. Guo, C. Xu, and C. Xu, "GhostNet: More features from cheap operations," in *Proc. IEEE/CVF Conf. Comput. Vis. Pattern Recognit. (CVPR)*, Jun. 2020, pp. 1577–1586.
[141] R. Zhang and C. Wen, "SOD-YOLO: A small target defect detection algorithm for wind turbine blades based on improved YOLOv5," *Adv. Theory Simul.*, vol. 5, no. 7, Jul. 2022, Art. no. 2100631.
[142] P. W. Power and J. A. Schoonees, "Understanding background mixture models for foreground segmentation," *Proc. Image Vis. Comput. New Zealand*, vol. 2002, pp. 10–11, 2002.
[143] J. Illingworth and J. Kittler, "A survey of the Hough transform," *Comput. Vis., Graph., Image Process.*, vol. 43, no. 2, p. 280, Aug. 1988.
[144] J. A. Hartigan and M. A. Wong, "Algorithm AS 136: A K-means clustering algorithm," *Appl. Statist.*, vol. 28, no. 1, p. 100, 1979.
[145] S. Woo, J. Park, J.-Y. Lee, and I. S. Kweon, "CBAM: Convolutional block attention module," in *Proc. Eur. Conf. Comput. Vis.*, Sep. 2018, pp. 3–19.
[146] C. Yang, X. Liu, H. Zhou, Y. Ke, and J. See, "Towards accurate image stitching for drone-based wind turbine blade inspection," *Renew. Energy*, vol. 203, pp. 267–279, Feb. 2023.
[147] C. Wang and Y. Gu, "Research on infrared nondestructive detection of small wind turbine blades," *Results Eng.*, vol. 15, Sep. 2022, Art. no. 100570.
[148] H. Sanati, D. Wood, and Q. Sun, "Condition monitoring of wind turbine blades using active and passive thermography," *Appl. Sci.*, vol. 8, no. 10, p. 2004, Oct. 2018.
[149] X. Chen, A. Shihavuddin, S. H. Madsen, K. Thomsen, S. Rasmussen, and K. Branner, "AQUADA: Automated quantification of damages in composite wind turbine blades for LCOE reduction," *Wind Energy*, vol. 24, no. 6, pp. 535–548, Jun. 2021.
[150] W. Zhou, Z. Wang, M. Zhang, and L. Wang, "Wind turbine actual defects detection based on visible and infrared image fusion," *IEEE Trans. Instrum. Meas.*, vol. 72, pp. 1–8, 2023.
[151] H.-H. Zhao, P. L. Rosin, Y.-K. Lai, and Y.-N. Wang, "Automatic semantic style transfer using deep convolutional neural networks and soft masks," *Vis. Comput.*, vol. 36, no. 7, pp. 1307–1324, Jul. 2020.
[152] A. Poudel and J. S. Chu, "Air-coupled ultrasonic testing of carbon-carbon composite aircraft brake disks," *Mater. Eval.*, vol. 71, no. 8, pp. 1–8, 2013.
[153] R. Raišutis, R. Kažys, and L. Mažeika, "Application of the ultrasonic pulse-echo technique for quality control of the multi-layered plastic materials," *NDT E Int.*, vol. 41, no. 4, pp. 300–311, Jun. 2008.
[154] S. K. Chakrapani, V. Dayal, R. Krafka, and A. Eldal, "Ultrasonic testing of adhesive bonds of thick composites with applications to wind turbine blades," in *Proc. AIP Conf.*, 2012, pp. 1284–1290.
[155] K. Kong, K. Dyer, C. Payne, I. Hamerton, and P. M. Weaver, "Progress and trends in damage detection methods, maintenance, and data-driven monitoring of wind turbine blades—A review," *Renew. Energy Focus*, vol. 44, pp. 390–412, Mar. 2023.
[156] A. Ghoshal, M. J. Sundaresan, M. J. Schulz, and P. Frank Pai, "Structural health monitoring techniques for wind turbine blades," *J. Wind Eng. Ind. Aerodynamics*, vol. 85, no. 3, pp. 309–324, Apr. 2000.
[157] A. Abouhnik and A. Albarbar, "Wind turbine blades condition assessment based on vibration measurements and the level of an empirically decomposed feature," *Energy Convers. Manage.*, vol. 64, pp. 606–613, Dec. 2012.
[158] P. Chen and B. Chen, "Influence of the blade size on the dynamic characteristic damage identification of wind turbine blades," *Nonlinear Eng.*, vol. 12, no. 1, Apr. 2023, Art. no. 20220261.
[159] B. Pinney, S. Duncan, M. Shekaramiz, and M. A. Masoum, "Drone path planning and object detection via QR codes; a surrogate case study for wind turbine inspection," in *Proc. Intermountain Eng., Technol. Comput. (IETC)*, 2022, pp. 1–6.
[160] B. Pinney, B. Stockett, M. Shekaramiz, M. A. Masoum, A. Seibi, and A. Rodriguez, "Exploration and object detection via low-cost autonomous drone," in *Proc. Intermountain Eng., Technol. Comput. (IETC)*, 2023, pp. 49–54.
[161] P. Hart, N. Nilsson, and B. Raphael, "A formal basis for the heuristic determination of minimum cost paths," *IEEE Trans. Syst. Sci. Cybern.*, vol. SSC-4, no. 2, pp. 100–107, Jul. 1968.
[162] S. Alqahtani, I. Riley, S. Taylor, R. Gamble, and R. Mailler, "MTL robustness for path planning with A*," in *Proc. 17th Int. Conf. Auto. Agents MultiAgent Syst.*, pp. 247–255, 2018.
[163] R. A. Krishnan, V. R. Jisha, and K. Gokulnath, "Path planning of an autonomous quadcopter based delivery system," in *Proc. Int. Conf. Emerg. Trends Innov. Eng. Technol. Res. (ICETIETR)*, Jul. 2018, pp. 1–5.
[164] E. Yanmaz, "Joint or decoupled optimization: Multi-UAV path planning for search and rescue," *Ad Hoc Netw.*, vol. 138, Jan. 2023, Art. no. 103018.
[165] Y. Chao, P. Augenstein, A. Roennau, R. Dillmann, and Z. Xiong, "Brain inspired path planning algorithms for drones," *Frontiers Neurorobotics*, vol. 17, Mar. 2023, Art. no. 1111861.

MAJID MEMARI received the bachelor's degree in industrial engineering, the M.S. degree in computer science, and the M.B.A. and Ph.D. degrees in computer science. He has established himself as a Proficient Data Scientist with over eight years of field experience, underpinned by a rich educational foundation. In the Ph.D. degree, he leveraged advanced deep learning and computer vision techniques to enhance the accuracy of systems interpreting text in images. His research interests include generative models and crafting synthetic images to bolster text recognition in diverse industry applications. He explored stock market trend prediction through news sentiment analysis during the M.S. degree. Currently, he is a Postdoctoral Researcher with Utah Valley University, he specializes in machine learning and computer vision, focusing on real-time drone and aerial imaging for wind turbine maintenance. Concurrently, he holds a position as a Data Scientist with Potentia Analytics, developing predictive models for patient flow in healthcare settings. Previously, he was a Research Assistant with the University of Pennsylvania and Southern Illinois University Carbondale, engaging in a gamut of projects from big data analytics to medical image synthesis.

PRAVEEN SHAKYA received the B.Tech. degree in aerospace engineering from Indian Institute of Technology (IIT) Kharagpur, India, in 2011, the M.Tech. degree from IIT Bombay, India, in 2013, and the Ph.D. degree in aerospace engineering from IIT Kharagpur, in 2021. In the Ph.D. degree, he did the flutter analysis of composite WTB by using finite element method (FEM) in the MATLAB environment. His master's dissertation was on dynamics and control where he did the flight dynamic analysis of sounding rocket and numerical simulations to analyze the rocket's trajectory, aerodynamic forces, and rotational motion. Currently, he is a Postdoctoral Researcher in mechanical engineering with Utah Valley University. His research interests include fatigue and crack analysis for WTBs.

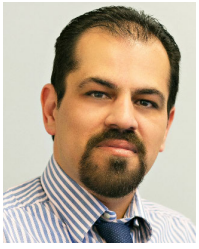

MOHAMMAD SHEKARAMIZ (Member, IEEE) received the M.S. degree in electrical engineering-controls from Isfahan University of Technology (IUT), Iran, in 2006, and the Ph.D. degree in electrical engineering-signal processing from Utah State University (USU), USA, in 2018. He was a Postdoctoral Researcher with the Information Dynamics Laboratory, USU, until August 2019, where he researched problems related to active noise cancellation. He is a member of Golden Key Honor Society, Phi Kappa Phi, and Tau Beta Pi. Since 2019, he has been with the Electrical and Computer Engineering Program, Utah Valley University (UVU), where he is currently an Assistant Professor. He is the PI of a grant proposal from the Utah System of Higher Education-Deep Technology Talent Initiative related to developing a fully automated system for the inspection of wind turbines using artificial intelligence and commercial drones. His current research interests include machine learning, deep learning, drone path-planning, statistical signal processing, and compressive sensing.

ABDENNOUR C. SEIBI received the B.S. degree in mechanical engineering and the M.S. and Ph.D. degrees in engineering mechanics from The Pennsylvania State University. He is currently a Distinguished Researcher in problems related to the energy sector and advanced materials. He is also a Professor with the Mechanical Engineering Program, Utah Valley University, Orem, UT, USA. He has published over 150 technical articles and 30 technical reports which earned him international recognition from ASME and SPE. He is a member of ASME and SPE.

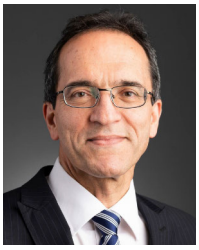

MOHAMMAD A. S. MASOUM (Senior Member, IEEE) received the B.S. and M.S. degrees in electrical and computer engineering from the University of Colorado Denver, Denver, CO, USA, in 1983 and 1985, respectively, and the Ph.D. degree in electrical and computer engineering from the University of Colorado Boulder, Boulder, CO, USA, in 1991. He is currently a Professor and the Chair/Head of the Engineering Department, Utah Valley University, Orem, UT, USA. He has published over 150 journal articles and 200 conference papers. He has coauthored *Power Quality in Power Systems and Electrical Machines* (Elsevier, 2008, 2015, and 2023) and the *Power Conversion of Renewable Energy Systems* (Springer, 2011 and 2012).